INFORMATION TO USERS

The most advanced technology has been used to photograph and reproduce this manuscript from the microfilm master. UMI films the text directly from the original or copy submitted. Thus, some thesis and dissertation copies are in typewriter face, while others may be from any type of computer printer.

The quality of this reproduction is dependent upon the quality of the copy submitted. Broken or indistinct print, colored or poor quality illustrations and photographs, print bleedthrough, substandard margins, and improper alignment can adversely affect reproduction.

In the unlikely event that the author did not send UMI a complete manuscript and there are missing pages, these will be noted. Also, if unauthorized copyright material had to be removed, a note will indicate the deletion.

Oversize materials (e.g., maps, drawings, charts) are reproduced by sectioning the original, beginning at the upper left-hand corner and continuing from left to right in equal sections with small overlaps. Each original is also photographed in one exposure and is included in reduced form at the back of the book. These are also available as one exposure on a standard 35mm slide or as a 17" x 23" black and white photographic print for an additional charge.

Photographs included in the original manuscript have been reproduced xerographically in this copy. Higher quality 6" x 9" black and white photographic prints are available for any photographs or illustrations appearing in this copy for an additional charge. Contact UMI directly to order.

U·M·I

University Microfilms International
A Bell & Howell Information Company
300 North Zeeb Road, Ann Arbor, MI 48106-1346 USA
313/761-4700 800/521-0600

Order Number 9009728

Charge transfer in polymeric systems

DiBerardino, Thomas, Ph.D.

City University of New York, 1989

U·M·I
300 N. Zeeb Rd.
Ann Arbor, MI 48106

A

CHARGE TRANSFER IN POLYMERIC SYSTEMS

by

THOMAS DiBERARDINO

A dissertation submitted to the Graduate Faculty in Chemistry in partial fulfillment of the requirements for the degree of Doctor of Philosophy, The City University of New York.

1989

This manuscript has been read and accepted for the Graduate Faculty in Chemistry in satisfaction of the dissertation requirement for the degree of Doctor of Philosophy.

9/1/89
Date

Chair of Examining Committee

9/28/89
Date

Executive Officer

Fitzgerald Bramwell

Arthur Woodward
Supervisory Committee

The City University of New York

ABSTRACT

Charge transfer complexes of polymeric donors having pendent heterocyclic rings and low molecular weight acceptors were studied. Electronic spectroscopy was used for the observation of charge transfer processes for systems with molecular iodine as the acceptor. The application of electron spin resonance, infrared spectroscopy and nuclear magnetic resonance spectroscopies lead to detailed information on the charge transfer complexes involving tetracyanoethylene (TCNE) as the acceptor. A new synthetic route for the synthesis of poly(4-vinylpyrimidine) (P4VPm), a polymer donor with diazine functionality, was developed and a mechanistic pathway of dehydration of an alcohol intermediate was proposed.

UV-Vis - Charge transfer complexes of iodine with the following donors were investigated: atactic high molecular weight (HMW) and low molecular weight (LMW) poly(2-vinylpyridine) (P2VP), isotactic (*i*-) P2VP, and pyridine. Reaction schemes for P2VP were developed based upon the position and intensities of the absorption bands. In non - polar solvents the perturbed visible band was found to be dependent on the type of donor and iodine concentration. Extinction coefficients increased with the extent of blue shift for the visible absorption band of iodine. The triiodide (I_3^-) absorption band at 366 nm showed a lower limit of donor to I_2 stoicheomtric ratio of 0.5:1. This ratio approached unity with a corresponding decrease in the degree of

blue shift for the visible absorption band of I_2. Based on extinction coefficients, formation constants, position and intensity of the absorption, it was concluded triiodide ion formed in the atactic HMW P2VP system while LMW and *i*-P2VP resulted in a species with both inner and outer complex characteristics. In solvent of lesser hydrogen bonding ability but of greater dielectric constant, iso P2VP and pyridine, unlike HMW P2VP, did not give triiodide. A mechanism for the different behaviors was given based on coiling of the chain. Formation constants and extinction coefficients obtained in different solvents supported the above mechanism.

NMR - Charge transfer complexes formed between *i*-P2VP donor and TCNE acceptor were observed in the liquid and the solid states by NMR spectroscopy. In the liquid state, formation constants (K) and the change in chemical shift accompanying the formation of the pure complex (Δ_0) were obtained. The nature of the molecular orbitals involved was employed to explain the order of Δ_0 values for the five aromatic carbon nuclei. Results for 2 - ethylpyridine (2EP) yielded an order for Δ_0 values different from the polymer systems. The difference was attributed to the lower extent of electron transfer for the 2EP complex. A mechanism for this difference was given based on Mulliken's orientation and overlap principle.

Formation constants were derived for the polymeric system by various algebraic approaches based on the law of mass expression

for the 1:1 complex. The value was found to be 21 kg/mole and the system was shown to be quickly saturated. Proton NMR of the polymeric charge transfer complex showed unique behavior of proton 3 (H_3) and proton 6 (H_6) of the ring. The value of K determined by proton NMR was the same as by carbon NMR but decreased at lower donor concentration. The higher apparent formation constant for H_3 and the unusual chemical shifts of H_6 were used to support a topographic model of the complex involving an anisotropic magnetic environment around the donor. The model was substantiated by an analysis of the 2EP complex. The formation constant for 2EP was found to be dependent upon Additional Unspecific Shielding (AUS). A formation constant of 6 Kg/mole was obtained for all protons. This value was independent of donor concentrations except at very low concentrations. Reasons for the behavior of the protons for both systems were given. The origin for AUS involved in 2EP but not in the polymer was given.

In the solid state, isotactic P2VP and P4VP complexes with TCNE were studied. The degree of electron transfer was estimated from infrared data and the degree of change chemical shifts for acceptor was found to be the same in P2VP and P4VP. Chemical shifts for the aromatic carbons confirmed the $n{:}\pi$ complex. No evidence for a $\pi{:}\pi$ complex was observed. ^{13}C absorption intensities as a function of contact time were obtained to give information including $T_1\rho(H)$, chain mobility and proximity of carbon nuclei on TCNE to the proton pool. Delayed decoupling

experiments confirmed assignments for the non - protonated carbons and yielded evidence for the model developed from solution studies.

ESR - P2VP, P4VP and P4VPm yielded free radicals upon complexation with TCNE both in the solid and the solution states. Complexes of TCNE formed in 2EP, 4EP and 4-methylpyrimidine as solvents were observed. For the polymeric systems, there are at least two radicals present i.e. the TCNE and the polymer radicals. One is expected to involve delocalization into the heterocyclic ring. In solution only the TCNE radical, a product of complete electron transfer, was observed. The signal originating from the 2EP complex was not well resolved; the radical may still be partially associated with the 2EP molecule. Spin density for the P4VP system reached a maximum at 2:1 donor ring to acceptor ratio. All P2VP polymers reached a maximum at a 4:1 ratio. The level of radical concentration in these systems is not high enough (ca. 0.1 mol %) to affect NMR measurements

P4VPm was synthesized by a new pathway with improved yield. The preparation used the formation of 4 - pyrimidinyllithium and its reaction with formaldehyde gas to give a reactive carbocation which lead to the formation of an alcohol intermediate. In addition, a second method was developed, involving the reaction of the alcohol with acetic anhydride to give a high yield of the vinyl product. Mechanistic schemes were given and discussed. Reactions of the alcohol confirmed the mechanism for its

dehydration. A six - member hydrogen bonded ring formed by the alcohol was found to be the primary cause of low yields through regeneration of starting material. Other exploratory synthetic methods were attempted but were less successful in obtaining high yields. These methods included: a)high pressure reaction of formalin solution with 4-methylpyrimidine to give an alcohol intermediate b)reaction of 4-methylpyrimidine, acetic anhydride and *a* - polyformaldehyde in a sealed tube to give the vinyl compound and c)reaction of 2 - bromopyrimidine with vinylmagnesium bromide to give the vinyl compound.

Acknowledgements

I would like to express my gratitude to Professors Fitzgerald Bramwell and Arthur Woodward for their time and contributions as members of my thesis committee. My appreciation goes out to Professor Nan-Loh Yang for acting as advisor, I will miss our many memorable discussions. I am also grateful to Professor Ruth E. Stark for her contributions.

I am deeply indebted to my family for exceptional support without which this work would not be a reality. My deepest thanks goes out to my wife Fei-Fei for being a constant source of inspiration by her hard work and emotional support and for making our years together the best.

Acknowledged are teaching support from the Department of Chemistry and the Department of applied Science and C.U.N.Y. - P.S.C. grants # 6-68253 and 6-67271.

This work is dedicated to the memory of my Father and to the future of my daughter.

TABLE OF CONTENTS

LIST OF FIGURES

I INTRODUCTION

The process of charge transfer interaction is important in chemistry. It is involved in the primary acts and the transient states of numerous chemical reactions, is the basis of many catalytic processes, determines the specific solvation in solutions and leads to the formation of numerous new compounds with different properties. Charge transfer complexes have long been the subject of intense investigation mostly by electronic spectroscopy and latter by solution NMR spectroscopy. Investigations have overwhelmingly been on small molecules. The most studied polymeric system have been complexes with poly-(N-vinylcarbazole) as the donor. Investigation of these systems has been confined mostly to the use of electronic spectroscopy.

For this thesis poly(vinylpyridine) as donor in charge transfer reactions was investigated by Fourier Transform Infra-Red spectroscopy (FT-IR), electronic spectroscopy, electron spin resonance and nuclear magnetic resonance. Much work has been done on the pyridine ring and it is of fundamental interest to study interactions of its polymer analog. Information for the polymer complexes is severely lacking in the literature although poly(2-vinylpyridine)(P2VP) is essential as a conductance - enhancing additive in lithium - I_2 cells. This work investigates P2VP and its analogs as donor for the acceptors iodine and tetracyanoethylene (TCNE).

Charge transfer complexes of polymeric donors with iodine were investigated by electronic spectroscopy. This technique enabled study of dilute solutions of donor and acceptor in a variety of solvents. The perturbed blue shift of the visible iodine absorption was studied in depth in relation to solvent and type of donor. Tacticity, molecular weight and solvent were important factors which influenced the equilibrium of iodine solutions. *i*-P2VP and 2EP with TCNE in DMSO-d_6 were studied by NMR spectroscopy. This is the first in depth study of a donor having magnetically non-equivalent nuclei in which each nucleus is analyzed. Overwhelmingly, highly symmetric small molecules are reported in the literature. A topographic model of the complexes was proposed based on NMR results.

II BACKGROUND

This background section will introduce the concept of the charge transfer via quantum mechanical treatment. Application of spectroscopies and mathematical treatments used in the analysis of parameters for charge transfer complexes will then be addressed.

II.A THEORY OF THE CHARGE TRANSFER COMPLEX

II.A.1 Description of the Charge Transfer Complex

The formation of charge transfer complexes involves an interaction of an electron on the donor moiety with a vacant molecular orbital on the acceptor moiety. The assumption is made that the electron occupies the highest occupied donor orbital, HOMO, and is transferred to the lowest unoccupied molecular orbital, LUMO of the acceptor. Intermolecular bonds are thus formed as the result of electron transfer. The degree to which electron transfer occurs is much less than what ordinarily occurs when new compounds are formed (1) and thus neither covalent or ionic bonds are formed.

A charge transfer system can be represented by donor (D) and acceptor (A) in a resonance hybrid of the structures I and II:

$$D + A \leftrightharpoons \underset{I}{(D,A)} \leftrightharpoons \underset{II}{(D^{+}A^{-})}$$

Scheme II.A.1.1

This resonance can be expressed as an approximate wave function Ψ_n which is the sum of two terms given in equation II.A.1.1

$$\Psi_n = a\Psi_0(D,A) + b\Psi_1(D^{+}\text{-}A^{-}) \qquad \text{II.A.1.1}$$

Wave function Ψ_0 refers to the "no-bond" state. In this state the molecules are situated at a distance equal to that in the complexed state while having the same geometrical configuration as in the complex. Wave function Ψ_1 represents the dative state. This state involves transfer of an electron from a molecular orbital on the donor to a vacant molecular orbital on the acceptor. The second electron located on the donor remains paired with the electron now present in the vacant acceptor orbital. The coefficients a and b characterize the fraction of the no - bond and dative state.

Normalization of Ψ_n results in:

$$\int \Psi_n \Psi_n dv = a^2 + b^2 + 2abS_{01} = 1 \qquad \text{II.A.1.2}$$

where $S_{01} = \int \Psi_0 \Psi_1 dv$ over all space. S_{01} represents the overlap (or non - orthogonality) integral between the function Ψ_0 and Ψ_1. The term S_{01} is proportional to the overlap integral of the filled donor orbital (Ψ_d) and the lower vacant orbital of the

acceptor (Ψ_a). The orientation of the donor - acceptor complex maximizes the overlap integral between Ψ_d and Ψ_a. This has been termed the orientation and overlap principle (2). The principle states that the partners in the donor - acceptor complex tend to assume a mutual orientation so that the orbital from which the electron is transferred has the greatest overlap integral with the orbital which accepts the electron. The need for maximizing overlap between orbitals of donor and acceptor is important. When a donor and an acceptor come in contact in a medium, the formation of a charge transfer complex depends on whether or not the collision is successful, ie., maximum overlap is required.

Quantum theory requires that for a ground state Ψ_n there must be an excited state. This excited state $\Psi_e$is given as:

$$\Psi_e = a^*\Psi_1(D^+\text{-}A^-) - b^*\Psi_0(D,A) \qquad \text{II.A.1.3}$$

Quantum theory also requires that the excited state wave function be orthogonal to the ground state function as follows:

$$\int \Psi_n \Psi_e dv = 0 \qquad \text{II.A.1.4}$$

Normalization of the excited state function results in:

$$\int \Psi_e^2 dv = a^{*2} + b^{*2} - 2a^*b^*S_{01} = 1 \qquad \text{II.A.1.5}$$

The specific case of pyridine and iodine will be considered

based on the fundamental approach discussed above. Pyridine acts as an increvalent *n* donor as discussed above. The electronic configuration of Iodine (I) is: $[Kr]4d^{10}5s^25p^5$ which makes iodine a sacrificial σ acceptor by addition of an electron into an anti - bonding orbital as seen in the diagram below.

Figure II.A.1.1: Molecular orbital diagram for I_2 showing the LUMO as anti-bonding.

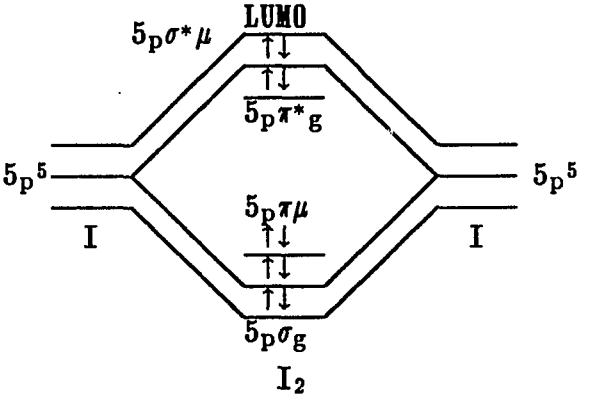

The equilibrium between pyridine and iodine is given

$$Py + I_2 \rightleftharpoons PY\cdot I_2 \rightleftharpoons PYI^+\text{–}I^-$$

Scheme II.A.1.2: Pyridine (Py) and I_2 in equilibrium

The ground and the excited states can be represented (from equations II.A.1.1 and II.A.1.3 respectively) as:

$$\Psi_n = a\Psi_0(Py\cdot I_2) + b\Psi_1(PyI^+\text{–}I^-) \qquad \text{II.A.1.6a}$$

$$\Psi_e = a^*\Psi_1(pyI^+\text{–}I^-) - b^*\Psi_0(Py\cdot I_2) \qquad \text{II.A.1.6b}$$

For a loose complex, S_{01} in equation II.A.1.2 is small and $a + b \simeq 1$. When b^2 is small the ground state wave function is dependent mostly on the first (no - bond) term.

The coefficients a and b represent respectively the fraction of no-bond and dative contribution to the wave function Ψ_n. When the value of b is low, the fraction of charge transfer is small and the system is stabilized mainly by classic electrostatic forces. At high values of b the contribution of charge transfer may be much greater than the classic intermolecular forces. Coefficients a, b and a^*, b^* in equation II.A.1.1 and II.A.1.3 are related to the orthogonality (equation II.A.1.4) and normalization conditions of functions Ψ_n and Ψ_e, leading to equations II.A.1.2 and II.A.1.5. As a result, $a^* \cong a$ and $b^* \cong b$. If S_{01} were 0 then $a = a^*$ and $b = b^*$ would be true exactly. In the case where there is mostly no-bond in the ground state ($a^2 >> b^2$) there is a short wavelength absorption. That is, in the excited state there is mostly dative character and $a^{*2} >> b^{*2}$.

II.A.2 CLASSIFICATION OF DONORS AND ACCEPTORS

Classification of charge transfer complexes has been developed by Mulliken (3) in which donor and acceptors are each divided into three major groups. The principle used in categorizing the molecule is based upon the type of orbital taking part in the interaction. The first group of donors, represented by n, are those in which the energetically highest

orbital, HOMO, accommodates a lone pair of n - electrons of a heteroatom such as R_2O, R_2S, R_3N, etc. In the second group the electron pair is in a sigma orbital and this group is denoted as σ. The third group constitute those donors in which the electrons are in a π - orbital of an unsaturated or aromatic compound and represented as π.

Acceptors are also divided into three major categories and are grouped according to the character of the lowest unoccupied molecular orbital, LUMO, capable of accepting electron density. The first group consist of acceptors with v - vacant orbitals of the metal atom (metal halides, some organometalic compounds) and designated as v acceptors. The second group contains a non - bonding σ - orbital such as iodine, bromine and iodine monochloride and is given the symbol σ. The third group are those which accept electron density into the π - orbitals and are represented by π. Commonly seen in the literature are the symbols b and a, which stand for base (donor) and acceptor respectively, placed in front of the symbols π and σ to differentiate the functionalities.

Donor and acceptors can both be termed increvalent and sacrificial. Increvalent complexes are of the type $n \cdot v$ with increased valence of both the donor and the acceptor, such as the complex of a nitrogen heteroatom with that of boron. In the complex $R_3N \cdot BR_3$, the nitrogen valence as well as the boron valence, is increased from 3 to 4 and thus the term increvalent.

Replacing the boron moiety with the acceptor I_2 gives an example of a sacrificial acceptor. The complex is designated as $n \cdot a\sigma$, i.e. an electron is transferred from a n - orbital of nitrogen to a σ - antibonding orbital of I_2. Accepting electron density into an antibonding orbital weakens the bond between the acceptor I - I atoms, thus it is a sacrificial acceptor.

These classifications are important in predicting stability. The strongest complexes tend to be those in which both donor and acceptor are increvalent while the weakest are those in which both donor and acceptor are sacrificial. An interesting and significant situation arises for benzene and its derivatives. The benzene ring may act as either a donor or acceptor but is always sacrificial, as are all π donor and acceptors. Figure II.A.2.1 represents the energy level of the π molecular orbital of benzene.

Figure II.A.2.1: Energy levels of the Benzene π orbitals

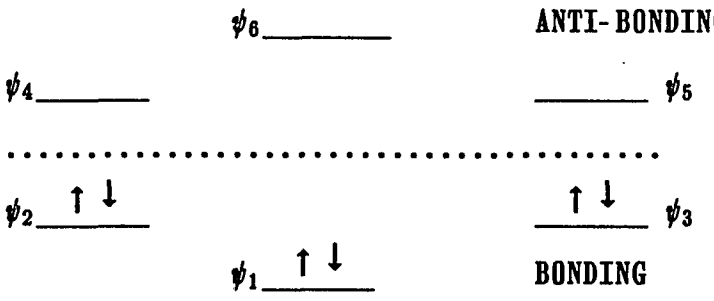

The six π - electrons in benzene are distributed with two in each of the three bonding MO's. Thus, if one is removed to form Bz^+ in donor action, the bonding is weakened. The lowest unfilled π

- orbital in Figure II.A.2.1 is antibonding, thus if an electron is added to form Bz^- in acceptor action, the bonding is weakened relative to neutral benzene. It is interesting and informative to compare benzene, a π system, with that of pyridine in the formation of a charge transfer complex. Pyridine has two sp^2 electrons available for donor action. Therefore pyridine may act as an increvalent donor by the action of the non - bonding electrons. This has important implications on the stability as well as the topography of its complex. Thus iodine forms a complex collinear with the nitrogen heteroatom of pyridine (4) whereas in benzene the complex is along the C_6 axis (5).

II.B.1 THE ELECTRONIC ABSORPTION SPECTRUM

It is not difficult to realize why electronic spectroscopy has been so popular in the study of charge transfer complexation. Both the theory of electronic excitation and the instrumentation necessary for its precise observation has been well established before the theory of charge transfer was developed. The occurrence of absorption bands, usually in the visible region, was ideal for studies by electronic spectroscopy. A survey of the vast amount of literature reveals that the theory of charge transfer complexation developed from a need to explain the appearance of the new absorption band rather than from a need to explain complexing itself. It is therefore appropriate to detail the theoretical aspects of what is known as the charge transfer transition.

According to theory (6) the transition of an electron from a donor to acceptor is expected to cause an intense absorption corresponding to the transition $\Psi_e \leftarrow \Psi_n$ which represents the wavefunctions as defined by equation II.A.1.1 and II.A.1.3. It should be emphasized that the two wavefunctions arise from interaction between two separate moieties which fulfill the roles of the acceptor and the donor. The transition requires the participation of both a donor and acceptor and this can serve as a means of identifying a charge transfer complex. Therefore, the term charge transfer transition has been used to distinguish those type of absorption band due to an intramolecular transition

of an electron from a ground state to a higher energy molecular orbital. It is advantageous at this point to consider simple molecular orbital theory to better visualize the transition.

Figure II.B.1.1: Molecular orbital diagram representing the transfer of electron density from the HOMO of donor to LUMO of acceptor

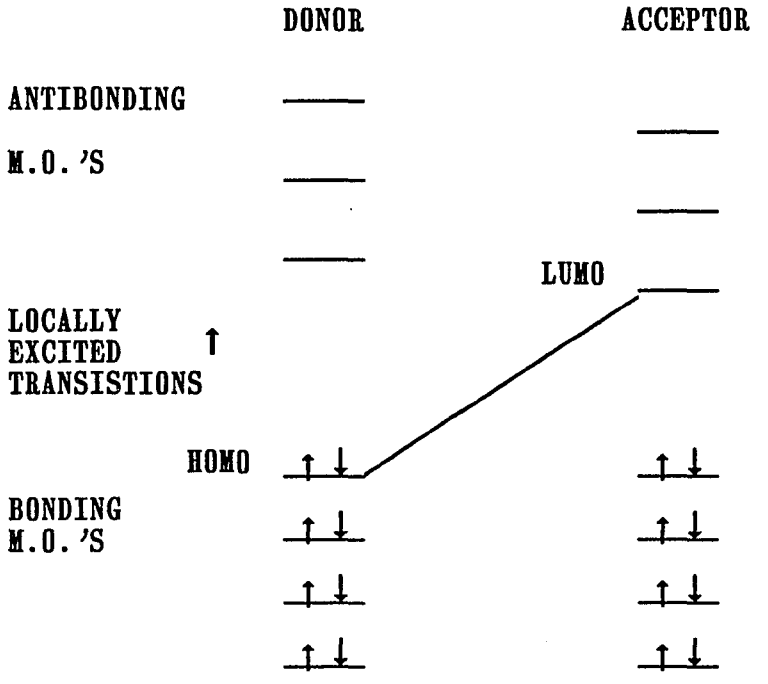

As seen in Figure II.B.1.1, the charge transfer transition is represented as an electron being transferred from the highest occupied molecular orbital (HOMO) of the donor to the lowest unoccupied molecular orbital (LUMO) of the acceptor. The transition can then be considered as arising from the transfer of an electron from a filled orbital of the donor to an empty orbital in the acceptor. The Figure is informative because it pictures the transition which would occur with the absorption of

energy. The ground state would then be a low energy state which has the same geometry and distance between donor and acceptor as in the excited state. It is also seen that the LUMO of the acceptor is of a lower energy state than the LUMO of the donor. This is the essence of a charge transfer transition relative to an absorption of energy by a lone moiety.

II.B.2 EVALUATION OF THE EQUILIBRIUM CONSTANT AND EXTINCTION COEFFICIENT BY ELECTRONIC SPECTROSCOPY

The parameters of interest in the study of charge transfer complexes are the equilibrium (or formation) constant K and the extinction coefficient of the charge transfer complex, ϵ_c. For the case in which donor (D) and acceptor (A) are in a one to one equilibrium with complex (AD) as in:

$$A + D \leftrightharpoons AD$$

Scheme II.B.2.1

the equilibrium constant is expressed as:

$$K = \frac{[AD]}{([A]_0 - [AD])([D]_0 - [AD])} \qquad \text{II.B.2.1}$$

where [AD] is the concentration of the complex and A and D represent acceptor and donor moieties and the subscripts 'o' represent initial concentrations in units of mole/liter. In the case of a one to one complex, equation II.B.2.1 can be rearranged to give:

$$\frac{1}{K} = \frac{[A]_0[D]_0}{[AD]} - ([A]_0 + [D]_0) + [AD] \qquad \text{II.B.2.2}$$

The first application of the above general equation toward evaluation of the equilibrium constant and extinction coefficient in a charge transfer system was presented by Benesi and Hildebrand (7). Their publication resulted in an influx of

articles dealing with both experimental and theoretical aspects of charge transfer complexation. The expressions used to obtain the parameters are detailed below.

The absorption of a species in solution is given by Beer's law

$$\text{Abs} = l\epsilon_c C \qquad \text{II.B.2.3}$$

where l is the optical path length and C the concentration. Equation II.B.2.3 may be rewritten in terms of the concentration of the complex

$$[AD] = \text{Abs}/\epsilon_c l \qquad \text{II.B.2.4}$$

Experimental conditions are chosen such that the concentration of the complex in equation II.B.2.2 is small relative to $[A]_0 + [D]_0$. This is assured by setting the condition that $[D]_0 >> [A]_0$ or $[A]_0 >> [D]_0$. Under such conditions, the last term in equation II.B.2.2 becomes negligible. Eliminating the term [AD] in the denominator of equation II.B.2.2 by equation II.B.2.4 yields equation II.B.2.5.

$$\frac{[A]_0[D]_0 l}{\text{Abs}([A]_0 + [D]_0)} = \frac{1}{K\epsilon_c([A]_0 + [D]_0)} + \frac{1}{\epsilon_c} \qquad \text{II.B.2.5}$$

If, for example, a large excess of donor is used then equation II.B.2.5 can take the form:

$$\frac{[A]_0 l}{Abs} = \frac{1}{K\epsilon_c [D]_0} + \frac{1}{\epsilon_c} \qquad \text{II.B.2.6}$$

Other conditions necessary in the use of the above equations are that the complex absorbs at a wavelength which no other components absorb and the charge transfer complex has a 1:1 stoicheometry. A linear relation between the left side of equation II.B.2.6 and $1/[D]_0$ is commonly used to verify a 1:1 relation.

Equation II.B.2.6 has been criticized (8) for its dependence on extrapolation to higher concentrations. Alternative expressions for equation II.B.2.6 have been given to avoid this type of extrapolation (9):

$$\frac{[A]_0 [D]_0}{Abs} = \frac{1}{K\epsilon_c} + \frac{[D]_0}{\epsilon_c} \qquad \text{II.B.2.7}$$

$$\frac{Abs}{[D]_0} = -K(Abs) + K[A]_0 \epsilon_c \qquad \text{II.B.2.8}$$

Both assume the same experimental conditions as stated above and rely on extrapolation to infinitely dilute solutions.

A method, applicable to systems showing a decrease in the free absorption band corresponding to an increase in a new absorption band of the complexed state, will be discussed. The method depends upon the blue shift of the acceptor, e.g. iodine, which has an intensity proportional to the amount of complex formed. The method is ideal for study of iodine with pyridine

ring systems which show significant perturbation of the free iodine absorption band. The equations

$$\Delta OD \propto [I_2]_0 - [I_2]_c \qquad \text{II.B.2.9a}$$

$$OD_c \propto [I_2]_c \qquad \text{II.B.2.9b}$$

define the relations between absorption of the free and complex states of iodine with added donor at a constant iodine concentration. ΔOD is defined as the difference between the absorption of iodine in solution free of donor and the absorption at the same wavelength after addition of donor. OD_c is defined as the absorption of the complex band and is proportional to the concentration of iodine in the complexed state: $[I_2]_c$. The number of moles of the complex, n, can be expressed as:

$$\frac{\Delta[I_2]_f}{\epsilon_{I_2}} = n \qquad \text{II.B.2.10}$$

where $\Delta OD = \Delta[I_2]_f$, the change in free iodine as a result of complexation and ϵ_{I_2} is the extinction coefficient for iodine. The extinction coefficient of the complex ϵ_c is then:

$$\epsilon_c = \frac{OD_c}{n} \qquad \text{II.B.2.11}$$

from which the concentration of the complex is determined:

$$\frac{OD_c}{\epsilon_c l} = [AD] \qquad \text{II.B.2.12}$$

where OD_c is the absorption of the perturbed band for each increment of donor concentration.

II.C.1 DEVELOPMENT OF NMR IN THE STUDY OF COMPLEX EQUILIBRIA

II.C.1.a BASIC EQUATIONS

For a NMR observable nucleus located on one of the components of Scheme II.B.2.1, a relation between the resonance absorption frequency (hereafter referred to as chemical shift) and the concentrations of the free and the complexed moieties can be established. Let us consider an observable nucleus to be contained in the acceptor molecule. From scheme II.B.2.1, the nucleus is partitioned between two magnetically nonequivalent sites, i.e. the free and the complexed. If the exchange between sites is fast on the NMR time scale (as is usually the case) then the observed chemical shift is actually a weighted average of the site frequencies. This observed chemical shift, $\delta_{obs}{}^{a}$, of a nucleus on the acceptor molecule is thus represented by equation II.C.1.1

$$\delta_{obs}{}^{a} = f_f \delta_f + f_c \delta_c \qquad \text{II.C.1.1}$$

where f_f and f_c are the fraction of free and bound acceptor while δ_f and δ_c are the chemical shift of the nucleus under observation while in the free and the complexed states respectively.

The use of nuclear magnetic resonance as a method to obtain the equilibrium constant and the chemical shift of pure complex (Δ_o) in a recognized charge transfer system of small molecules was first reported by M.W. Hanna and A.C. Ashbough (10). Development of the

equation used to relate the observed chemical shift to the equilibrium constant and shift of pure complex was based on a method previously used to study hydrogen-bonded systems (11). Following such treatments (12), it was shown that

$$\delta_{obs}{}^{a} - \delta_{f}{}^{a} = \frac{[D]_{o}K}{1 + [D]_{o}K} (\delta_{c}{}^{a} - \delta_{f}{}^{a}) \qquad \text{II.C.1.2}$$

where $\delta_{f}{}^{a}$ is the chemical shift of acceptor nucleus in the uncomplexed form and $\delta_{c}{}^{a}$, the chemical shift of accepter nucleus in the pure complex. For $\Delta = \delta_{obs}{}^{a} - \delta_{f}{}^{a}$ and $\Delta_{o} = \delta_{c}{}^{a} - \delta_{f}{}^{a}$, equation II.C.1.2 becomes:

$$\Delta = \frac{\Delta_{o}[D]_{o}K}{1 + [D]_{o}K} \qquad \text{II.C.1.3}$$

which is the NMR 1:1 binding isotherm. Linearization of equation II.C.1.3 is accomplished by taking the reciprocal form:

$$\frac{1}{\Delta} = \frac{1}{\Delta_{o}[D]_{o}K} + \frac{1}{\Delta_{o}} \qquad \text{II.C.1.4}$$

Equation II.C.1.4, which can also be written for the shift of a nucleus in the donor moiety, is analogous to the Benesi-Hildebrand equation for electronic spectroscopy given in section II.B.2. Examination of equation II.C.1.3 reveals that if the denominator is a constant, a plot of Δ vs $[D]_{o}$ will be a straight line with the slope equal to the product ($K \times \Delta_{o}$). Under such conditions the parameters K and Δ_{o} can only be obtained as a product. The conditions in which the denominator of equation II.C.1.3 would be constant are if

$(K \times [D]_0) << 1$, or if $(K \times [D]_0)$ remains unchanged over the concentration range studied. Therefore, in order to obtain values for both K and Δ_0 a plot of Δ vs $[D]_0$ must be a curved line.

Although for some systems the above conditions have been met and values for K have been found consistent with optical data, (13) the use of equation II.C.2.4 has been criticized (14,15). The application of equation II.C.1.4 suffers in that an extrapolation to solutions of high concentration has to be made. Particularly in systems where the association constants are small, the extrapolation may lead to incorrect values of Δ_0 and consequently incorrect values of K. The use of equation II.C.1.5

$$\Delta/[D]_0 = -\Delta K + \Delta_0 K \qquad \text{II.C.1.5}$$

was suggested (15) which is the algebraic form of equation II.C.1.3, corresponding to the equation used in the optical determination described by Foster, Hammick and Wardley (16). In contrast to equation II.C.1.4, a plot of $\Delta/[D]_0$ vs Δ requires extrapolation to an infinitely dilute solution, and the evaluation of K is obtained directly from the slope of the line without recourse to an extrapolation.

The above treatments all assume that the term [AD] in equation II.B.2.1 is negligible compared to $[D]_0$. Therefore, the condition that $[D]_0 >> [A]_0$ must be met. From the relation $[D]_0 = [D] + C_c$ and $C_c = K[A][D]$ equation II.C.1.6 can be obtained

$$[D]_o = [D](1 + K[A]) \qquad \text{II.C.1.6}$$

Assuming $[D] = [D]_o$ is therefore essentially the same as assuming $K[A] \ll 1$ (17). When the condition can not be met, such as when K is large or the excess component is not very soluble, then the term for the concentration of complex must be considered. It then becomes necessary to use an iterative procedure to calculate K and Δ_o (18).

The observed chemical shift can be expressed by equation II.C.1.7 (19)

$$\delta_{obs}{}^a = \left[\frac{[A]_o - [AD]}{[A]_o}\right]\delta_f^a + \frac{[AD]}{[A]_o}\,\delta_c^a \qquad \text{II.C.1.7}$$

where $[A]_o$ is the initial amount of species containing the nuclei under observation. Solving equation II.C.1.7 in terms of the concentration of complex yields equation II.C.1.8

$$[AD] = \frac{\delta_{obs} - \delta_f^a}{\delta_c^a - \delta_f^a}\,[A]_o \qquad \text{II.C.1.8}$$

Equation II.B.2.1 can be rearranged to give

$$K[D]_o[A]_o - K[AD]([D]_o + [A]_o - [AD]) = [AD] \qquad \text{II.C.1.9}$$

From equations II.C.1.8 and II.C.1.9, equation II.C.1.10 is obtained

$$\frac{[A]_o}{\Delta} = \frac{1}{\delta_c^a - \delta_f^a}([D]_o + [A]_o - [AD]) + \frac{1}{K(\delta_c^a - \delta_f^a)} \qquad \text{II.C.1.10}$$

The above equation can be written so that the nuclei being observed is either the donor or acceptor. The two unknowns, [AD] and δ_c^a, are then determined by successive approximations which conclude when $[A]_o/\Delta$ vs $[A]_o + [D]_o - [AD]$ for two successive cycles yield essentially identical convergent values for the slope. K is calculated from the limiting slope and intercept values. δ_c^a, and thus Δ_o is obtained from the final slope. The technique has been found to be successful when $[A]_o$ and $[D]_o$ are comparable in concentration (20). Difficulties with very strong complexes have been reported (21). The reason for unreliable values of K with strong interactions were given in terms of hydrogen-bonding systems. K for a strong hydrogen-bond system was found very sensitive to small changes in the intercept value of the final regression line. Other complicating factors are that NMR chemical shifts of a proton in a hydrogen-bond is dependent on the concentration of the proton acceptor and that most proton donors show a tendency to self associate and to form other then 1:1 complexes with the acceptor (22).

An additional expression for graphical determination of K and Δ_o is as follows. Taking the reciprocal of equation II.B.2.1 allows the equilibrium constant to be expressed as equation II.C.1.11

$$1/K = ([A]_o[D]_o/[AD]) - ([A]_o+[D]_o) + [AD] \qquad \text{II.C.1.11}$$

When the sum of the initial concentrations of donor and accepter are large enough that the complex concentration is small by comparison, then the last term of equation II.C.1.11 can be dropped. Rearranging

equation II.C.1.8 after making the usual substitutions with Δ and Δ_o results in equation II.C.1.12

$$[A]_o + [D]_o = ([A]_o\Delta_o)/\Delta - 1/K \qquad \text{II.C.1.12}$$

The above equation was written such that a nucleus on the donor moiety is being observed. Equation II.C.1.12 has the advantage of extrapolation to dilute solutions (as does equation II.C.1.5) and both the parameters Δ_o and K can be determined directly. Another less obvious advantage of equation II.C.1.12 is the dependence of the ordinate on both donor and accepter concentrations. This is important if addition of one to the other causes the constant component to change by affecting the total weight or volume of the solution. Obviously, mole fraction units can not be used in application of equation II.C.1.12.

II.C.1.b ADDITIONAL UNSPECIFIC SHIELDING

When a nucleus within the acceptor molecule is being observed for the evaluation of the equilibrium constant (K) and chemical shift of the pure complex, Δ_0, it is required that the values δ_f^a and δ_c^a remain constant in the presence of donor even when the donor is in large excess. Because the of need for maximum overlap to occur between the highest occupied donor orbital and the lowest vacant acceptor orbital, unfavorable topographic arrangement of the colliding molecules will result in unsuccessful collisions (23). Additional unspecific shielding (AUS) is the net result of unsuccessful collisions on the

observed chemical shift of the acceptor in the free and complexed states.

Evaluation of AUS can be made based on equation I.C.1.13(24).

$$\frac{\Delta - a[D]_0}{[D]_0} = - K(\Delta - a[D]_0) + \text{constant} \qquad \text{II.C.1.13}$$

The above equation was derived based on equation II.C.1.5 where a is the AUS coefficient. For a plot of the left side term vs $(\Delta - a[D]_0)$ the constant term in equation II.C.1.13 (intercept) is an approximation of the product $(K \times \Delta_0)$. The term Δ_0 can not be derived by this treatment. The value of a depends on the geometric position of the observed nucleus relative to the position of the complexing species in a complex. The relative value of a will increase if the observed nuclei can be exposed to collisions with a complexing moiety. A nucleus less exposed to collisions when complexed will need less correction, resulting in a lower value for a. In complexes of 1,3,5-triacetylbenzene with benzene, the value for a was found to be appreciably greater for the acetyl protons than that of the aromatic protons (24). This result was attributed to exposed position of the acetyl protons in the complex relative to the aromatic protons.

II.C.1.c SATURATION FRACTION

Application of spectroscopy to the evaluation of formation parameters usually involves the titration of a dilute component at fixed concentration $[P]_0$ by a second component with total

concentration $[X]_0$. The formation constant is defined by the mass law expression of equation II.C.1.14

$$[PX] = K[P][X] = K([P]_0 - [PX])([X]_0 - [PX]) \qquad \text{II.C.1.14}$$

and the saturation fraction, s, is given by equation II.C.1.15

$$s \equiv [PX]/[P]_0 = K[X]/(1 + K[X]) \qquad \text{II.C.1.15}$$

where the species without subscript are equilibrium concentrations and s is $0 \leq s \leq 1$ (25). When the concentration of the free (unbound) excess component approaches the concentration of complex to within the same order of magnitude, the substitution $[X] = [X]_0 - [PX]$ is required. This has been addressed for evaluation of the parameters in electronic (26) and NMR (18) spectroscopy. The usual experimental condition is arranged so that a large excess of one component allows for the assumption that $[X] \simeq [X]_0$. This approximation leads to a specific error given by equation II.C.1.16

$$(K' - K)/K = -s[P]_0/[X]_0 \qquad \text{II.C.1.16}$$

where K' is the value calculated using the approximation $[X] \simeq [X]_0$ and K is the value calculated from the exact solution. From equation II.C.1.16 the value of K obtained from the approximation is always smaller then the true K.

The saturation fraction can be related to the concentration of

the complex and the concentration of the dilute component by some parameter which is directly proportional to the concentration of the complex. For electronic spectroscopy Beer's law relates the absorption (A) to the complex concentration by the proportionality constant ϵ, the extinction coefficient. If $A = \epsilon[PX]$ then a maximum absorption (A_{max}) can be expressed as $A_{max} = \epsilon[P]_0$, that is when all of the dilute component is complexed $[P]_0 = [PX]$. Equation II.C.1.17 expresses s in these terms.

$$A/A_{max} = A/\epsilon[P]_0 = [PX]/[P]_0 \equiv s \qquad \text{II.C.1.17}$$

Spectroscopic treatment for evaluation of K and ϵ was derived from equations II.C.1.15 and II.C.1.17. For the case of NMR spectroscopy, the observed chemical shift δ is proportional to the ratio of PX to P and the proportionality constant is δ_0 as seen in equation II.C.1.18.

$$\delta = \delta_0[PX]/[P]_0 \qquad \delta/\delta_0 \equiv s \qquad \text{II.C.1.18}$$

Combination of equations II.C.1.15 and II.C.1.18 yield equation II.C.1.4.

In determining the range of s which would minimize the error, equations II.C.1.19 and II.C.1.20 are considered.

$$\frac{\Delta K}{K} \geq \Delta s\left[\frac{1}{s^2} + \frac{1}{(1-s)^2}\right]^{\frac{1}{2}} \qquad \text{II.C.1.19}$$

$$\Delta\epsilon/\epsilon = \Delta\delta_0/\delta_0 \geq \Delta s\sqrt{2}/s \qquad \text{II.C.1.20}$$

when the relative error, $100\Delta K/K$ and $100\Delta\epsilon/\epsilon = 100\Delta\delta_0/\delta_0$, given by the above equations are plotted as a function of s the minimum error in ϵ and δ_0 are obtained when the concentration of complex is maximized ($s = 1$). For K the most accurate values are obtained when s is between 0.2 and 0.8. Since K is linked to ϵ and δ_0 the best data should be obtained when $0.2 \leq s \leq 0.8$.

II.C.2 SOLID STATE NUCLEAR MAGNETIC RESONANCE

Charge - transfer systems have been studied primarily by electronic spectroscopy and later by proton NMR spectroscopy. Through advancements in theory and instrumentation the study of these complexes by NMR in the solid state was made possible. The technique of solid state NMR has been applied to the study of the complex with tetracyanoethylene (TCNE) as the acceptor with hexamethylbenzene as the donor (27). The one to one complex was isolated as crystalline material in which the six aromatic carbons were equivalent and gave one sharp signal. The methyl carbons were also equivalent giving one sharp signal. The purpose of their work was to investigate changes in the isotropic chemical shift values in the aromatic donor carbons. Topographic arrangements of benzoid π - type donors and TCNE have been well defined. It is known that the plane of the TCNE molecule lies above the plane of the benzene ring. The geometry of this complex was expected to be influenced by the replacement of a carbon with a nitrogen heteroatom in the ring. It is of interest to study the complexes of TCNE with pyridine ring systems of the polymers poly(2 - vinylpyridine) and poly(4 - vinylpyridine). Polymers play an important role in contemporary science, including engineering materials and semi - conductors. The charge transfer complex of I_2 with P2VP is currently used in the lithium battery, an important new technology. Analysis of the geometry of the charge - transfer complex with TCNE would be of great interest. Information obtained may help contribute to an

understanding of complexation in the amorphous solid state. For this work results from solid state NMR studies were complemented by high resolution NMR.

Carbon - 13 resonance absorption may be obtained in the solid state by the technique of combining cross-polarization and magic angle spinning, CP/MAS. Rapid motion of the molecule in solution, which reduces dipolar interactions, chemical shift anisotropy and spin-spin coupling to isotropic averages, is not present in the solid state. In order to overcome this disadvantage, the technique of magic angle spinning (MAS) is used. To overcome the long relaxation times of the ^{13}C nuclei in the solid cross-polarization (CP) is used. The two techniques can be coordinated to yield well resolved resonance absorption spectra. Details of the CP/MAS experiment will be given followed by application to the charge transfer system.

The three main contributions to anisotropy in the solid state are dipolar interactions, chemical shift interactions and spin - spin coupling. All three comprise part of the general Hamiltonian. The general Hamiltonian for the interactions experienced by a nucleus is given in equation II.C.2.1

$$H = H_z + H_d + H_{cs} + H_{sc} + H_q \qquad \text{II.C.2.1}$$

Here H_z and H_q represent the Zeeman interaction and quadrupolar interactions respectively The remaining three terms are of

interest and will be discussed further. The Zeeman interaction is a function of the applied magnetic field and an intrinsic part of the experimental condition not under control. Therefore this contribution will not be addressed further.

For a system containing a dilute spin state S (^{13}C spins) and an abundant spin state I (^{1}H spins) only the interactions between I - S spin states are important in observation of the dilute component. Interaction between S - S states are essentially non-existent due to statistical improbability of contact between such states. For such a system the dipolar coupling term to the general Hamiltonian is given in the equation:

$$H_d = H_{is} = \frac{\gamma_i \gamma_s}{r_{is}^3} \hbar^2 \vec{I} \cdot \hat{D} \cdot \vec{S} \qquad \text{II.C.2.2}$$

where γ's are the respective magnetogyric ratios and $\hbar$ Plank's constant divided by 2π. $\vec{I}$ and $\vec{S}$, vector quantities for the interaction between an isolated pair of unlike spins, are related to each other by the dipolar coupling tensor $\hat{D}$. The strength of the interaction depends on the magnetogyric ratios, is independent of the applied field and falls off rapidly with distance. These factors will be important in experimental pulse sequences applied to obtain important information.

The chemical shift interaction is represented by equation II.C.2.3

$$H_{cs} = \gamma_i \hbar \vec{I} \cdot \hat{\sigma} \cdot \vec{H}_0 \qquad \text{II.C.2.3}$$

Here the field strength, $\vec{H}_0$, is related to the spin vector by the shielding tensor, $\hat{\sigma}$. The tensor relates the indirect coupling of nuclei to the static magnetic field by interaction with the electron(s). The spin - spin coupling interaction for spins I and S is represented by the equation:

$$H_{sc} = \vec{I} \cdot \hat{J} \cdot \vec{S} \qquad \text{II.C.2.4}$$

The interaction is 1 - 2 orders of magnitude less then the chemical shift and dipolar interactions.

The above relations show that for a system of dilute nuclear spins the main contribution to broadening are dipolar interactions and chemical shift anisotropy. In the solid sample the former condition can be eliminated by conventional decoupling fields applied at the proton resonance frequency. The chemical shift anisotropy therefore remains the dominant source of line broadening in the solid state. Improvement in resolution by eliminating, as much as possible, this source of line broadening is possible for dilute and abundant spin systems. The spins are related to the applied field by the tensor $\hat{\sigma}$. This tensor is a 3 x 3 matrix represented by the equation

$$\sigma = \begin{bmatrix} \sigma_{11} & \sigma_{12} & \sigma_{13} \\ \sigma_{21} & \sigma_{22} & \sigma_{23} \\ \sigma_{31} & \sigma_{32} & \sigma_{33} \end{bmatrix} \qquad \text{II.C.2.5}$$

For a coordinate system with the applied field H_0 lies along the z axis, conversion to a diagonal form of the above matrix yields the principle elements σ_{11}, σ_{22} and σ_{33}. In a polycrystalline sample the chemical shift consist of a dispersion of orientation where each spin state has direction defined by angles relative to the principle axis. The chemical shift tensor element which describes the interaction between $\vec{I}$ and $\vec{H}_0$ of equation II.C.2.4 is given in equation II.C.2.6

$$\sigma = \sigma_{iso} + (8/2)(3\cos^2\theta - 1) - (\delta\eta/4)\sin^2\theta(e^{i2\theta} + e^{-i2\theta}) \quad \text{II.C.2.6}$$

where

$$\sigma_{iso} = (1/3)(\sigma_{xx} + \sigma_{yy} + \sigma_{zz}) \quad \text{II.C.2.6a}$$

$$\delta = (2/3)\sigma_{zz} - 1/3(\sigma_{xx} + \sigma_{yy}) \quad \text{II.C.2.6b}$$

$$\eta = 3(\sigma_{yy} \quad \sigma_{xx})/(2\sigma_{zz} - \sigma_{yy} - \sigma_{xx}) \quad \text{II.C.2.6c}$$

δ is referred to as the shielding anisotropy and η is the shielding asymmetry factor. These latter terms give rise to the broad lines in solid state NMR. They represent instantaneous spin direction for all possible orientations. These terms can be shown to be dependent upon the term $(3\cos^2\beta - 1)$. When the angle β is chosen so that this term vanishes then

$$\sigma = \sigma_{iso} \quad \text{II.C.2.7}$$

The angle which satisfies equation II.C.2.7 is termed the magic angle. The sample is spun around an axis inclined at β (55°44'', the magic angle) relative to H_0, the laboratory field.

The technique of magic angle spinning does not reduce anisotropy to the isotropic value for powder samples because the anisotropy is on the order of 10^5 Hz whereas spinning rates commonly obtained are on the order of kHz. MAS alone is not entirely effective for observation of ^{13}C nuclei in solids because of long relaxations. A technique which enhances S/N and makes observation of the resonance absorption practical is cross - polarization.

The method of cross - polarization (CP) involves a polarization transfer of magnetization from a source (^1H nuclei) with a low spin temperature (I spins) to a nuclear sink (^{13}C nuclei) of high spin temperature (S spins). The technique of spin - lock polarization transfer was applied in which simultaneous rf irradiation of I and S spins bring the two spin systems in contact. The two systems are in thermodynamic equilibrium when the magnitudes of the spin locking fields for the I and S spins satisfy the Hartmann - Hahn condition:

$$\gamma_i I_{slf} = \gamma_s S_{slf} \qquad \text{II.C.2.8}$$

where γ represent the gyromagnetic ratio for the respective spins and I and S are spin locking fields for each species of nuclei. In the usual case I refers to ^1H and S refers to ^{13}C and the ratio of γ_i/γ_s is approximately 4. In order to satisfy equation II.C.2.8 the ^{13}C locking field must be 4 times that of the ^1H locking field. Under such conditions the energy of the spin

states are identical for both types of spins. The dilute spin states adopt the more favorable spin distribution of the abundant spin states as equilibrium is established. The entire pulse sequence may be repeated within a timescale relative to the proton relaxation and not the much longer ^{13}C relaxation.

A typical CP sequence involves polarization of the ^{1}H spins along the y' axis of the rotating frame followed by an on - resonance pulse applied to the ^{13}C spins in order to orient the spins along the y' axis. When the Hartmann - Hahn condition is satisfied, polarization of the (cold) ^{1}H spins with the (hot) ^{13}C spins takes place. The time in which the two states are allowed to equilibrate is the contact time, T_{ct}. After cross - polarization the ^{13}C resonance absorption is recorded during heteronuclear decoupling. Therefore, the effectiveness of the CP technique depends on the dipolar coupling of the carbon nuclei to the proton nuclei. This interaction, according to equation II.C.2.2, depends on the negative third power, r^{-3} of distance. Further, evolution of the ^{13}C resonance absorption is dependent upon the proton $T_1\rho$. These conditions manifest themselves as a maximum value of T_{ct} and a spatial dependency of ^{1}H spins to ^{13}C spins. ^{13}C nuclei which are further away from the proton 'pool' of spin states will not be observed if the contact time is lengthened because of decay of the 'cold' ^{1}H spin states by a $T_1\rho$ process with the lattice (spin - lattice relaxation). Non - protonated carbons can not be observed under the conditions of a CP/MAS experiment if the carbons are not within close spacial

proximity to the proton spin states. The substantial difference of the effect of the dipolar interaction on a carbon attached to a proton (r ~ 1.1 Å) and with carbons with protons only on nearest neighbors (r ~ 2.0 Å) allows differentiation of the two types of carbons possible. This is achieved by inserting a delay after evolution of the ^{13}C spin states during the CP period.

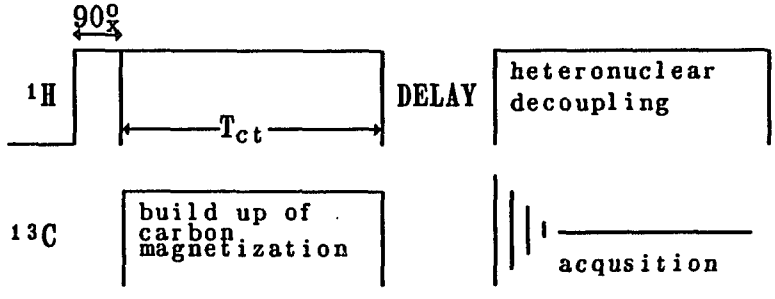

FIGURE II.C.2.1: Basic pulse sequence

This is a basic pulse sequence. The delay is eliminated in a typical cross - polarization experiment. 90°_{x} represents a $\pi/2$ pulse along the X' axis of the rotating frame which orients the ^{1}H magnetization along the Y' axis. A ^{13}C on resonance pulse orient the ^{13}C spins along the Y' axis. When the equality of II.C.2.8 is satisfied as described above, the spin states equlibrate whereby the dilute spins adopt the more favorable spin distribution of the abundant spins.

There are three different experiments described in Figure II.C.2.1. The first is the cross - polarization sequence usually associated with magic angle spinning in which the delay is removed. The second can be a study of the contact time

dependency upon carbon magnetization. $T_1\rho(H)$ may be obtained as a function of contact time due to the carbon signal's dependency upon proton magnetization. The carbon absorption intensity is maximized at a certain contact time and falls off as spin - lattice processes begin to dominate as described above. A third experiment involves the introduction of a delay between the build - up of ^{13}C magnetization during cross - polarization and data acquisition with decoupling (28,29). During the delay no radio frequency is applied (the ^{1}H locking field is eliminated) and the ^{13}C spins are allowed to precess in their local ^{1}H dipolar fields. The time for a polarized carbon nucleus to loose its magnetization depends upon the magnitude of the dipolar coupling. The carbon spins which are strongly associated with the attached proton dephase quickly in the y' axis (spin - spin diffusion). All three types of experiments were used successfully in the present work to investigate the charge transfer system.

III EXPERIMENTAL

III.1 MATERIALS

All solvents were purchased as anhydrous materials of the highest available purity. Further purification involved refluxing over appropriate drying agents and redistillation. The first and last portions of the distillate were discarded, using only the middle portion. Solvent were stored in sealed deep - red ground glass reagent bottles over freshly activated molecular sieves. Deuterated dimethylsulfoxide (DMSO-d_6) was purchased as 99.9% deuterated product. The solvent was stored over molecular sieves for a few days before use without further purification.

Tetracyanoethylene was purchased from Aldrich Chemical Co. and resublimed under reduced pressure at least three times. The crystalline material was sealed and stored in a desiccator with drierite and phosphorus pentoxide. Iodine was purchased from Aldrich chem. co. with 99.999% purity and used without further purification. Iodine of lower purity (99.8%) was resublimed at least twice before use. Polymers were reprecipitated from methylene chloride solutions by heptanes. Only the first fraction to precipitate from solution was isolated and reprecipitated at least twice. The wet polymer was dried at ca. 80°C under reduced pressure overnight. Liquid donors were distilled over appropriate drying agents and the middle portion of the distillate redistilled again. The liquid was stored in a

sealed bottle over molecular sieves inside a desiccator.

III.2 PROCEDURES

Solution to be studied by UV - Vis spectroscopy were prepared by mixing the required amount of stock solutions of donor and acceptor. All solid starting materials were weighed directly. Liquid materials were weighed by delivering the required amount, estimated by density, into a small vessel and taking the difference. Solvent would then be used to transfer the liquid to a volumetric flask. Readings were taken at room temperature in either 0.1, 0.2 or 10 mm quartz cells.

For NMR solutions solid TCNE was weighed directly to which stock solution of donor in deuterated solvent was added. The total weight was then recorded and concentration units reported in moles/KG solution. Units based on weight were used because the total volume was shown to change upon addition of a constant amount of donor stock solution to various amounts of solid TCNE. Samples for observation in the solid state were prepared by mixing a 1:1 mole ratio of TCNE and polymer as solids. The solid was thoroughly mixed by mortar and pestle followed by introduction of methylene chloride to form a slurry. The solvent was removed at room temperature under vacuum with occasional mixing. The resultant fine powder was further mixed with mortar and pestle. The same method was applied to solid samples for use in electron spin resonance spectroscopy.

III.3 INSTRUMENTATION

Nuclear magnetic resonance spectra were recorded at a proton resonance frequency of 200 MHz with an IBM WP - 200SY spectrometer. Solutions were run at 303° K and the temperature controlled by a Bruker Instruments B - VT 1000 unit. The spectrometer was equipped with a solid accessory for cross polarization and high-powered decoupling. A cylindrical double air bearing MAS probe from Doty Scientific Co. was used with rotors having a sample volume of 0.36 cm^3 made of Al_2O_3. Transients of 2K points each were coadded, zero filled to 4K points, multiplied by a decaying exponential (line broadening of 50 Hz unless otherwise noted) and fourier transformed. Recycle delays of at least 2 s were employed during averaging, in order to permit repolarization of the ^1H spin reservoir as well as to minimize heating. Chemical shift calibration was based on the methyl carbon (31 ppm) of p-di-*tert*-butylbenzene (PDTBB). The $\pi/2$ pulse lengths were determined for each experiment by adjusting the pulse length such that PDTBB intensities are null (180°) and taking half the value. Because the Hartmann-Hahn matching condition had been fulfilled, the ^1H $\pi/2$ and the ^{13}C $\pi/2$ pulse lengths are the same. Typically the $\pi/2$ pulse length was found to be $\sim$ 5 μs. Cross polarization times were varied from 0.2 ms to 10 ms. Delayed decoupling experiments were run with a cross polarization time of 4.2 ms. This value led to strong intensities for the carbons of interest in the CP/MAS experiments. Spinning rates were varied between 2 and 4.7 kHz.

Electron spin resonance measurements were made on a JOEL model JES-Me-3X, X-band, ESR spectrometer (Cranford, N.J.) with a TE_{105} cylindrical dual cavity. Spin density measurements were made against a known quantity of crystalline di-phenylpicrylhydrazyl, DPPH. The quantity of DPPH was determined experimently by measurements of its optical density in benzene, λ_{max} = 519 nm, log ϵ = 4.89. All first derivative curves were doubly integrated by the Wyard method (30). Spin density calculations are based on the assumption of one spin per DPPH molecule.

Electronic absorption spectra were recorded on a Cary 118 double beam scanning spectrometer. A Bio-rad FTS-40 fourier transform infrared spectrometer with a 3240-SPC data station was used for IR absorption spectra of solid samples.

III.4 POLYMER SYNTHESIS

Low Molecular Weight poly(2 - vinylpyridine) (LMW P2VP) was prepared by solution polymerization in toluene with AIBN as the initiator at 70°C for one hour under nitrogen. The concentration of 2 - vinyl pyridine was 2.50 mol/L and AIBN, 0.609 mol/L. The molecular weight as determined by vapor pressure osmometer in toluene is: $\bar{M}_n = 2.65 \times 10^3$. Figure III.4.1 is a GPC curve for this polymer. Isotactic polymer was prepared according to literature (31). A three necked, round bottomed flask (3 L) was equipped with a dropping funnel, mechanical stirrer and a

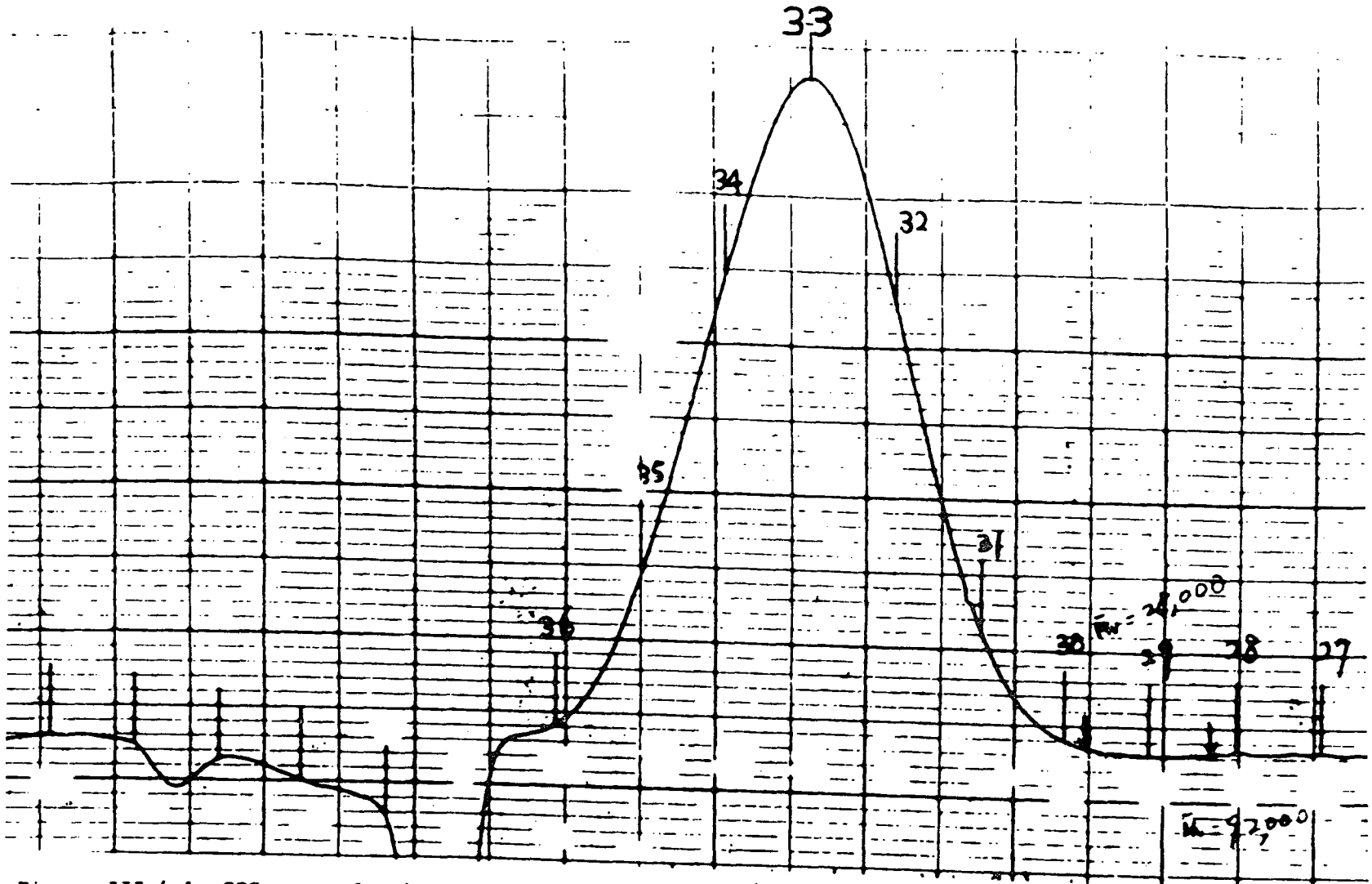

Figure III.4.1: GPC curve for low molecular weight poly(2-vinylpyridine)

condenser capped with a drying tube. The set-up was flame dried by passing prepurified grade nitrogen gas while under vacuum. 2 L of toluene (dried by CaH_2, then redistilled) was added into the flask followed by 40 ml of 3 M phenylmagnesium bromide (Alfa Chem. Co.) injected through a serum stopper into the flask. 375 ml of 2-vinyl pyridine (dried by CaH_2, then vacuum distilled) was added into the solution through a dropping funnel. A small amount of monomer was added each time and the reaction mixture was stirred efficiently by an overhead mechanical stirrer. The entire volume of the monomer was added dropwise with the polymerization system cooled by a water bath. The mixture was stirred for ca. 7 hours. The polymer solution was poured into a 5% hydrochloric acid solution and stirred until the polymer dissolved completely in the aqueous phase. The aqueous solution was added dropwise to a well stirred solution of NH_3 containing NH_4Cl. The polymer precipitated in white flocks, which on standing converted into a semi-solid product. the polymer was redissolved in chloroform and precipitated by a non - solvent. The high tacticity of the polymer is verified by its ^{13}C NMR spectrum (Figure III.4.2). $\bar{M}_w$ is 2.5×10^4 and $\bar{M}_n$ is 1.8×10^4, giving a dispersity of 1.4. Figure III.4.3 shows a GPC trace for this polymer. P2VP standards used for calibration were purchased from Polyscience. Commercially available high molecular weight atactic poly(2-vinylpyridine) was purchased from Aldrich Chem. Co. Its $\bar{M}_w$ is ca. 40×10^3.

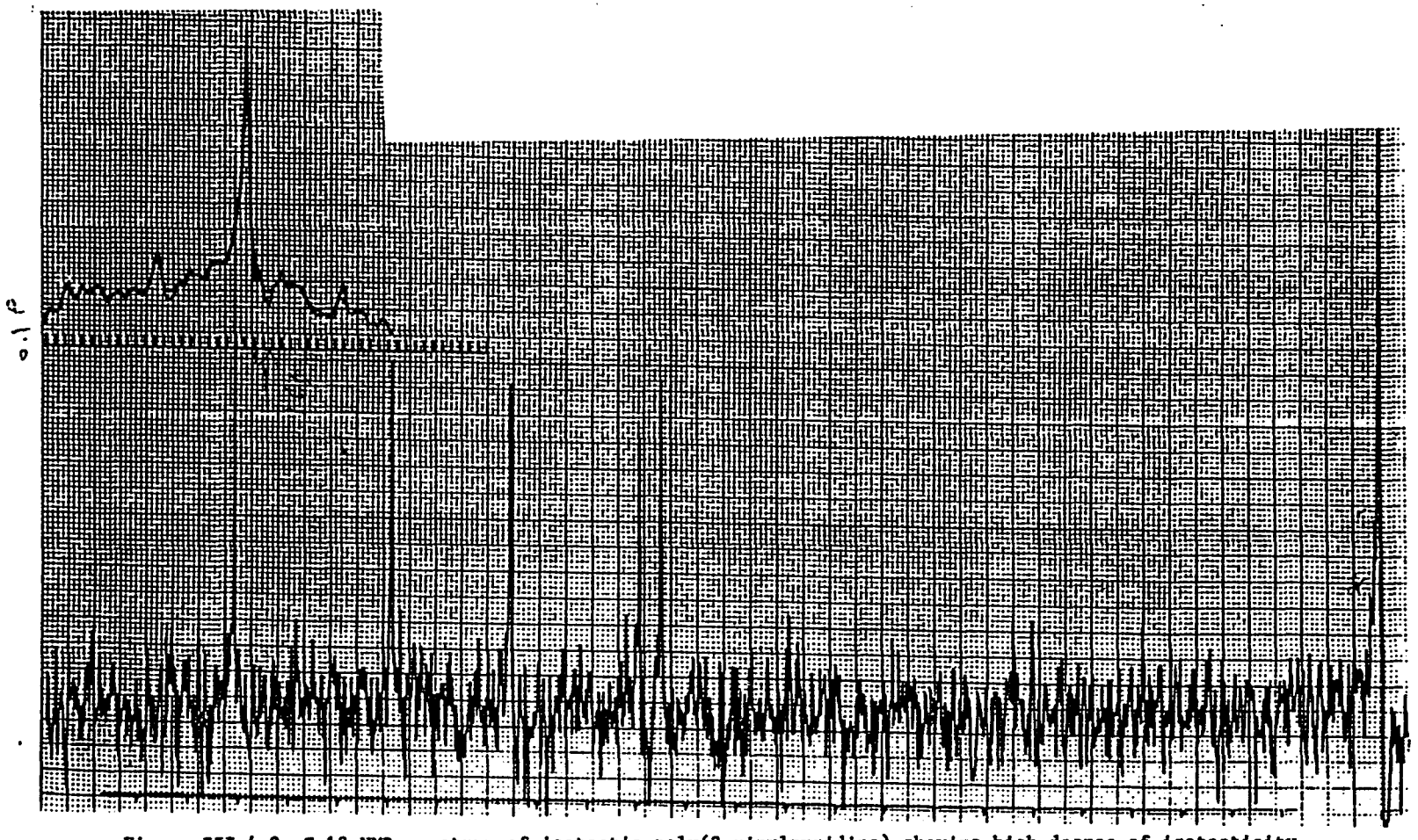

Figure III.4.2: C-13 NMR spectrum of isotactic poly(2-vinylpyridine) showing high degree of isotacticity

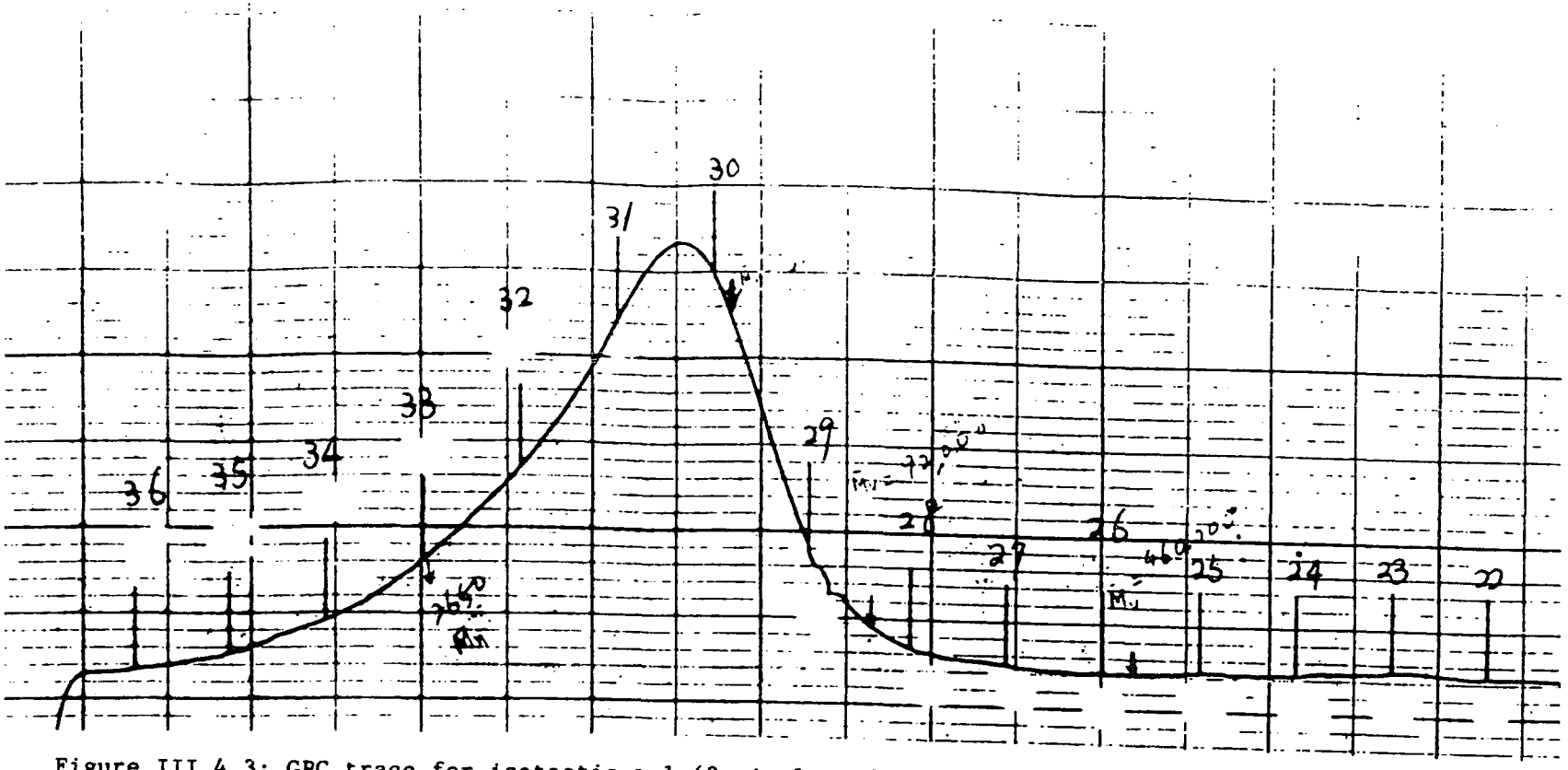

Figure III.4.3: GPC trace for isotactic poly(2-vinylpyridine)

IV RESULTS AND DISCUSSION

IV.A ELECTRONIC ABSORPTION SPECTROSCOPY

For the pyridine - iodine system, extensive study on electronic absorption spectroscopy has been performed. A comparison of pyridine with its polymeric donor, poly(2-vinylpyridine), should be of fundamental interest. This section is concerned with the charge transfer system of iodine and poly(2 - vinylpyridines)(P2VP) plus its analogs in a series of solvents with a gradation of their polarity and ability in acting as a donor in hydrogen bonding.

IV.A.1 POLAR SOLVENT

Ethanol was selected as a polar solvent with a strong tendency to act as a hydrogen bonding donor. The discussion of the absorption spectrum of iodine in ethanol has been documented (32). Solvated iodine, in a non - complexing solvent absorbs at wavelengths longer then 500nm. Iodine dissolved in ethanol absorbs at $\sim$ 440nm. No absorption band was observed at the longer wavelength, indicating all the iodine is complexed with the solvent. An intense absorption occurs at 230nm which was also observed as the charge transfer band of ethanol - iodine in non - polar solvents (33). Absorptions also occur at 358nm (ϵ = 2.5 x 10^4 cm·l/mol) with a corresponding absorption at 284nm (ϵ = 4.5 x 10^4 cm·L/mol) which shows approximately twice the intensity

of the 358nm band. These two bands were attributed to the triiodide ion (34,35) which was identified by absorption bands of triiodide from the dissociation of tetramethylammonium triiodide. The intensities of these bands for iodine in ethanol corresponds to a very low concentration of triiodide. In pyridine as solvent, iodine formed small amounts of triiodide when the iodine concentration is 10^{-3} to 10^{-5} mol/L. The mole fraction of triiodide within this range is increased upon dilution (36). These absorption bands for iodine in ethanol may be explained by the following equilibria:

$$\text{ETOH}\cdot I_2 \leftrightharpoons (\text{ETOH}\cdot I)^+I^- \qquad (1)$$

$$(\text{ETOH}\cdot I)^+I^- \rightleftharpoons (\text{ETOH}\cdot I)^+ + I^- \qquad (2)$$

$$(\text{ETOH}\cdot I)^+ + I^- \overset{I_2}{\rightleftharpoons} \text{ETOH}\cdot I^+ + I_3^- \qquad (3)$$

Scheme IV.A.1.1

Reaction (2), involving the separation of the negative charge I^- from a positive species, should be facilitated by solvents with a strong tendency to act as a donor in hydrogen bonding:

$$(\text{EtOH}\cdot I)^+I^-\cdots H\overset{\delta+}{-}O\overset{\delta-}{-}CH_2\text{-}CH_3.$$

The polymeric donor, P2VP, absorbs in the UV range with a maximum at 262nm. Upon introduction of P2VP to the ethanol solution of iodine the following changes were observed. The absorption band at 440nm is largely eliminated with a corresponding significant loss in intensity of the absorption at 230nm. Both these bands

are ascribed to the outer complex of ethanol and iodine, $ETOH \cdot I_2$. Their simultaneous disappearance is a strong indication that the ring of P2VP interacts more favorably with iodine than ethanol. As the concentration of P2VP is increased the absorption of the triiodide also increases. These results can be explained by the scheme:

$$ETOH \cdot I_2 \overset{P_2VP}{\rightleftharpoons} P_2VP \cdot I_2 + ETOH \quad (1)$$

$$P_2VP \cdot I_2 \rightleftharpoons (P_2VP \cdot I)^+ I^- \quad (2)$$

$$(P_2VP \cdot I)^+ I^- \rightleftharpoons (P_2VP \cdot I)^+ + I^- \quad (3)$$

$$(P_2VP \cdot I)^+ + I^- \overset{I_2}{\rightleftharpoons} (P_2VP \cdot I)^+ + I_3^- \quad (4)$$

Scheme IV.A.1.2

Since the absorption bands of 440nm and 230nm decrease significantly with the introduction of P2VP, the forward reaction in step 1 of Scheme IV.A.1.2 is clearly favored. The absorption in the range of 330 to 410 nm is dominated by triiodide. However, P_2VP - iodine (outer complex) and the inner complex and perhaps the dissociated monoiodide may be formed but their direct observation is precluded by the intense absorption of the triiodide band. The solvent ethanol should facilitate reaction (2) due to hydrogen bonding:

$$(P2VP \cdot I)^+ I^- \cdots H\overset{\delta^+}{\text{---}}O\overset{\delta^-}{\text{---}}CH_2CH_3 .$$

For a system 7.2×10^{-4} mol/L in iodine and 8.9×10^{-4} mol/L in P2VP, about one - half of the iodine are converted to triiodide.

Mulliken (36) proposed the following scheme for iodine dissolved in pyridine:

$$Py + I_2 \leftrightharpoons Py \cdot I_2 \quad (1)$$

$$Py \cdot I_2 \leftrightharpoons (PYI)^+I^- \quad (2)$$

$$(PYI)^+I^- \leftrightharpoons PyI^+ + I^- \quad (3)$$

Scheme IV.A.1.3

The complex $Py \cdot I_2$ was termed an outer complex and $(PYI)^+I^-$, an inner complex. Here pyridine acts both as electron donor and as a polar medium in assisting reactions 2 and 3. Kleinberg (37) studied iodine in pyridine and concluded that inner complex was formed, liberating monoiodide ion which can form triiodide with iodine.

In the system of I_2 in ethanol, pyridine failed to compete with the solvent to form a charge transfer complex. For the system of P2VP - iodine in ethanol the formation of triiodide is clearly indicated by the appearance of the intense 290nm absorption band and decrease in the 230nm absorption band (Figure IV.A.1.1). Therefore, if an equilibrium as described by Scheme IV.A.1.2 exist, an isosbestic point should be observed upon the addition of P2VP to the ethanol - iodine solution. The above figure clearly shows an isosbestic point (245nm) which is where the molar extinction coefficient for the $EtOH \cdot I_2$ complex is equal to one half that of triiodide, i.e. two moles of $EtOH \cdot I_2$ give one mole of triiodide. It should be noted that this 290nm triiodide

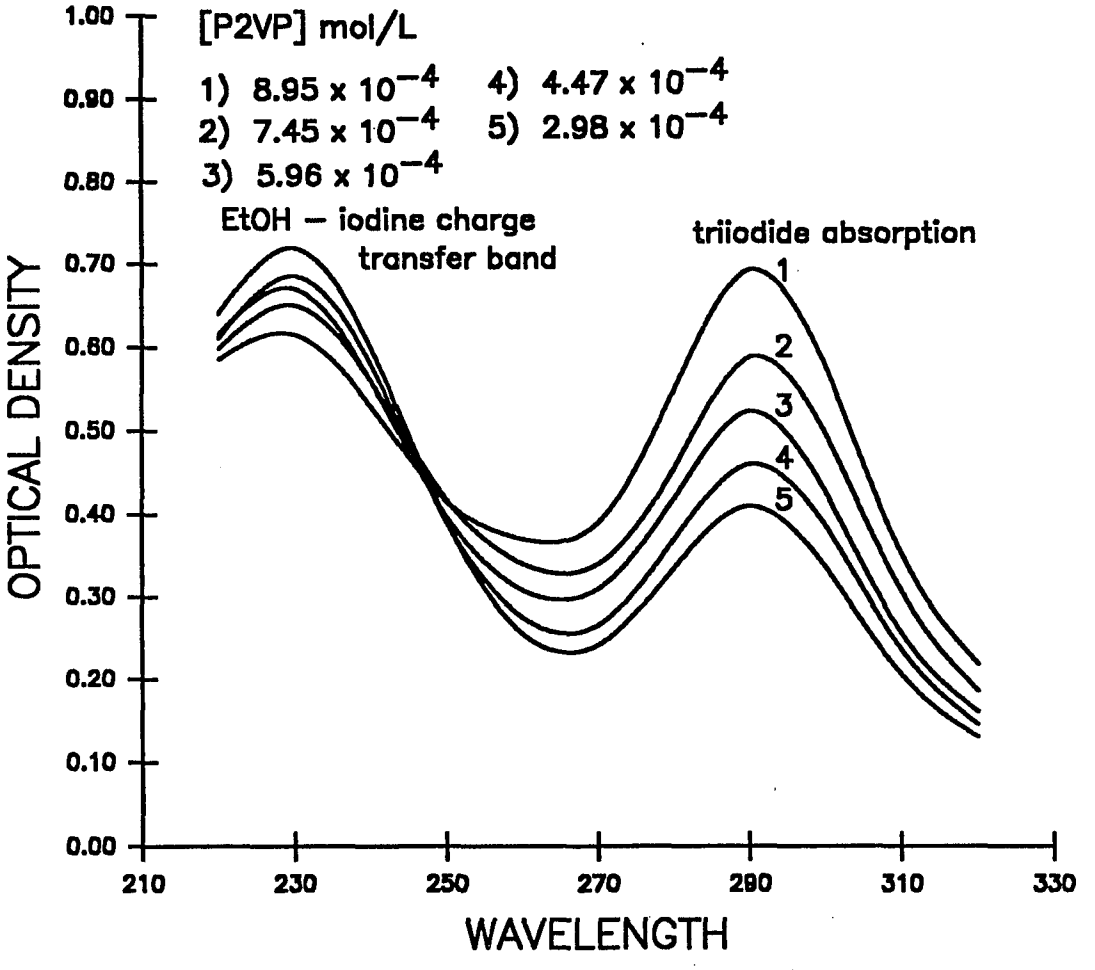

Figure IV.A.1.1: Effect of HMW P2VP on electronic absorption spectra of iodine/ethanol solution

peak is at a wavelength 6nm longer than in the case of triiodide in ethanol formed by the dissociation of tetramethylammonium triiodide. This may be due to the weaker interaction of the pyI^+ species with I_3^- compared to $(C_2H_5)_4N^+$. The absorption at 360 nm attributed also to triiodide exhibits ca. half of the intensity of the 290 nm band as reported in the literature. These observations clearly shows the significant differences between the donor pyridine and its polymer.

IV.A.2 NON - POLAR SOLVENT

In non - polar solvents the various aspects of a polymeric effect can be better demonstrated. Reid and Mulliken (36) have shown that when [Pyridine] >> $[I_2]$ in non - polar solvent the visible absorption band of iodine is shifted to shorter wavelengths with a limiting value of 389 nm. This wavelength limit was observed for the iodine concentration level of 10^{-4} mole/L. A limiting extinction coefficient of 2,120 was found for iodine at these concentrations in pure pyridine. Lowering the iodine concentration from 10^{-4} to 10^{-5} mole/L in pure pyridine caused the absorption maximum to shift to 368 nm. The formal extinction coefficient, based on iodine, rose to a maximum value of 9×10^4 cm·L/mol. This was attributed to triiodide formation. Based on this extinction coefficient they suggested that about half of the iodine remains as bound iodine (ie. $Pyr \cdot I_2$) and about half reacted to form triiodide. Sazkin et al (38) observed the formation of triiodide for PVP and iodine in 1,2 -

dichloroethane. An increase of iodine concentration caused a displacement of the 360 - 365 nm band to longer wavelength of 388 - 395 nm. This observation was not elaborated upon; the study was focused on the conductivity of the solution and its relation to absorption bands of triiodide. A more comprehensive study of a polymer with iodine in non - polar solvent was made by Tomono et al (39). This study was concerned with a polyamine polymer containing aliphatic amines as part of its backbone. By use of model compounds they established the existence of a 1:1 molecular complex with iodine. The monomeric model compounds, unlike the polymer did not give rise to triiodide formation. The study was restricted to low initial iodine concentrations of 10^{-4} to 10^{-5} mole/L which has been shown to favor triiodide formation. They concluded that triiodide formation is accelerated by the polymer due to a "stacking effect" of neighboring groups which set the condition [Donor]>>[I_2] within the local reaction field. They did not comment on the concentration dependency of iodine on the absorption maximum of the perturbed visible band of iodine. This band is of importance in evaluating formation constants between donor - iodine systems and the nature of the concentration dependent shift has not been adequately addressed. The present work will address this phenomenon in the systems involving P2VP polymers and model compounds.

IV.A.2.a CHLOROFORM AS SOLVENT

Equilibrium constants are commonly evaluated by monitoring

the perturbed visible band of iodine. For the present study iodine complexes with several donors were evaluated by this method (Section II.B.2). These systems showed different characteristics for an iodine concentration level of 10^{-3} mol/L. Low molecular weight P2VP shows a more intense absorption at a shorter wavelength compared to pyridine (Figure IV.A.2.1). Compared to HMW P2VP, *i*-P2VP shows a broader and weaker absorption band at a slightly longer wavelength maximum (Figure IV.A.2.2) Table III.B.1 lists values of the equilibrium constants and extinction coefficients in chloroform obtained from quantitative measurement of the donors in solutions of iodine (See section II.B.2).

Table III.B.1: Results obtained for donors with chloroform as solvent

DONOR	K (l/mol)	λ_{max} (nm)	ϵ (cm·L/mol)*
Py	60 ± 1	400	1.9×10^3
LMW P2VP	50 ± 10	370	4.4×10^3
i-P2VP	100 ± 20	368	5.0×10^3
HMW P2VP	93 ± 6	366	1.01×10^4‡

* Formal ϵ based on mole of I_2 reacted

‡ Corrected $\epsilon = 2 \times 10^4$ based on 2 mole I_3^- generated per one mole I_2 reacted

The assumed perturbed iodine absorption band in the polymeric systems is located in the region of the long wavelength absorption for triiodide. Therefore, caution must be taken in direct evaluation of this band as rising from bound iodine only. These slight shifts toward shorter wavelength may be due to the

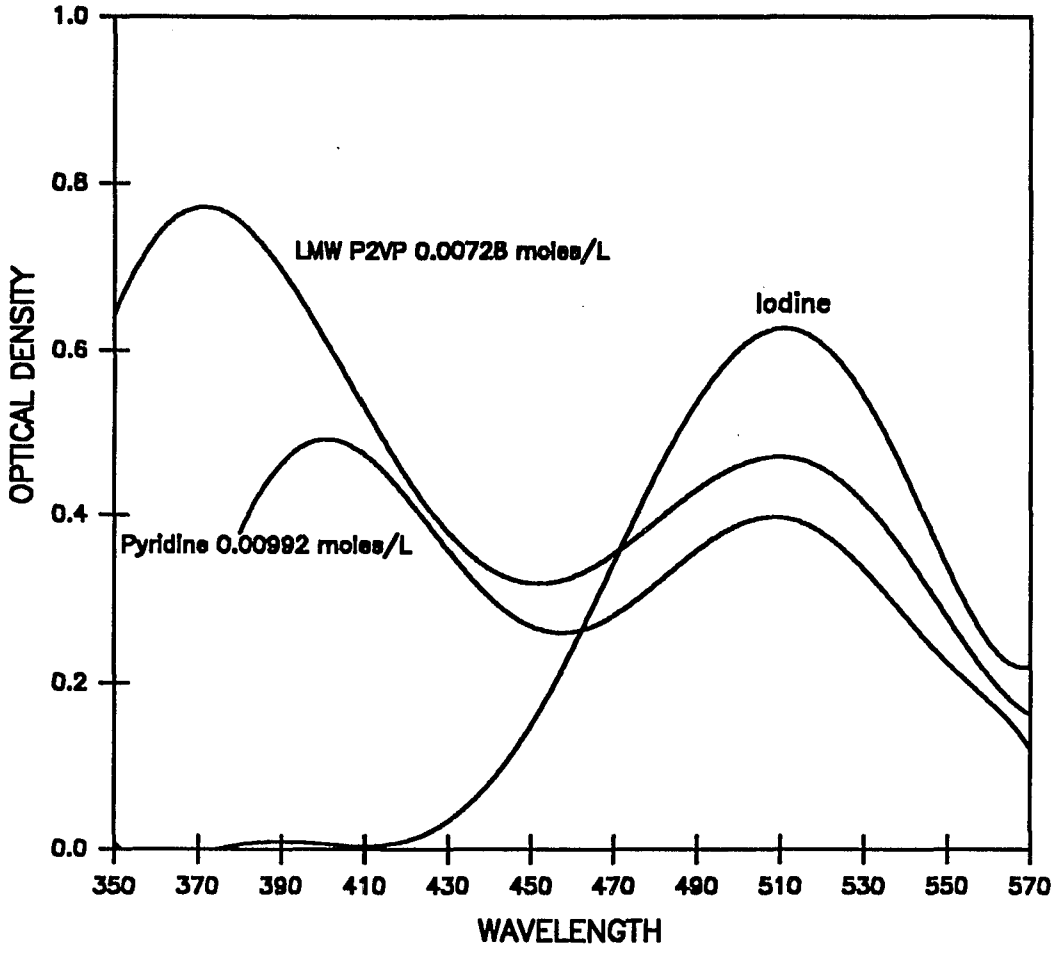

Figure IV.A.2.1: Effect of LMW P2VP and pyridine on electronic absorption spectrum of iodine/chloroform solution

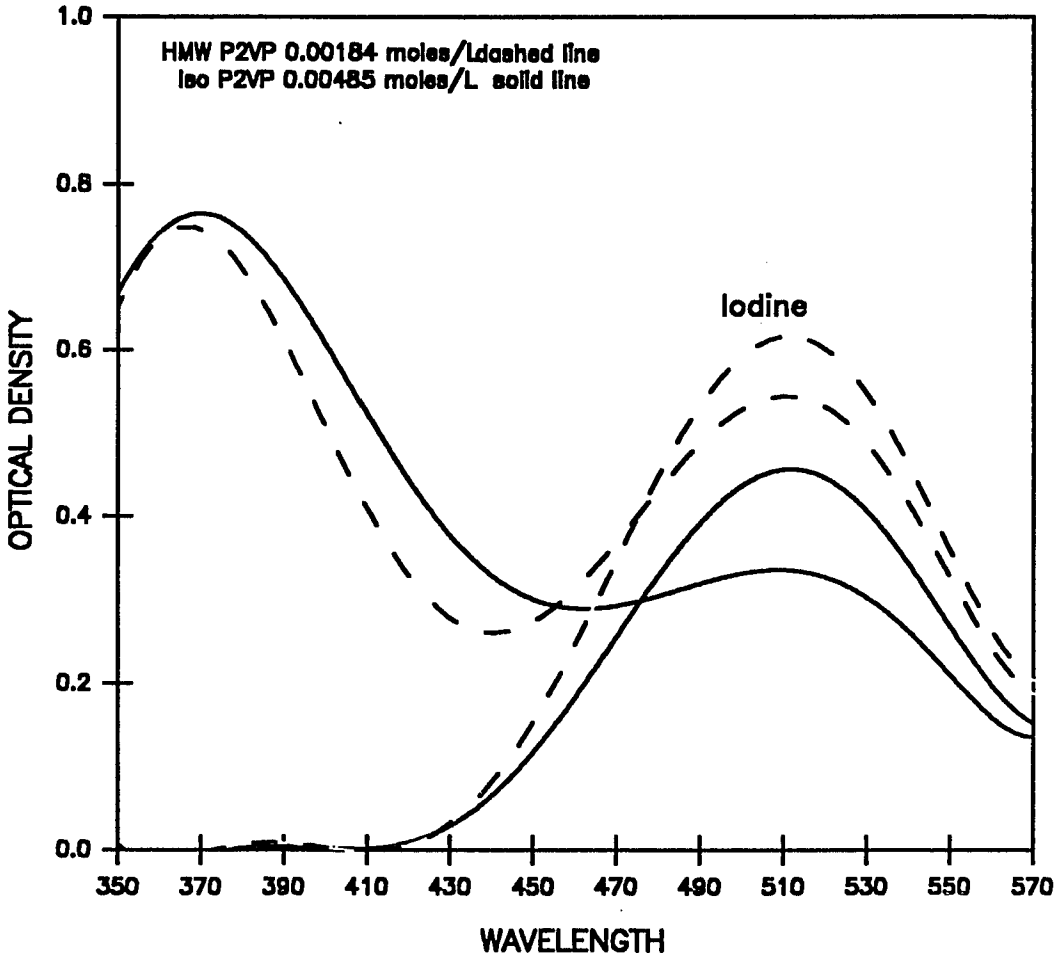

Figure IV.A.2.2: Effect of HMW and i–P2VP on the electronic absorption spectrum of iodine/chloroform solution

formation of strong absorbing triiodide. The extinction coefficient decreases as the extent of blue shift is decreased. The blue shift is an important parameter and an understanding of its origin is vital in interpreting data obtained by its analysis. The reason for a blue shift has been given (40) as follows. The lowest unoccupied molecular orbital of iodine which accepts electron density from the donor is strongly antibonding and therefore large i.e. more extended. Acceptance of electron density into this molecular orbital should considerably increase the effective size of the molecule. When the iodine molecule in its complexed state is excited by visible light absorption, its suddenly swollen size due to charge transfer introduces an exchange repulsion between the acceptor and the donor. The blue shift is a result of the required repulsion energy added to the usual energy of the excited iodine molecule. In the present polymeric systems the blue shift is quite large. Accompanying the large perturbation is an increased extinction coefficient. The extinction coefficient for py·I_2 is ca. 2 x 10^3 cm·L/mol; for I_3^-, 25 x 10^3 cm·L/mol. A molar extinction coefficient above the 2 x 10^3 level is a strong indication of the presence of triiodide. Observations of such large difference of extinction coefficients and λ_{max} (Table III.B.1) indicate the possibility of an inner complex or triiodide existing in equilibrium with the outer complex. Equilibrium constants reported under such conditions may not reflect the true values for the outer complex. It can be concluded that pyridine in ethanol only forms an outer complex with iodine. For the three polymers, triiodide formation

due to the polymeric effect in chloroform is in the descending order of HMW P2VP > Iso P2VP > LMW P2VP.

IV.A.2.b METHYLENE CHLORIDE AS SOLVENT

Methylene chloride, a weaker donor for hydrogen bonding compared to chloroform, shows weak interaction with iodine. The absorption of iodine in the concentration range 10^{-3} to 10^{-5} mol/L has an absorption maximum at 504nm with negligible absorption at shorter wavelengths. Unlike the case in polar solution, upon dilution no triiodide or monoiodide is formed. Introduction of P2VP had a marked effect on the equilibrium of iodine in this solution. The addition of P2VP led to a decrease in intensity of the 504nm band and the appearance of a new absorption band at 364nm. For a constant polymer concentration this absorption shifted from ~364nm to 388nm with increased iodine concentration. The absorption maximum remained relatively constant at ca. 365 nm for the iodine concentration range of 10^{-5} to 10^{-4} moles/L. The greatest change in absorption maximum occurred when iodine concentrations increased from 10^{-4} mol/L to a range of 10^{-3} mol/L. This pattern of change closely resembles the case of iodine in polar solvents. It implies that the polymer, although relatively very dilute compared to solvent, was responsible for the same driving force in the formation of triiodide in polar solvents. The polyamine polymer reported by Tomono et. al. (39) differs from P2VP in that it contains only aliphatic amines which are much stronger bases than the aromatic

amine of P2VP. The polyamine has all nitrogen atoms contained in the backbone while pendent rings of P2VP are subject to more stringent steric requirements. In both cases triiodide formation was observed. Tomono et. al. restricted their concentration of iodine to 10^{-4} moles/L. The formation of triiodide, in the present system, can be decreased if the concentration of iodine is increased. The position of the 366nm triiodide band was seen to shift to a limiting value of 380nm by increasing the iodine concentration to 10^{-3} mol/L in the presence of HMW P2VP. It should be noted that pyridine and iodine when mixed in non - polar solvents did not favor triiodide formation as evident from results of table III.B.1, nor did the substituted pyridines (41) in the same concentration ranges. As will be seen below, iso P2VP also did not favor triiodide formation at low iodine concentrations.

Outer complex coexisting with triiodide in methylene chloride for the HMW P2VP donor is suggested by the following observation. Monitoring charge transfer absorption at 254nm yields important information in regard to the species involved. Figure IV.A.2.3 shows a plot of log of absorbance vs log [P2VP] for HMW P2VP. The slope of the resulting straight line is equal to one, i.e. one pyridine ring per complex. The same results were observed for LMW P2VP and pyridine at the charge transfer absorption band. Treatment of absorptions at 366 and 290nm, the absorption bands for triiodide, yield slopes of 0.5 for the HMW P2VP donor (Figure IV.A.2.4). This implies that half of the

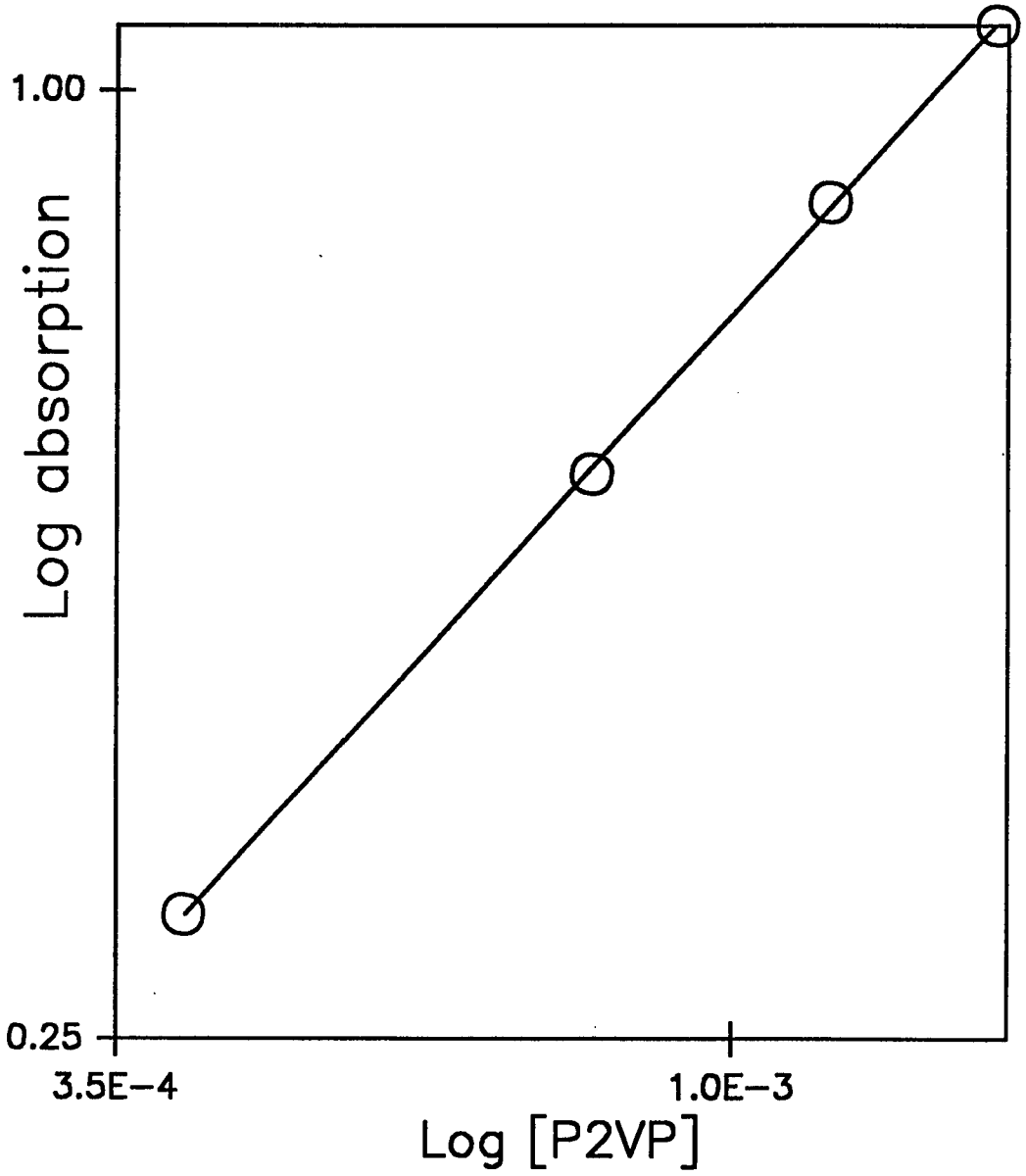

Figure IV.A.2.3: Log absorbtion 254nm vs log [P2VP] for HMW P2VP

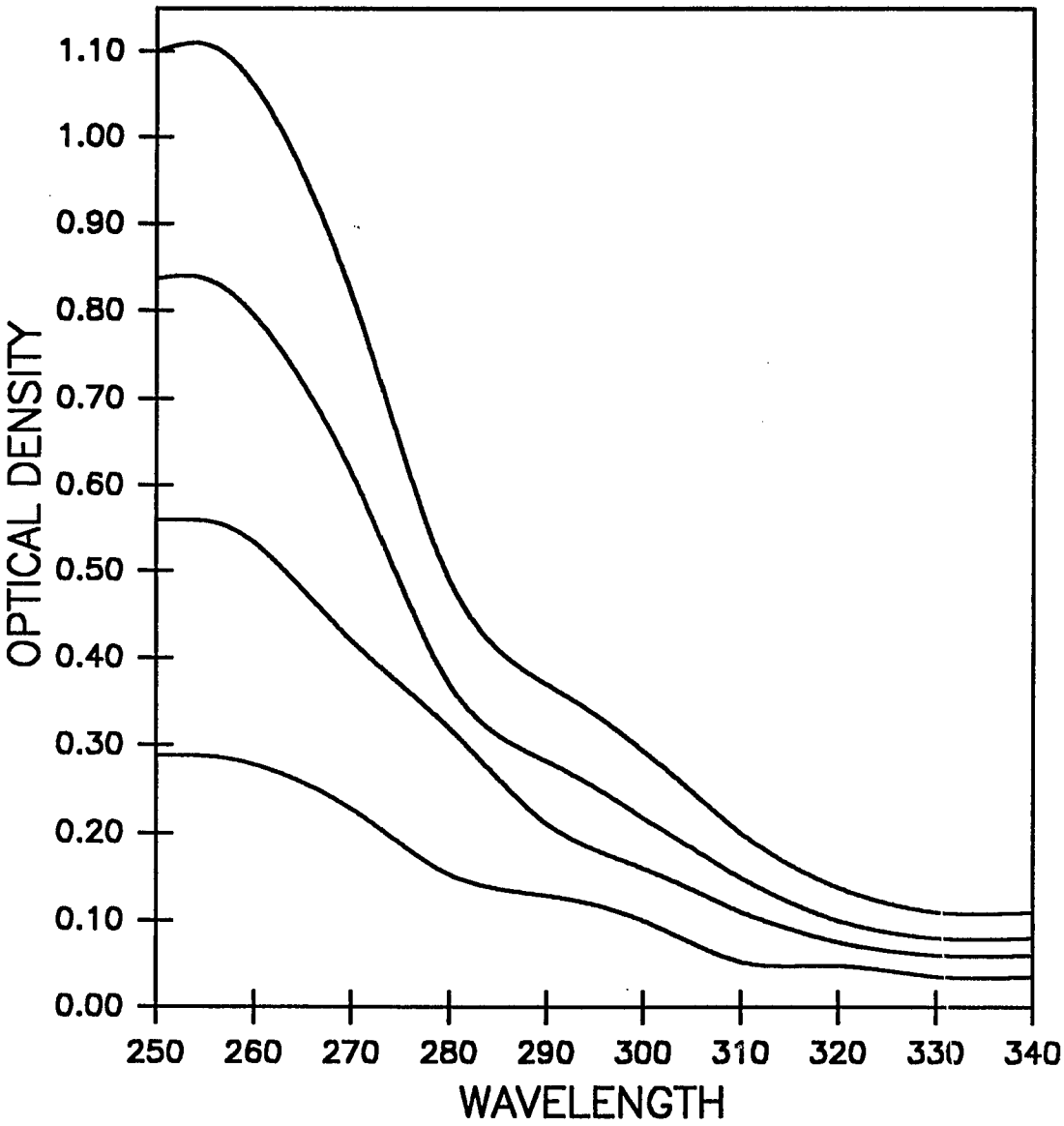

Figure IV.A.2.3a: Absorption curves used to obtain data in figure IV.A.2.3

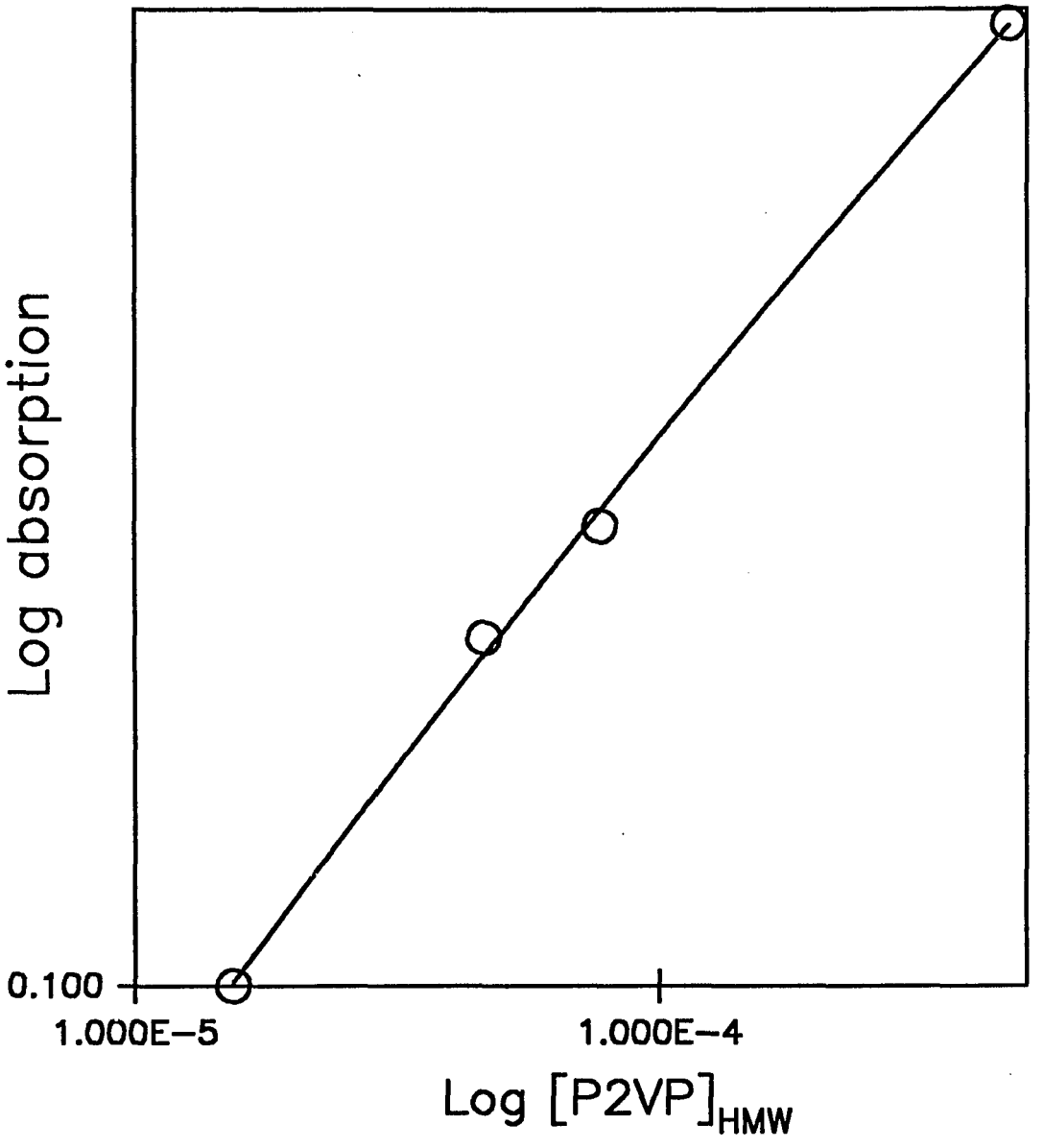

Figure IV.A.2.4: Log absorption 366nm vs log P2VP for HMW P2VP

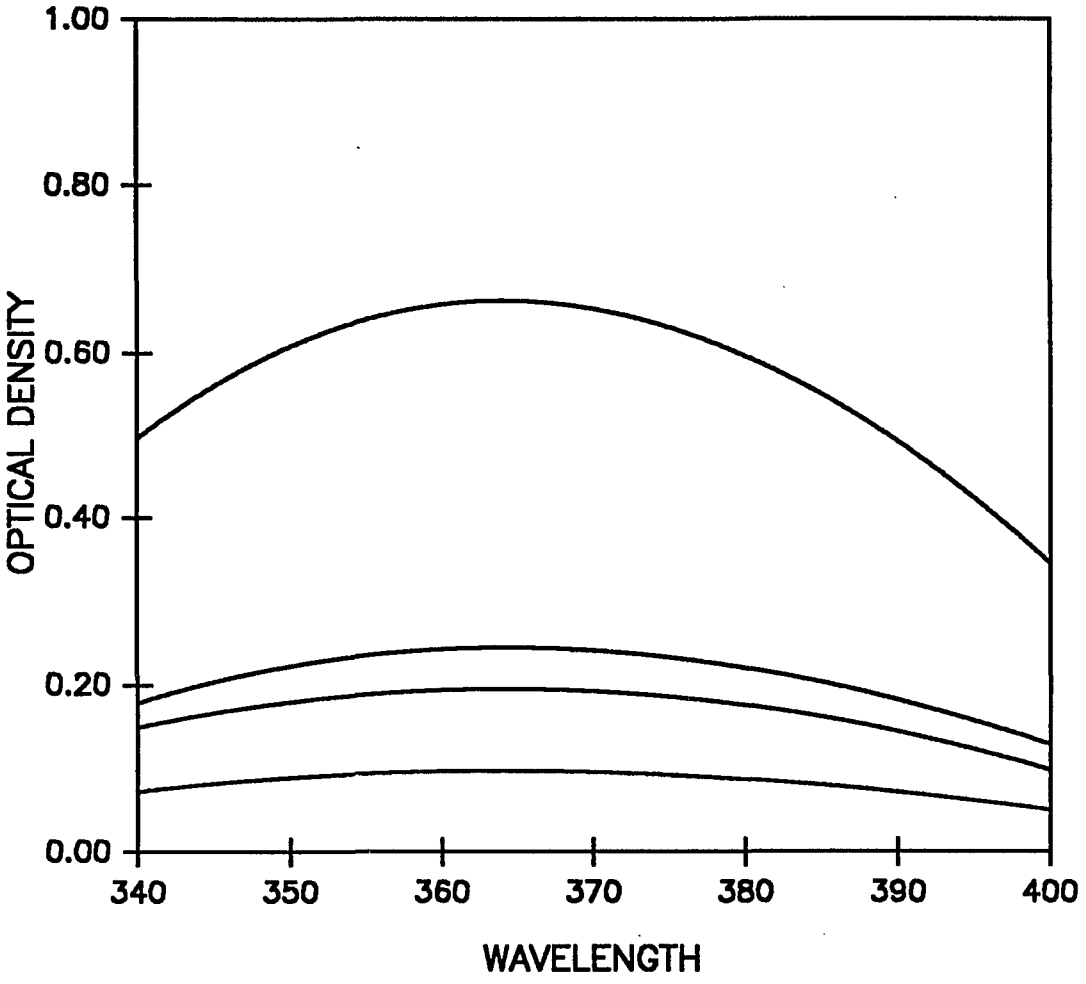

Figure IV.A.2.4a: Absorption curves used to obtain data in figure IV.A.2.4

pyridine rings participate in the equilibrium resulting in conversion of iodine to triiodide. This is consistent with the conclusion of Reid and Mulliken that about half of the iodine is bound when the donor is in excess (36). For the present system and that studied by Reid and Mulliken a single isosbectic point was observed. Under favorable conditions molecular iodine near an outer complex can be converted to triiodide readily. In the outer complex, donation of nitrogen electron density into the σ_u antibonding orbital of iodine, causes the iodine bond to weaken due to lowering bond order. The enlarged electron cloud of iodine is polarized and then becomes susceptible to attack by a nearby iodine or solvent to form a hydrogen bond and triiodide is formed. In methylene chloride, HMW P2VP is the only donor which leads to formation of triiodide. For an initial iodine concentration of 8.5×10^{-4} mol/L, a P2VP concentration of 3×10^{-3} mol/L lead to 16% conversion of iodine to triiodide.

The blue shift of iodine in the complexed state was examined in methylene chloride quantitatively. *i*-P2VP yielded absorption at 390nm with an iodine concentration range of 10^{-4} M while 2 - Picoline (2 methylpyridine) absorbed at 400nm. Figures IV.A.2.5 - IV.A.2.7 are graphs based on equation II.B.2.6 which all yield high correlation coefficients. The formation constant of 2 - picoline was found to be 231 L/mol and extinction coefficient 1352 cm·l/mole in excellent agreement with the reported values (41). Iso P2VP yielded a formation constant of 55 L/mol and ϵ of 4.6×10^3 cm·L/mol. Both absorption spectrums

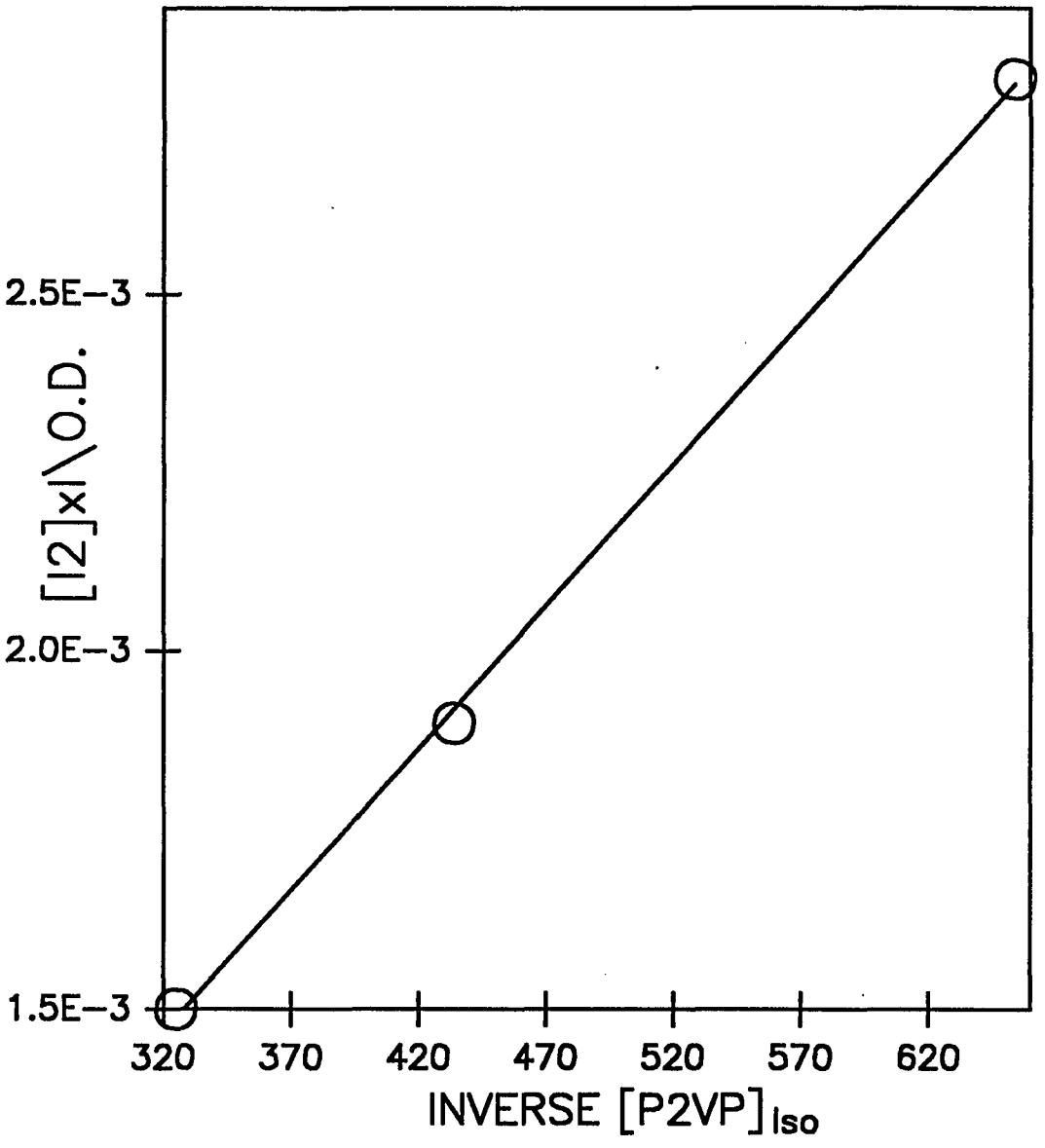

Figure IV.A.2.5: Benesi–Hilderbrand (equation II.B.2.6) plots of i–P2VP for solution of iodine in methylene chloride

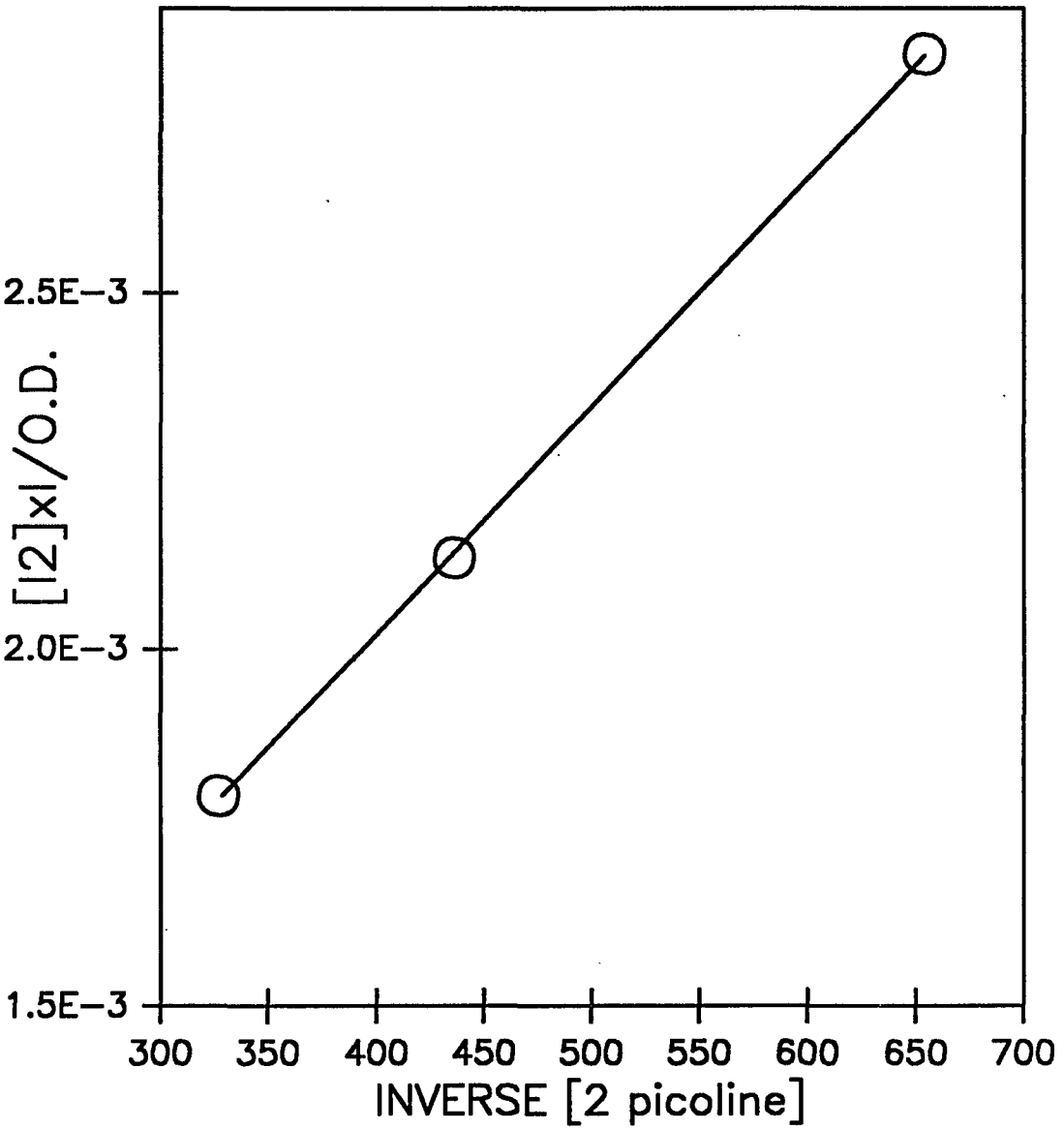

Figure IV.A.2.6: Benesi–Hilderbrand (equation II.B.2.6) plot of 2 picoline for solution of iodine in methylene chloride

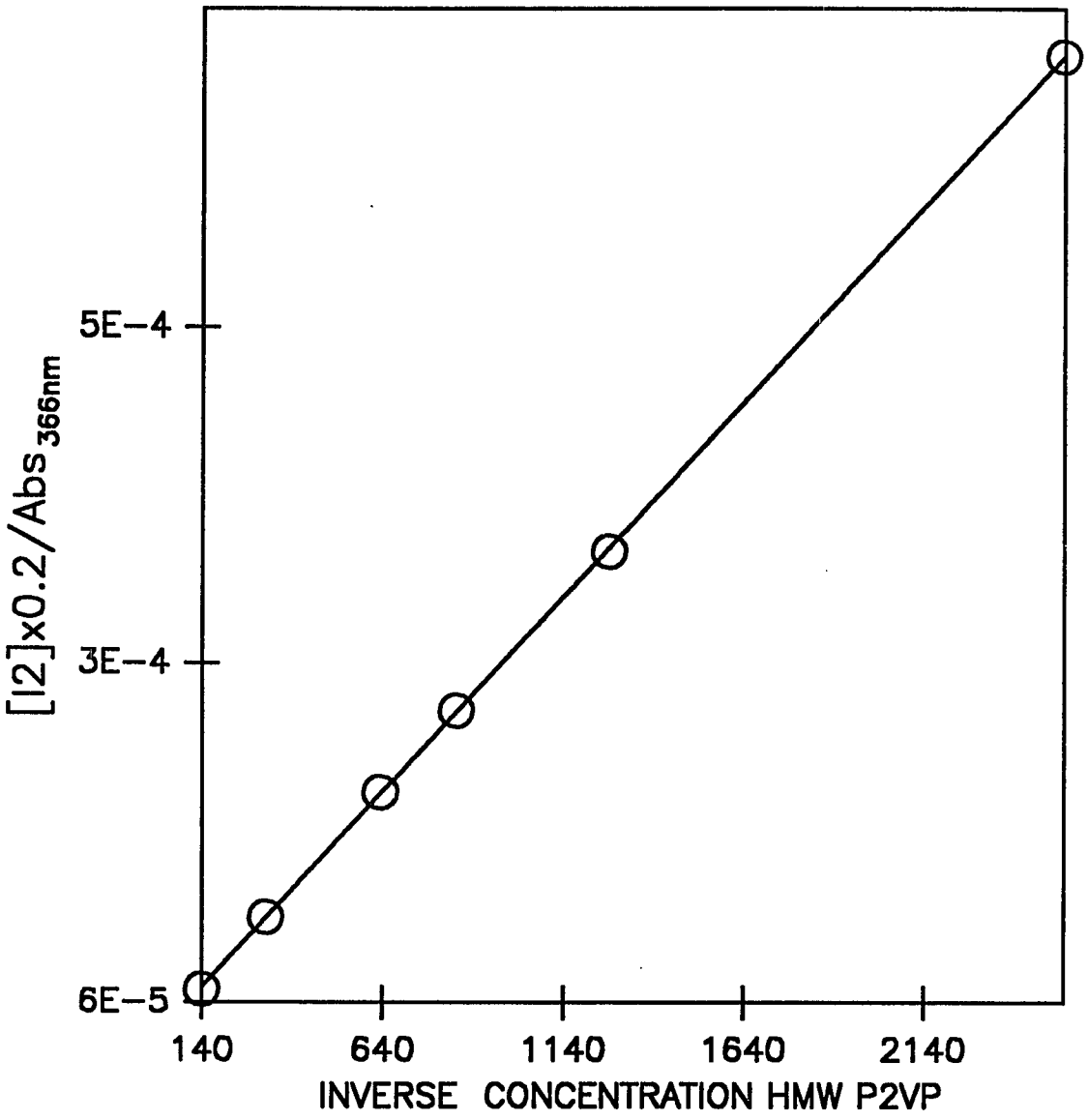

Figure IV.A.2..7: Benesi–Hilderbrand (equation II.B.2.6) plot of HMW P2VP for solutions of iodine in methylene chloride

shows no indication of triiodide. The formal equilibrium constant for HMW P2VP to form I_3^- was determined to be 160 l/mol and ϵ, 23.5 x 10^4 cm·l/mol at a wavelength of 366 nm. The absorption maximum at a long wavelength of 390nm for *i*-P2VP is due to its helical conformation in methylene chloride solvent. Its 3_1-helix may be better preserved and the chain does not form an extended coil as extensively as in chloroform. For this polymer, most of the pyridine rings are located on the surface of the helical cylinder. The lower equilibrium constant for the two polymers is expected due to steric hindrance from the backbone and is common in polymeric systems for bulky donor and acceptor moieties. Here the steric effect dominates the local concentration effect due to polymer.

IV.A.3 POLYMER EFFECT

The results from the present electronic absorption spectroscopy study of poly(2 - vinylpyridine) clearly indicate the dramatic difference between the two systems of the monomeric and the polymeric donors. The spatial distribution of the donor moieties attached to the macromolecule is dictated by the chain conformation controlled, by polymer tacticities and molecular weight as well as the solvent. For the processes involved in charge transfer from pyridine ring to molecular iodine, the polymer effect originates mainly from the polymer segmental distribution leading to a high local donor concentration and polar reaction medium. In a polar solvent ethanol, the P2VP

chain forms with iodine inner complex and triiodide readily, in contrast to the case of the pyridine molecule in methanol. In chloroform, a less polor solvent, the effect due to polymer molecular weight and conformation was systematically demonstrated (Table III.B.1). A random coil segmental distribution favored triiodide formation. The process of complete electron transfer to form triiodide requires charge separation and is facilitated by media with a high dielectric constant and a high tendency to act as a donor in hydrogen bonding. The trends of K, blue shift and extinction coefficient shown in the Table establish the validity of this principle. Compared to pyridine, the three P2VP polymers show a gradation in their manifestation of polymer effect in chloroform. HMW P2VP, assuming a conformation of extended coil, leads to the formation of the highest level of triiodide. LMW P2VP and the isotactic polymer showed less effect compared to atactic HMW polymer. LMW P2VP does not contribute to triiodide formation as readily because its small size precludes formation of regions of high pyridine ring concentration. *i*-P2VP does not contribute to triiodide formation as readily as HMW P2VP because of its helical conformation. However, because chloroform may cause the helical structure to partially break down, i.e. increases helical to coil transitions, the local concentration of pyridine rings is increased significantly enough to contribute to triiodide formation. The slightly lower K value for LMW P2VP compared to pyridine can be explained by the failure of the polymer effect of a low molecular weight species to compensate for the steric effect. For methylene chloride, the clear

contrast between HMW P2VP and *i*-P2VP is evident. No triiodide was formed for *i*-P2VP. The helical structure of the isotactic polymer is better preserved in methylene chloride and triiodide is not favored because the lack of large domains contributing to a local concentration effect. For the atactic P2VP system, 16% of the reacted iodine formed triiodide as stated previously. A lower equilibrium constant is obtained for the *i*-P2VP donor compared to 2 - picoline as would be expected. The results obtained in the present polymer systems compared to that obtained by Reid and Mulliken for solutions of pyridine reveal important differences for iodine in charge transfer interaction between a small molecule donor and a macromolecule carrying such donor functional groups. For the aromatic amine pyridine, a much weaker base than aliphatic amine, the polymer P2VP donor interacting with iodine acceptor can lead to complete electron transfer, i.e. formation of triiodide under conditions where the monomeric donors, pyridine and aliphatic amine fail to form even outer complexes. The polymer effect is controlled by molecular size, tacticity and conformation. Solvents can influence the charge transfer intermediates through their effect on polymer conformation, dielectric constant of the reaction medium and hydrogen bonding.

IV.B HIGH RESOLUTION NUCLEAR MAGNETIC RESONANCE

IV.B.1 ^{13}C NMR

Introduction of tetracyanoethylene (TCNE) to dilute solutions of P2VP causes changes in the chemical shift of the magnetically non - equivalent ^{13}C nuclei of the pyridine ring. These changes are represented in Figure IV.B.1.1a and 1b for free and complexed donor respectively. The signal to noise ratio for the absorption is poor due to the constraint in P2VP concentration required for the experiment. The number of transients ranged from ca. 5,000 for donor alone in solution to ca. 20,000 when TCNE is present. The spins were alowed to recover only within the time frame of the aquisition of ca 0.65 sec. The peak assignments are based on reproducibility for a collection of spectra. The direction of the chemical shift change for carbons 2 and 6 was to high field while carbons 3, 4 and 5 move downfield. These changes were important in interpreting the nature of the complex. There was a gradual change in chemical shift dependent on the concentration of TCNE. A plot of this dependency (Figure IV.B.1.2) shows the difference in chemical shift as a function of TCNE concentration. From this relation both the equilibrium constant K, and the change in chemical shift for the pure complex Δ_0, were obtained.

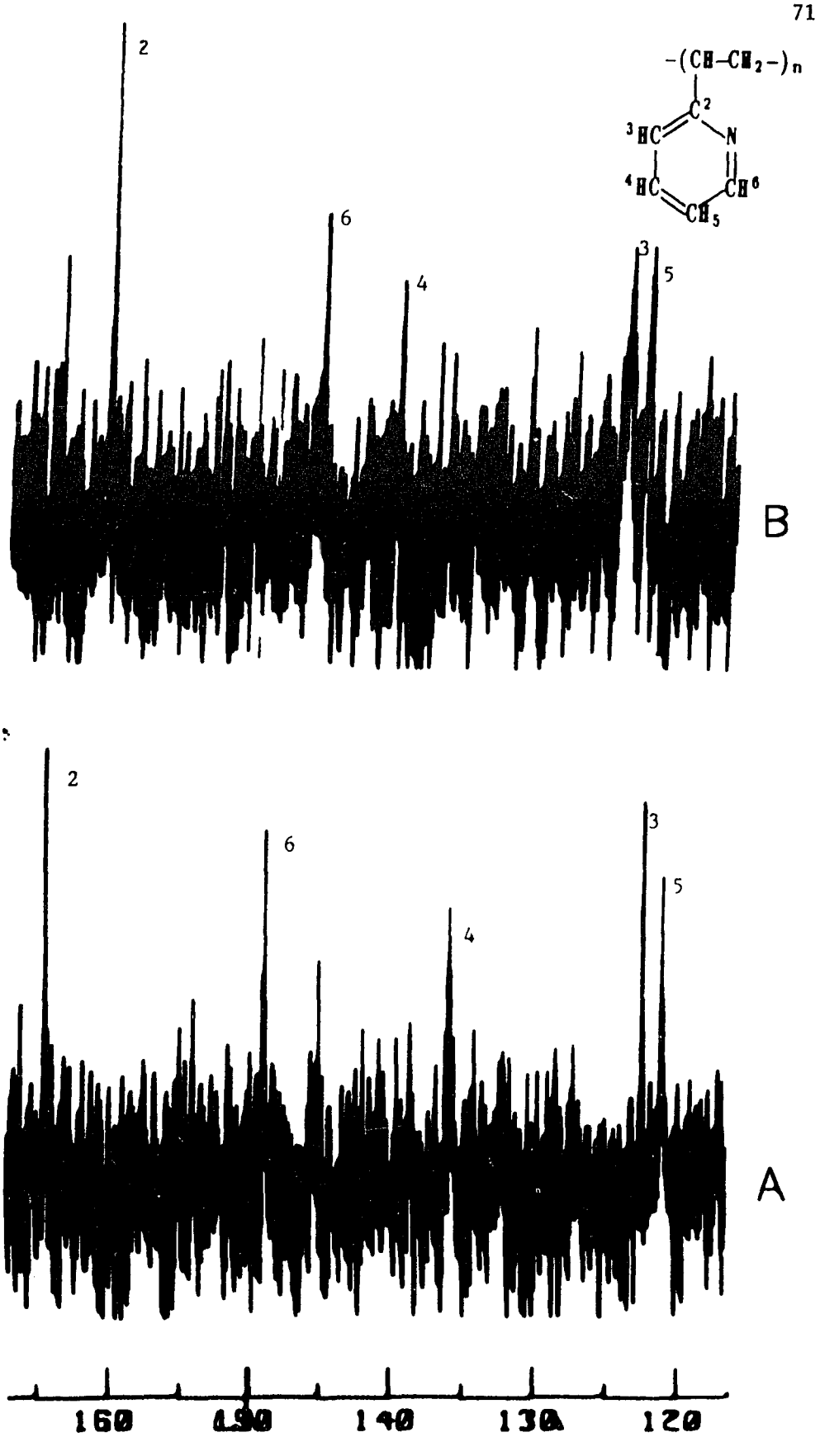

Figure IV.B.1.1: ^{13}C NMR spectra for Isotactic P2VP (0.06 mole/Kg) a)free and b)in the presence of TCNE

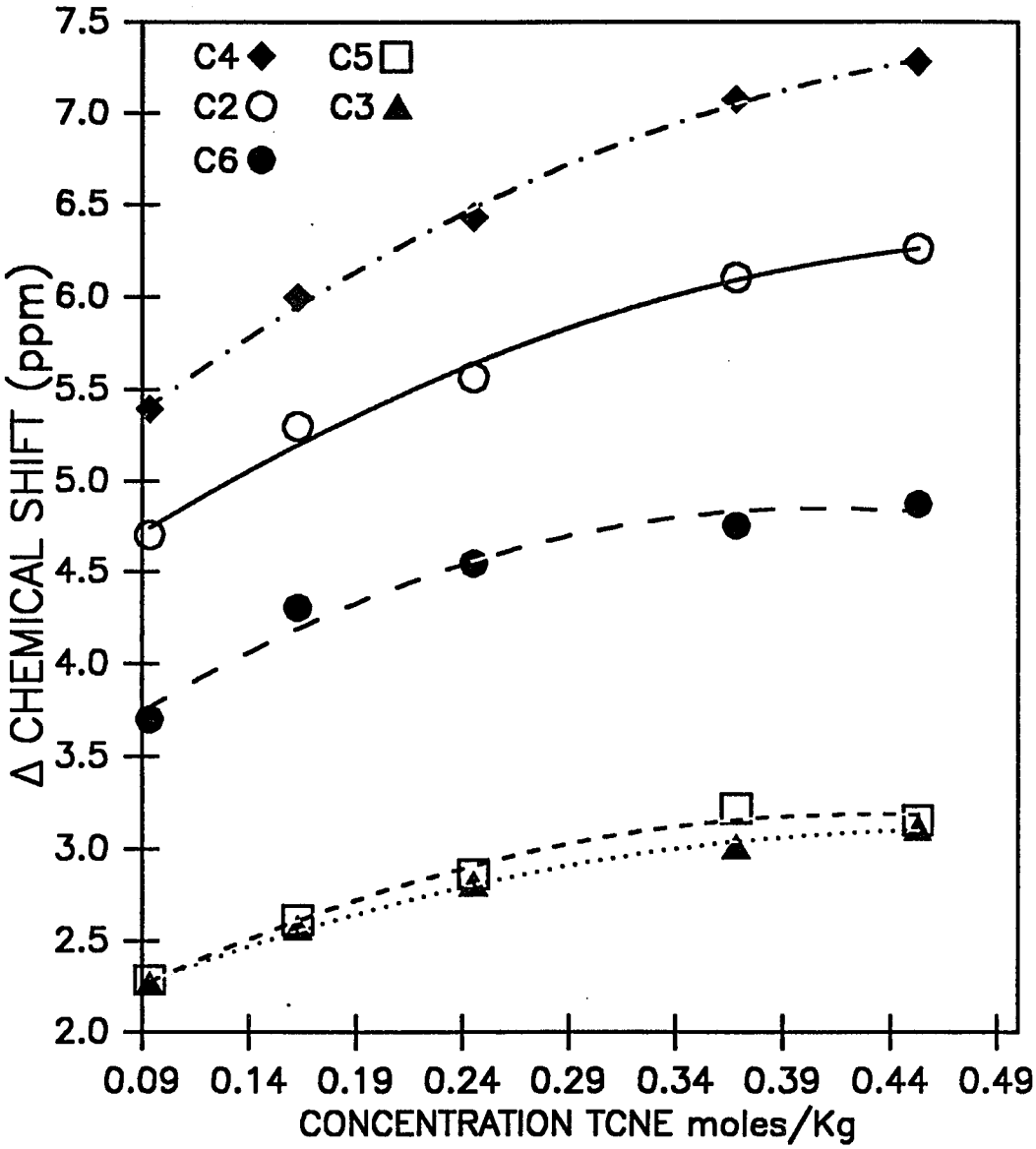

Figure IV.B.1.2: Change in chemical shift as a function of acceptor concentration for donor carbons

Table IV.B.1.1 list Δ_0 results as obtained for different mathematical expressions for each ring carbon atom.

Table IV.B.1.1: Values of Δ_0 for each nuclei as obtained by the equations listed

EQUATION	II.C.1.5	II.C.1.4	II.C.1.10
Nucleus	Δ_0	Δ_0	Δ_0
C_2	5 ± 2	5 ± 2	5 ± 2
C_6	4 ± 1	4 ± 1	4 ± 1
C_4	6 ± 2	6 ± 2	5 ± 2
C_3	3 ± 1	2 ± 1	2 ± 1
C_5	3 ± 1	2 ± 1	2 ± 1

An example of a plot obtained by equation II.C.1.4 for ^{13}C chemical shift is given in Figure IV.B.1.3. From such data the order of the parameter Δ_0 was found to be:

$$C_4 > C_2 > C_6 > C_3 \geq C_5$$

The order and the direction of the change in chemical shift for each of the carbons yielded information concerning the electronic configuration within the aromatic framework. To account for direction of the chemical shift, the relation given by Karplus and Pople (42) in equation IV.B.1.1 was considered:

$$\sigma_p^n = -(e^2h^2/2m^2c^2)(\Delta E^{-1})< r^{-3} >_{2pn} [Q_{nn} + \sum_b Q_{nb}] \quad \text{IV.B.1.1}$$

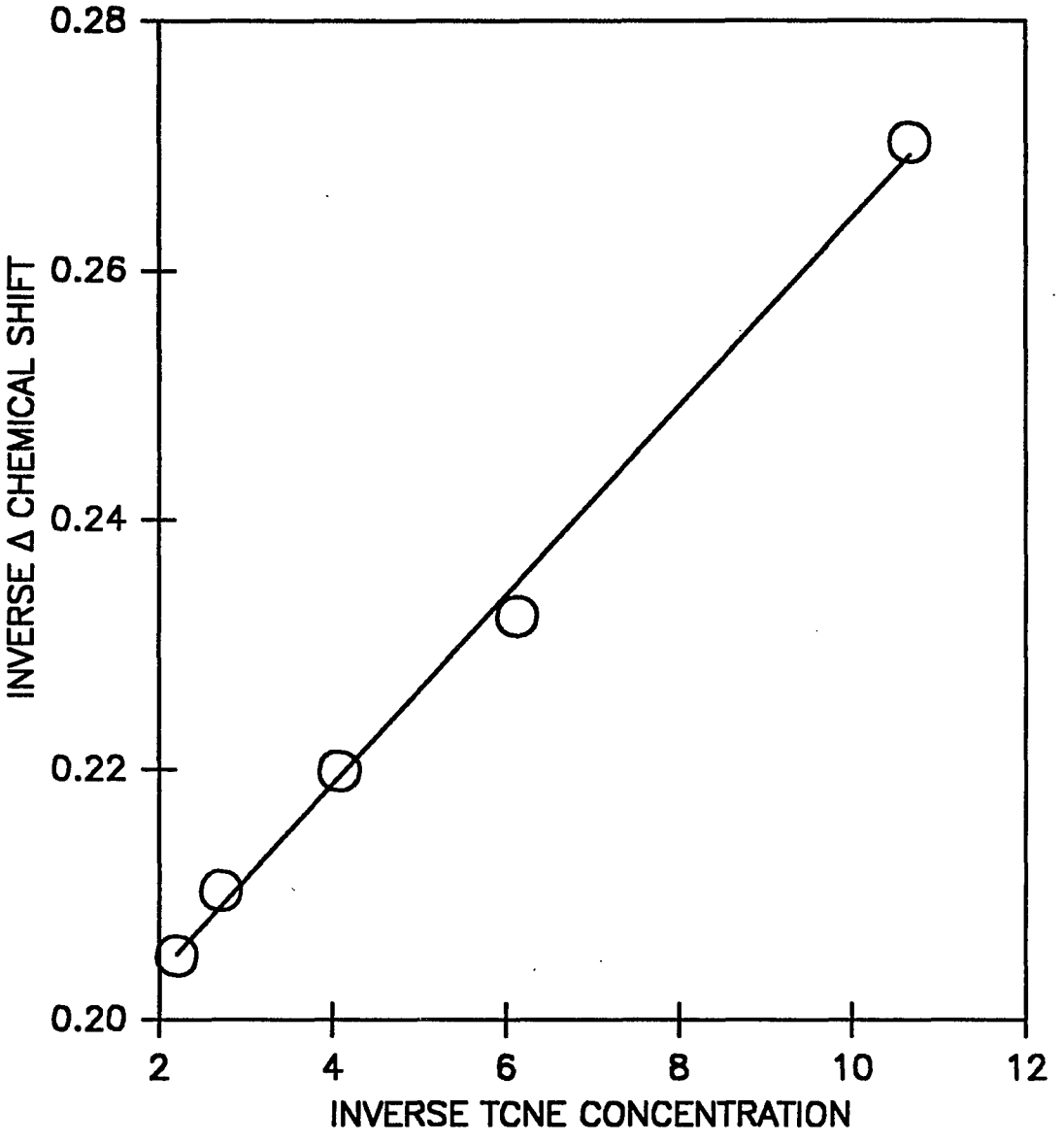

Figure IV.B.1.3: Inverse Δ chemical shift for C6 of P2VP vs inverse TCNE concentration (from equation II.C.1.4)

Here σ_p^n represents the contribution to the chemical shift by the paramagnetic component which dominates the position of a chemical shift for a nucleus, n, with p-orbitals. The first factor on the right side of the equation is constant for any nucleus. ΔE is the mean electronic excitation energy for the system and is the same for the nuclei under consideration. Because only one system is considered here these terms are not important in the present application and need not be considered. The Q terms which are functions of charge and bond orders contribute to the chemical shift but are essentially constant. The $< r^{-3} >_{2pn}$ term represents the average distance of the nucleus and the electron in the 2p orbital. It is of predominant importance in rationalizing ^{13}C chemical shift (43). T. Tokuhiro and G. Fraenkel (44) have discussed chemical shifts in terms of a simplified version of equation IV.B.1.1, i.e. equation IV.B.1.2:

$$\sigma_p^n = < r^{-3} >_{2pn} \chi_p^n \qquad \text{IV.B.1.2}$$

where χ_p^n contains the Q terms of equation IV.B.1.1. In predicting the absorptions of carbons attached to a nitrogen heteroatom, they concluded that the mean radius term dominates. Large downfield shifts for carbons attached to nitrogen heteroatoms relative to benzene were expected due to orbital contraction resulting in an increase in the $< r^{-3} >_{2pn}$ term which overrides the χ_p^n term. An explanation as to how this term affects chemical shifts will be given below.

The nitrogen atom in the pyridine ring contains two sp^2 electrons, each shared with an adjacent carbon atom to form a sigma bond, two sp^2 non - bonding electrons, and an electron in a p-orbital which takes part in resonance within the ring. Upon depletion of electron density from a non - bonding orbital in charge transfer, the density around the adjacent carbons can appear to increase. The electron in the p-orbital is perturbed toward the nitrogen heteroatom due to formation of a partial positive charge. This results in an increase in electron density in the vicinity of the nitrogen atom as electron density within the p orbital is shifted to compensate for loss of electron density within the non - bonding orbital. The increase in electron density is unique to the adjacent carbons to the nitrogen as an overall decrease in electron density is expected upon complex formation. This behavior had been observed previously by ^{13}C NMR which was enforced by theoretical calculation predicting an increase in electron density around the *a* carbons of pyridine when hydrogen bonded (45). Higher electron density around the adjacent carbons decreases the $< r^{-3} >_{2pn}$ term. The observed result is a high field shift for the adjacent carbons. Accompanying this high field shift is a low field shift for the remaining carbons of the ring. Such changes are consistent with redistribution of electron density within the ring as described. The high field shift for C_2 and C_6 can also be explained by a decrease in bond order of the carbon - nitrogen bond due to charge transfer from the nitrogen atom to TCNE. Here the bond order effect overwhelms the polarization effect. For

C_3, C_4 and C_5, the polarization effect prevails

In terms of magnitude, the carbon which is symmetrically opposite the site of electron transfer is most affected. Such behavior is commonly referred to as a para affect. The relative magnitude may be explained by C_4 loosing more electron density from its 2p orbital than the two meta carbon atoms. An important observation was made when the polymeric ring system was compared to 2 ethylpyridine in terms of magnitude for chemical shift changes upon complexation. Figure IV.B.1.4a and 4b show ^{13}C spectra for 2-ethylpyridine free and in the presence of acceptor respectively. All carbons of the free 2EP were observed except C_2 which had a very low signal to noise ratio, common for quaternary nuclei of small molecules. In the presence of TCNE, C_2 absorption was clearly observed. This may be due to the hindered rotation for the ethyl group because of the presence of the TCNE molecule next to the nitrogen atom. The direction of the chemical shift changes for the carbons are consistent with that of P2VP. Examples of graphical representation of Δ as a function of acceptor concentration are given in Figure IV.B.1.5. A minimum was observed for carbons 3 and 5 while a maximum occurred for carbons 4 and 6. Results for Δ_0 were obtained only from the region of the curve with positive slope. Results for Δ_0 are given in table IV.B.1.2

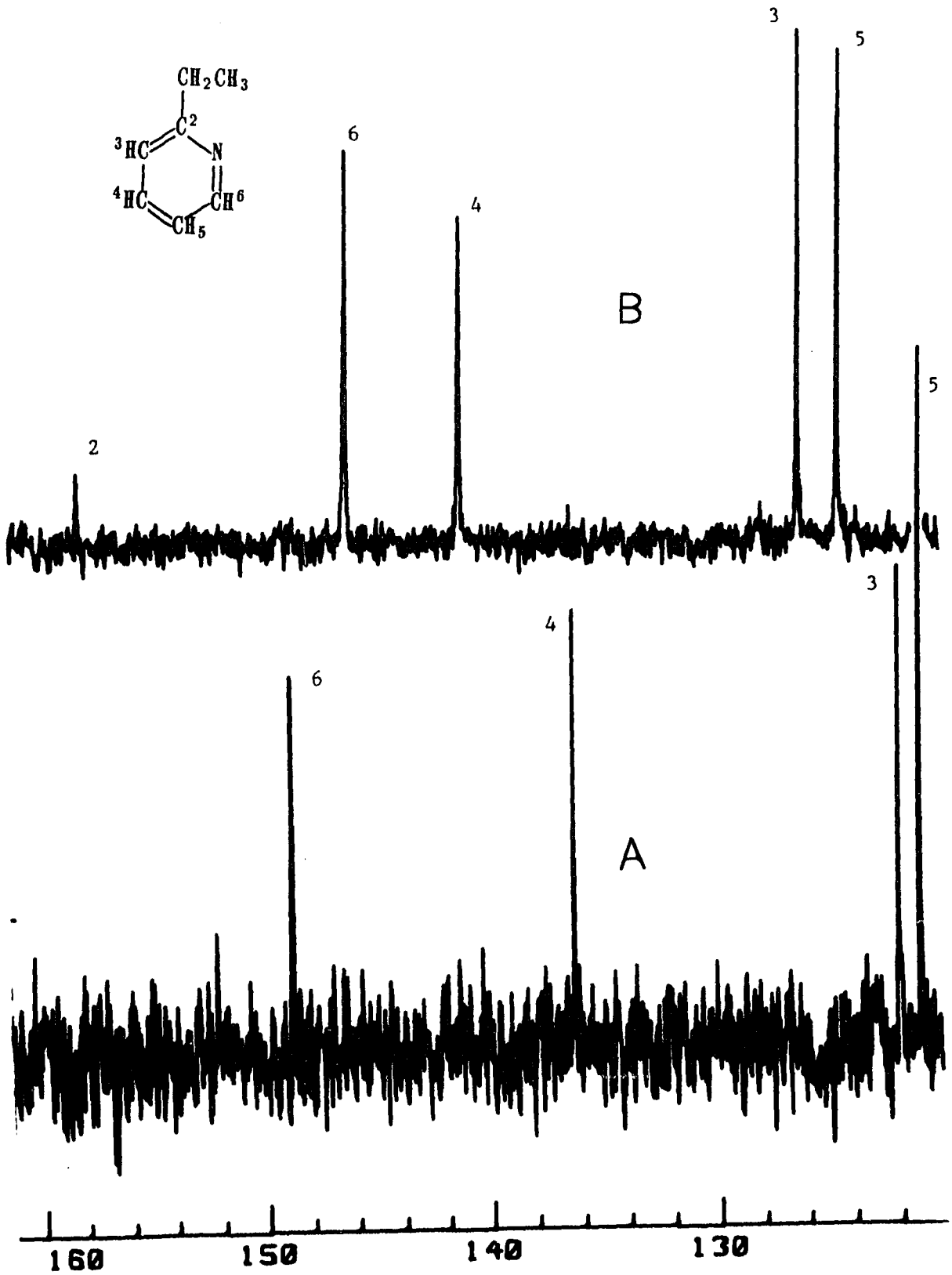

Figure IV.B.1.4: ^{13}C NMR spectra for 2EP in DMSO-d_6 a)free and b)in the presence of TCNE

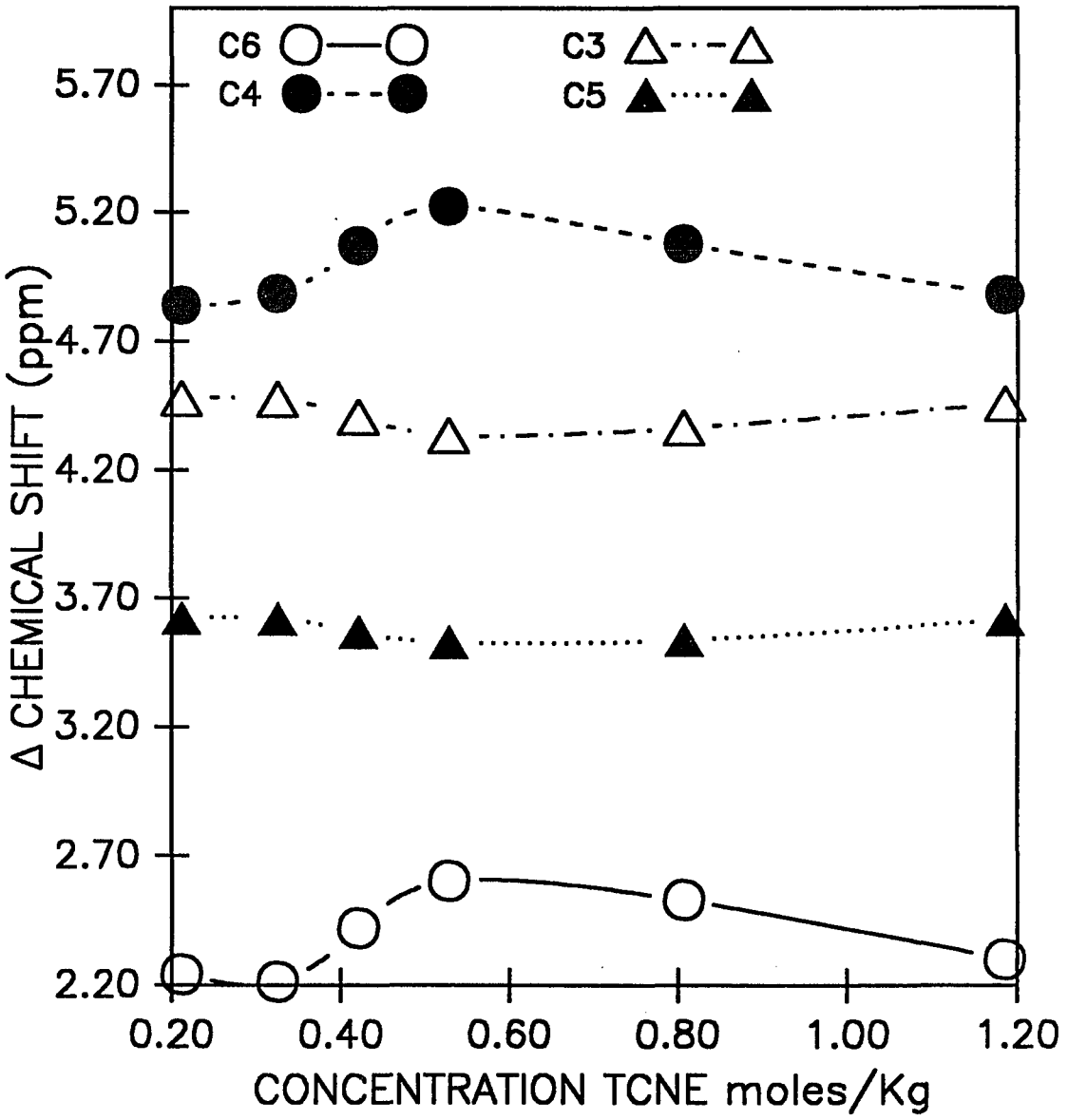

Figure IV.B.1.5: Change in chemical shift as a funnction of [TCNE] for the 2EP ring carbons

TABLE IV.B.1.2: Values of Δ_0 for 2 ethylpyridine

NUCLEUS	Δ_0
C_3	4.55 ± .07
C_5	3.63 ± .07
C_4	5 ± 1
C_6	3 ± 1

and the order of Δ_0 was found to be:

$$C_4 > C_3 > C_5 > C_6$$

Δ_0 values for the 2EP complex, obtained for carbons 3 and 5 were well reproduced over a wide concentration range while carbons 4 and 6 showed a greater error range. The average values for some of the carbons overlap within the error range of the measurement. The order as given is valid based on each individual experiment. This order is of interest in comparing results obtained for the polymeric system. The argument given below was based on the order obtained for the carbon nuclei of the two donor systems. It should be pointed out that the order obtained for the two systems was consistent for each experiment although the average values result in overlap. This overlap in Δ_0 for C_5 and C_6 does not place the order for Δ_0 in question. Conclusions to be arrived at are based on the order rather than the magnitude and has a sound experimental basis.

The difference in order was interpreted in terms of amount of electron density being transferred in the ground state. Pugmire and Grant (46) reported the order for the magnitude of chemical shift changes for carbons of pyridine to be: $C_4 > C_{2,6} > C_{3,5}$ upon protonation. This order is therefore expected for systems which show a high degree of electron transfer form non - bonding electrons upon complexation. Larkindale and Sinkin (47) reported the order: $C_4 > C_{3,5} > C_{2,6}$ for pyridine complexed with iodine, a condition which is expected to result in a relatively low degree of electron transfer from a non - bonding orbital. The order reported for P2VP and 2EP parallels the order for pyridine as obtained for protonation and iodine complex respectively. This infers a more complete transfer of electron density in the polymeric system as compared to the unattached alkylated ring. This condition was attributed to better overlap of non - bonding molecular orbitals with the lowest unoccupied molecular orbital of the acceptor in the polymeric system. This increased overlap found in the polymeric system was at first surprising since the backbone was expected to be a source of significant steric interference. Experimental results can be explained by the following argument. The pendent ring of P2VP is relatively fixed in a specific geometry relative to the backbone due to a high energy barrier of rotation with the plane of the ring oriented perpendicular to the backbone. Only a small deviation of 10 - 30^0 (48,49) is permitted due to steric interactions. Steric hindrance to complexation expected from the backbone is therefore minimized as the above condition places the

nitrogen heteroatom furthest away from the backbone. A second factor is that the nitrogen of the polymer is relatively fixed and the acceptor may be able to better position itself to achieve maximum overlap. Having the ring relatively fixed allows the complex to better stabilize and the acceptor to approach more efficiently than if the ring were moving freely at a faster rate. In the case of 2EP the alkyl group is freely rotating around the C_2 - Cα bond. The effect of this rotation is to sweep out a volume of repulsion which includes a region where the alkyl group is parallel to the nitrogen heteroatom. This is an area of maximum steric hindrance towards complexation, thus preventing the acceptor from achieving maximum overlap due to frequent repulsion by the alkyl chain. Such a condition does not apply to the polymer complex.

It can be concluded that in terms of the degree of chemical shift changes upon complexation the monomer donor and the macromolecular donor respond differently towards complexation. The type of complex must be the same in both cases as the direction of chemical shifts are the same for each carbon on both donor rings. From these findings, it was evident that the degree of charge transfer was greater in the polymeric system than in 2EP. This was attributed to a relatively fixed position of the pyridine ring of the polymer as compared to the ring of the small molecule 2EP. The high degree of electron transfer in the ground state was also supported by data from FT-IR, *vide infra*.

DETERMINATION OF FORMATION CONSTANTS BY ^{13}C - NMR

Table IV.B.1.3 lists values for the formation constant, K, obtained by different mathematical expressions for the P2VP donor system.

Table IV.B.1.3: Equilibrium constants obtained by equations listed for each nuclei of the IsoP2VP pyridine ring

EQUATION	I.C.1.5	I.C.1.4
Nucleus	K	K
C_2	20 ± 4	20 ± 6
C_6	21 ± 4	23 ± 2
C_4	21 ± 8	18 ± 5
C_3	22 ± 3	23 ± 3
C_5	22 ± 6	23 ± 2

The value of K in table IV.B.1.3 can be considered to have an average value of 21 Kg/mole solution. Values obtained from the iteration procedure were not well reproduced and ranged ~ 60 to 70 per cent higher. These higher values for iteration was expected from the application of equation II.C.1.10. Reason for poorly reproducible values may be attributed to strong interaction as stated previously (Section II.C.1). Although the problems were given in terms of hydrogen bonding systems, similarity is evident. The present system was sensitive to the intercept which in some cases was negative. There may also be a concentration effect which is known to causes dimerization in

hydrogen bonding systems. For various experiments the saturation fraction was seen to be optimized for ratios close to unity. This is an indication that saturation occurs quickly upon introduction of TCNE and that the complex is strong. Taking the value of K as 21 Kg/mole solution, the saturation fraction *s* is calculated and given in table IV.B.1.4. Values of initial donor concentration $[D]_0$, ratio of initial acceptor concentration to initial donor concentration, R and concentration of complex [AD] are also listed. The concentration of the complex was determined by iteration using the value of K and initial concentration of donor and acceptor in each solution.

Table IV.B.1.4: Saturation Fractions as determined with K of 21 Kg/mole

$[D]_0$	R	[AD]	*s*
0.0627	1.00	0.0286	0.456
0.0627	1.18	0.0319	0.510
0.0611	1.53	0.0341	0.558
0.0624	1.58	0.0374	0.600
0.0621	2.06	0.0421	0.678
0.0606	2.69	0.0434	0.716
0.0599	4.09	0.0483	0.806
0.0590	6.25	0.0513	0.870
0.0583	7.77	0.0521	0.894

Table IV.B.1.4 indicates that ratios close to unity better satisfy the condition for optimizing values of K. More

importantly are the relative concentrations of [AD] compared to $[D]_0$. This indicates that the assumption, $[AD] << [D]_0$, used to derive the equations starting from II.B.2.1 is not valid. The problem can not be rectified due to the need of a minimum concentration of donor necessary for observation of a NMR absorption.

Formation constants for the 2EP system were not well reproduced for a number of experiments. This is attributed to the irregular behavior of Δ on [TCNE] as given in Figure IV.B.1.5. The Δ_0 values were better reproduced because they depend on extrapolation to the intercept. The experimental values of Δ are close to the value for Δ_0, i.e. the variation of Δ is small. This condition improves the certainty for the Δ_0 value.

^1H NMR

Data for proton NMR were obtained at lower concentrations of donor as compared to that needed for carbon - 13 NMR data. Results obtained at the lower concentration range of ~.04 moles/Kg solution in donor will be presented first followed by results obtained in the same concentration range used to observe the carbon nuclei.

On addition of TCNE to the solutions of P2VP, NMR absorption for protons 3, 4 and 5 shift downfield while H_6 shifts slightly up field (Figure IV.B.1.6). Figure IV.B.1.7 represents a graph of Δ as a function of acceptor concentration. Table IV.B.1.5 lists results for Δ_0 and K obtained by the different algebraic approaches represented graphically in Figures IV.B.1.8 and IV.B.1.9.

Table IV.B.1.5: Values of K and Δ_0 as obtained for the various protons of the ring by the equations listed

EQUATION	II.C.1.5		II.C.1.4		II.C.1.10	
Nucleus	K	Δ_0	K	Δ_0	K	Δ_0
H_3	9 ± 2	.547±.008	8.1 ±.1	.544±.004	13 ± 3	.51 ±.02
H_4	8.6±.3	.32 ±.01	8.8 ±.1	.320±.008	11 ± 2	.295±.008
H_5	7.67±.04	.27 ±.03	7.9 ±.1	.26 ±.01	13 ± 4	.21 ±.06

Saturation fractions, *s*, are listed in table IV.B.1.6 over a range of acceptor concentrations. Values of table IV.B.1.5 were

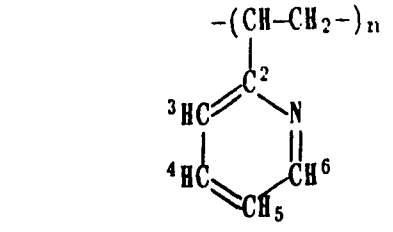

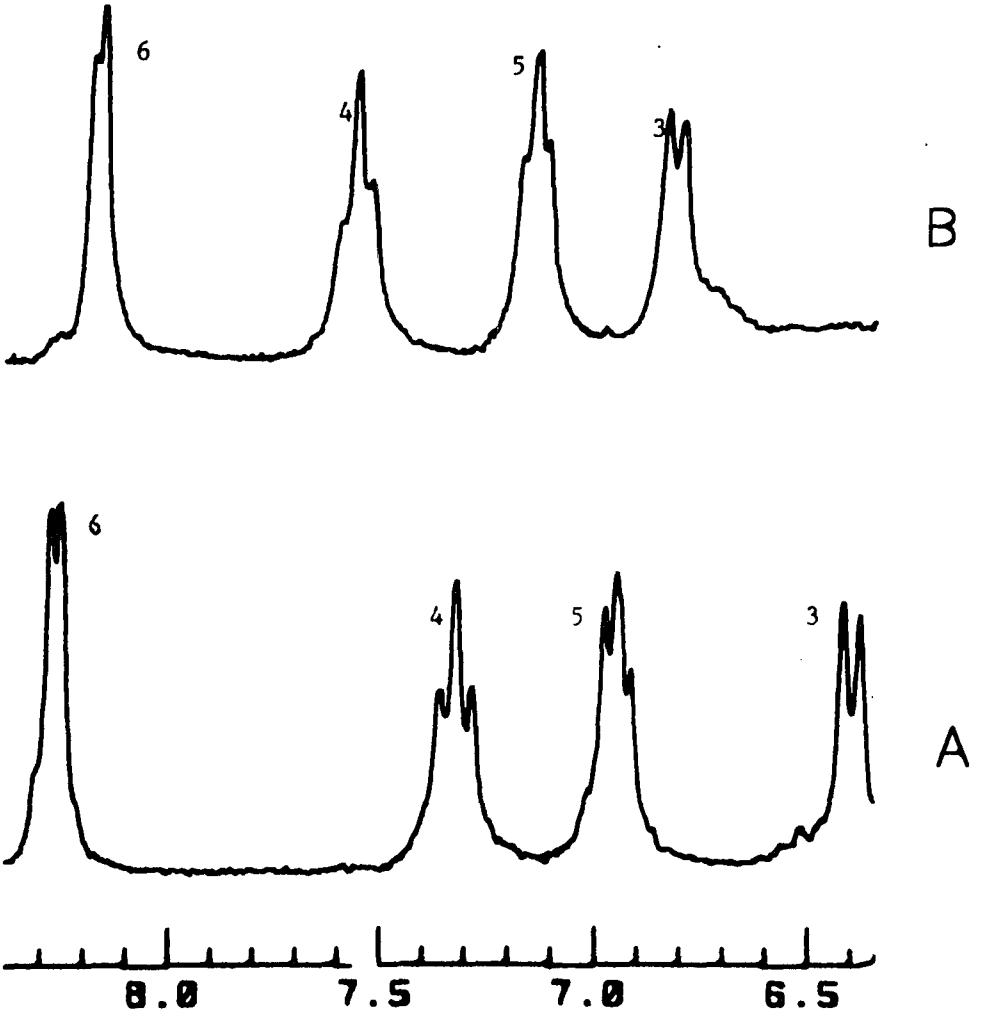

Figure IV.B.1.6: Proton NMR spectra for P2VP in DMSO-d_6 a) free and b) in the presence of TCNE

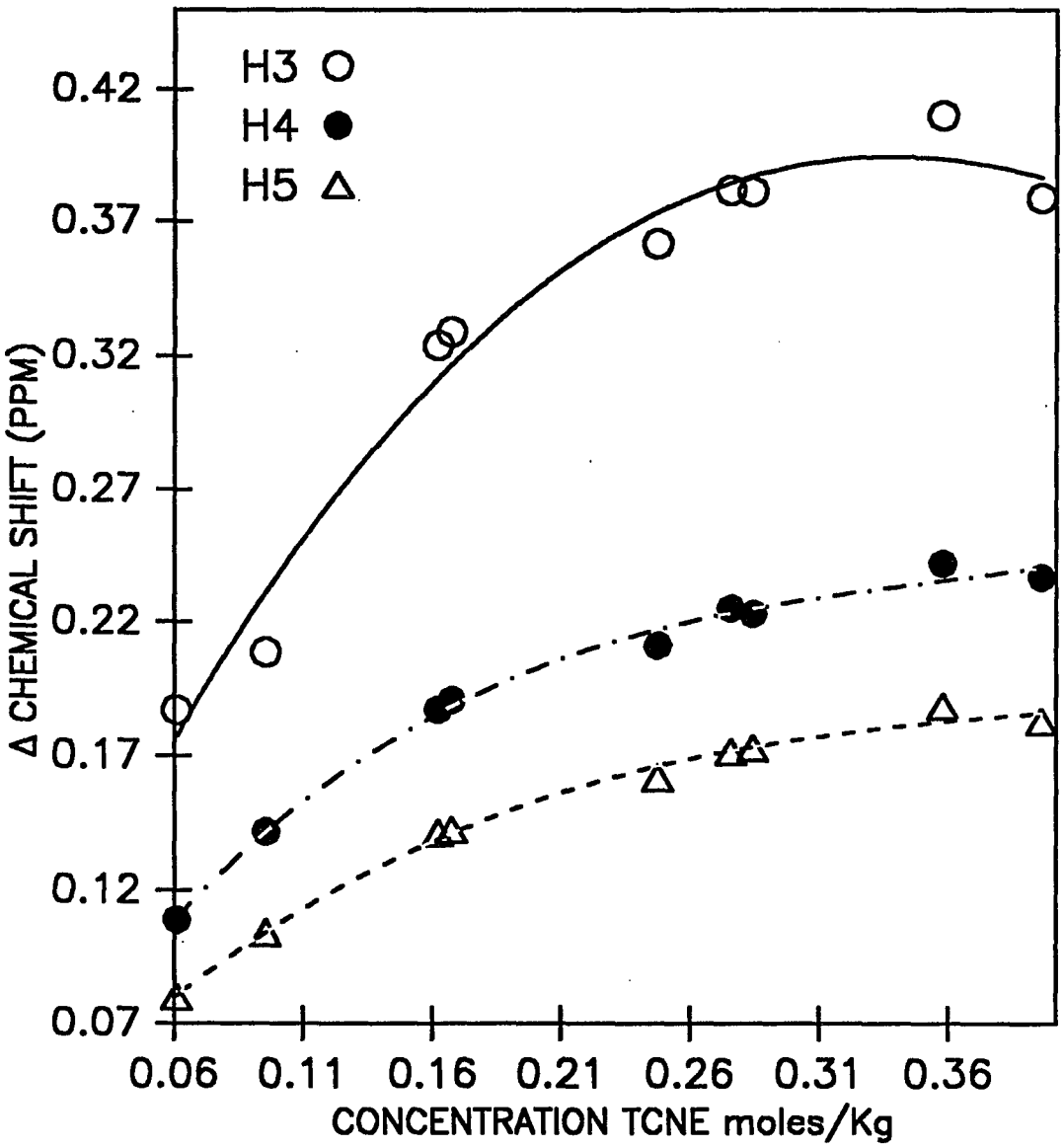

Figure IV.B.1.7: Change in chemical shift for P2VP ring protons as a function of acceptor concentration

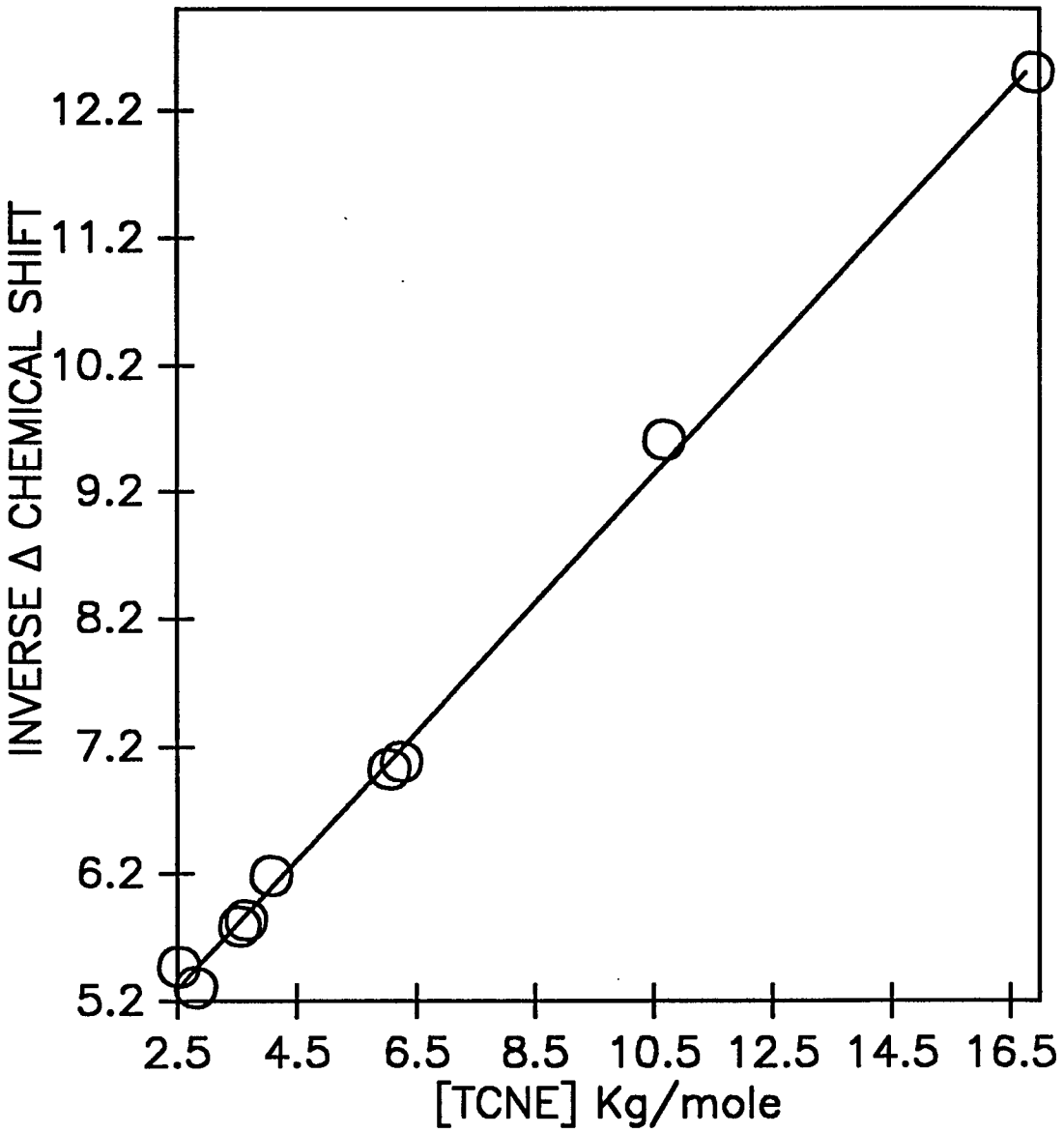

Figure IV.B.1.8: Inverse Δ chemical shift for H5 of P2VP vs inverse [TCNE] (from equation II.C.1.4)

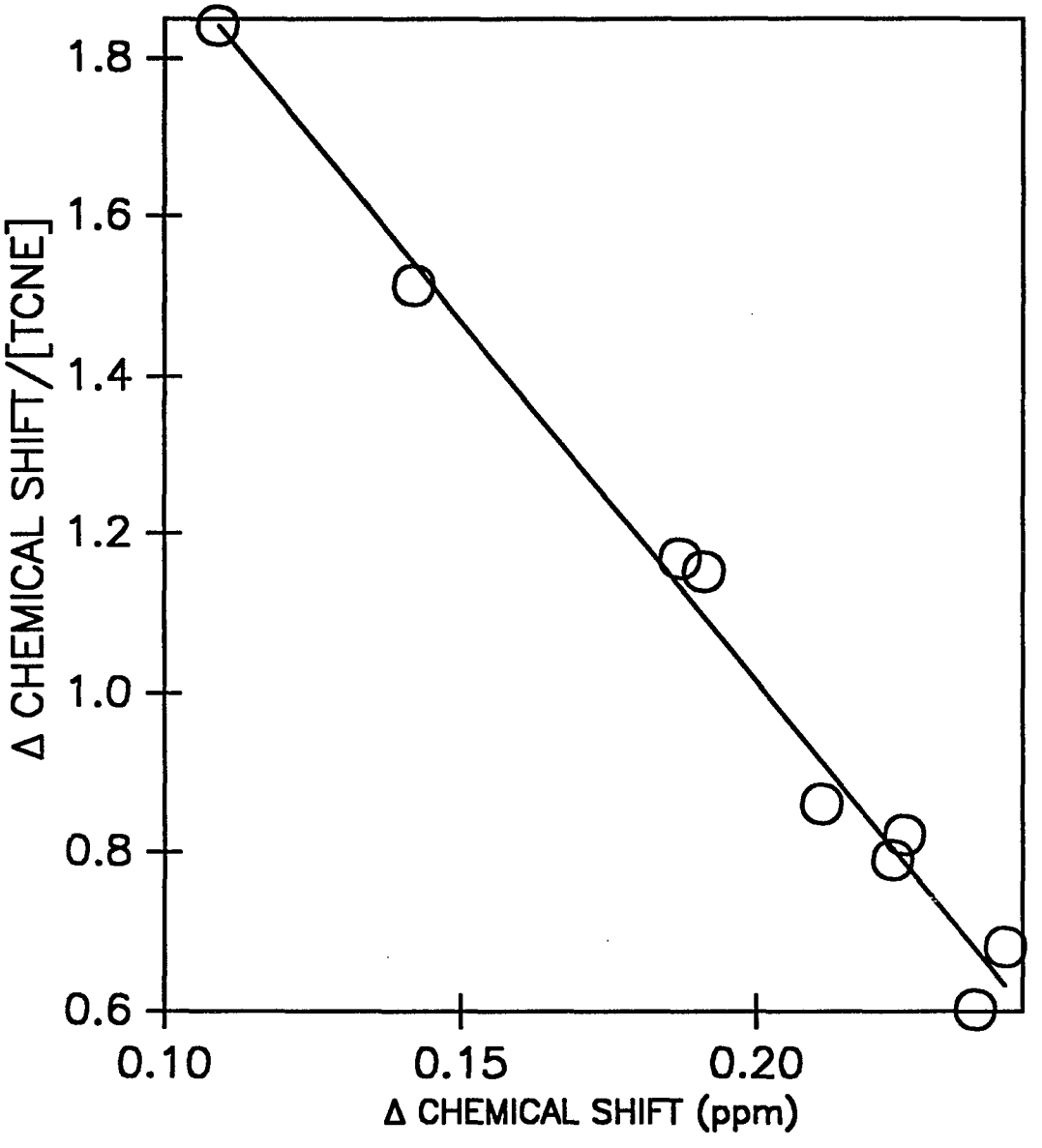

Figure IV.B.1.9: Δ Chemical shift divided by [TCNE] vs Δ chemical shift for H5 of P2VP (from equation II.C.1.5)

obtained over this range. Also listed are the initial donor concentrations $[D]_0$, ratio of acceptor to donor, R and concentration of the complex [AD] as obtained by iteration.

Table IV.B.1.6: Saturation Fractions based upon the results of table IV.B.1.5

$[D]_0$	[AD]	R	*S*
0.0413	0.0117	1.38	0.284
0.0431	0.0168	2.19	0.390
0.0405	0.0217	3.56	0.536
0.0412	0.0227	3.88	0.544
0.0435	0.0281	5.27	0.645
0.0421	0.0283	6.43	0.672
0.0407	0.0277	6.50	0.681
0.0435	0.0318	8.30	0.731

The range of *s* was optimized at the given donor concentration and the entire portion of acceptable values for *s* is between .2 and .8. Comparison of [AD] with $[D]_0$ indicates the same problem as described above but to a lesser extent. Plots of Δ vs. acceptor concentration as given in Figure IV.B.1.10, show a maximum. A comparison of this Figure with Figure IV.B.1.7 demonstrates the sensitivity of donor chemical shifts on TCNE concentration. A downward slope is seen for the last points in Figure IV.B.1.7. The concentration of TCNE was greater in Figure IV.B.1.10 and the inflection is better defined at higher acceptor concentrations. This concentration range is approximately where the value of *s* is

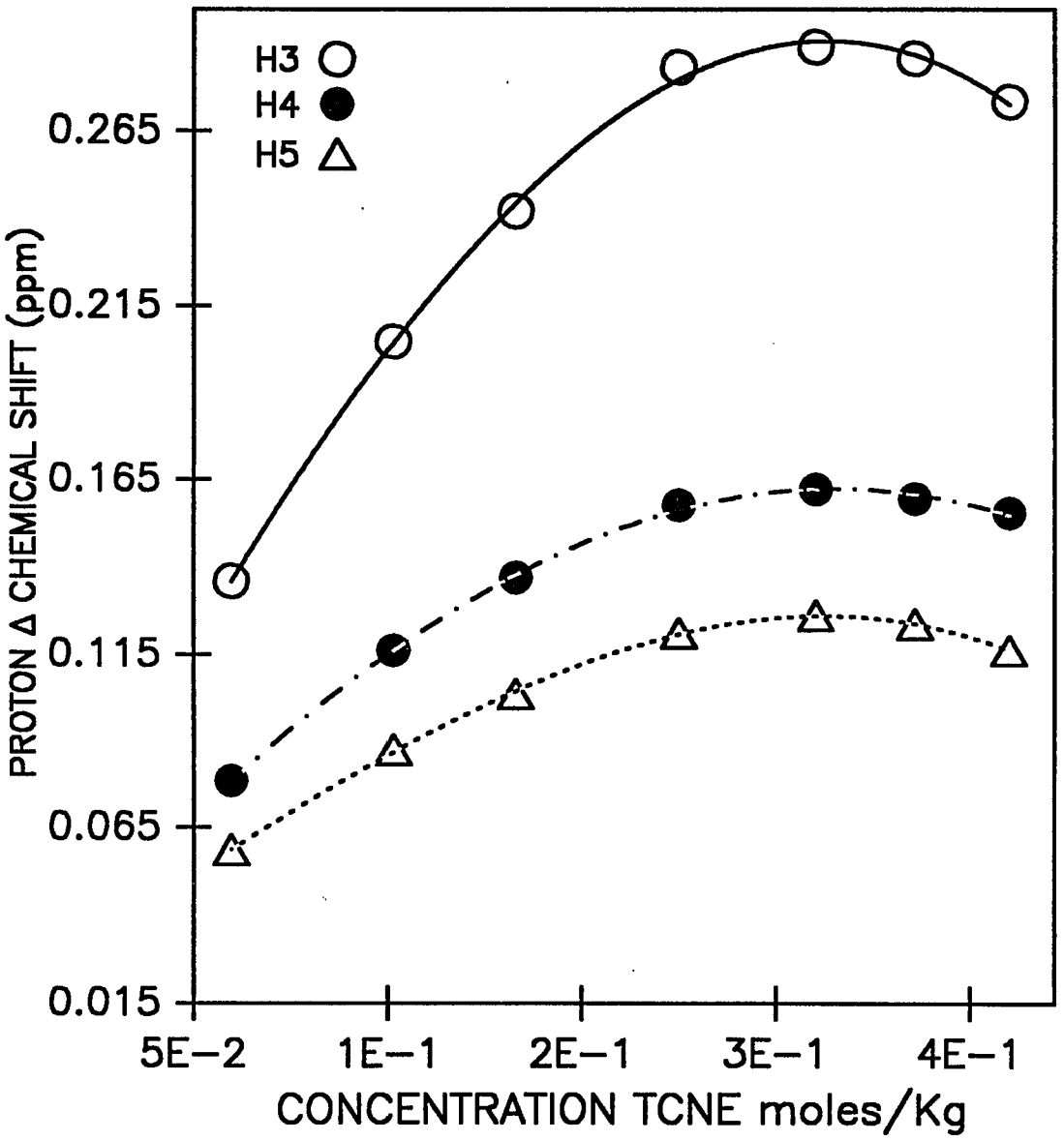

Figure IV.B.1.10: Change in chemical shift for P2VP ring protons as a function of acceptor concentration

reaching a maximum. Both the maximum in *s* and an inflection point on the graph indicate the system has reached saturation. A point of inflection has been observed by Pugmire and Grant (46) for the reaction of pyridine with increasing amounts of trifluoroacetic acid. The downward slope was attributed to a dilution effect with all protons giving the same slope to the right of the inflection. In the present system the slopes after the inflection point were equal for H_4 and H_5 but differed for H_3. This was our first indication that H_3 was responding differently to complexation. This observation along with the dependency of Δ upon acceptor concentration for H_6 will be discussed in more detail.

Values of Δ_0 and K for H_6 could not be obtained because the value of Δ changed very slightly with acceptor concentrations within the donor concentration range. The chemical shift of the pure donor was obtained within ± .002 ppm while changes in Δ for increasing acceptor concentrations were within this error range. The initial value of Δ upon the first introduction of acceptor was greater than this error and in an upfield direction. This direction was opposite to the remaining protons on the ring. The trend was better observed at higher donor concentrations and is given in Figure IV.B.1.11 as a plot of Δ as a function of acceptor concentration for the ring protons. The slope after the inflection for H_4 and H_5 are equal and different than that of H_3 as previously observed. H_6, in addition to moving upfield, has an initial negative slope. Graphical interpretation of H_6

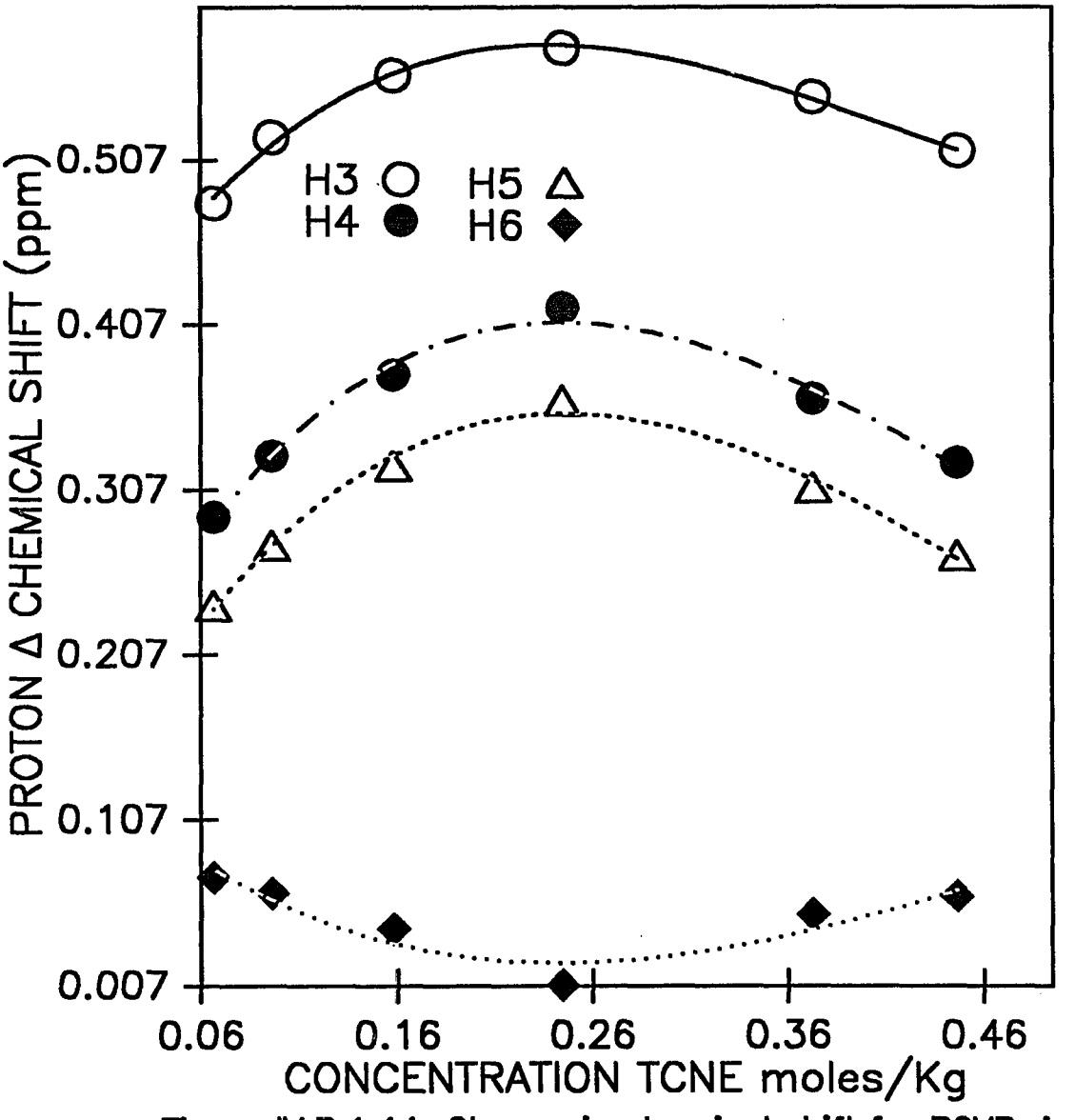

Figure IV.B.1.11: Change in chemical shift for P2VP ring protons as a function of acceptor concentration

chemical shift by the plot from equation II.C.1.4 is given in Figure IV.B.1.12. This pattern excludes extrapolation of data to obtain K and Δ_0 for this proton. However this unique behavior upon complexation proved to be very informative. Another important and informative observation was the high K value for H_3 as obtained at a concentration of ca. 0.06 mol/Kg solution:

TABLE IV.B.1.7: Values of K and Δ_0 for donor conentration range of ~.06 moles/Kg solution

Nucleus	K	Δ_0
H_3	43 ± 4	.61 ± .03
H_4	22 ± 3	.46 ± .06
H_5	20 ± 7	.42 ± .06

Figures IV.B.1.13 and IV.B.1.14 are typical lines obtained by equations II.C.1.4 and II.C.1.5 for the evaluation of K and Δ_0 listed in table IV.B.1.7. The order of Δ_0 was the same as in the low concentration range. However, the values of Δ_0 were higher. The equilibrium constant obtained by ^1H NMR was close to the value obtained by ^{13}C NMR. The difference in equilibrium constant as determined for the donor concentration of ca. 0.04 mole/Kg solution is attributed to an increase in polymeric domains. As a TCNE molecule leaves the vicinity of a polymer chain it is more likely to enter another domain if the volume occupied by polymeric domains is increased. An apparent equilibrium constant for H_3 was found to be twice that for the other nuclei within this donor concentration range. This unique behavior of H_6 and H_3 upon complexation gives support for a

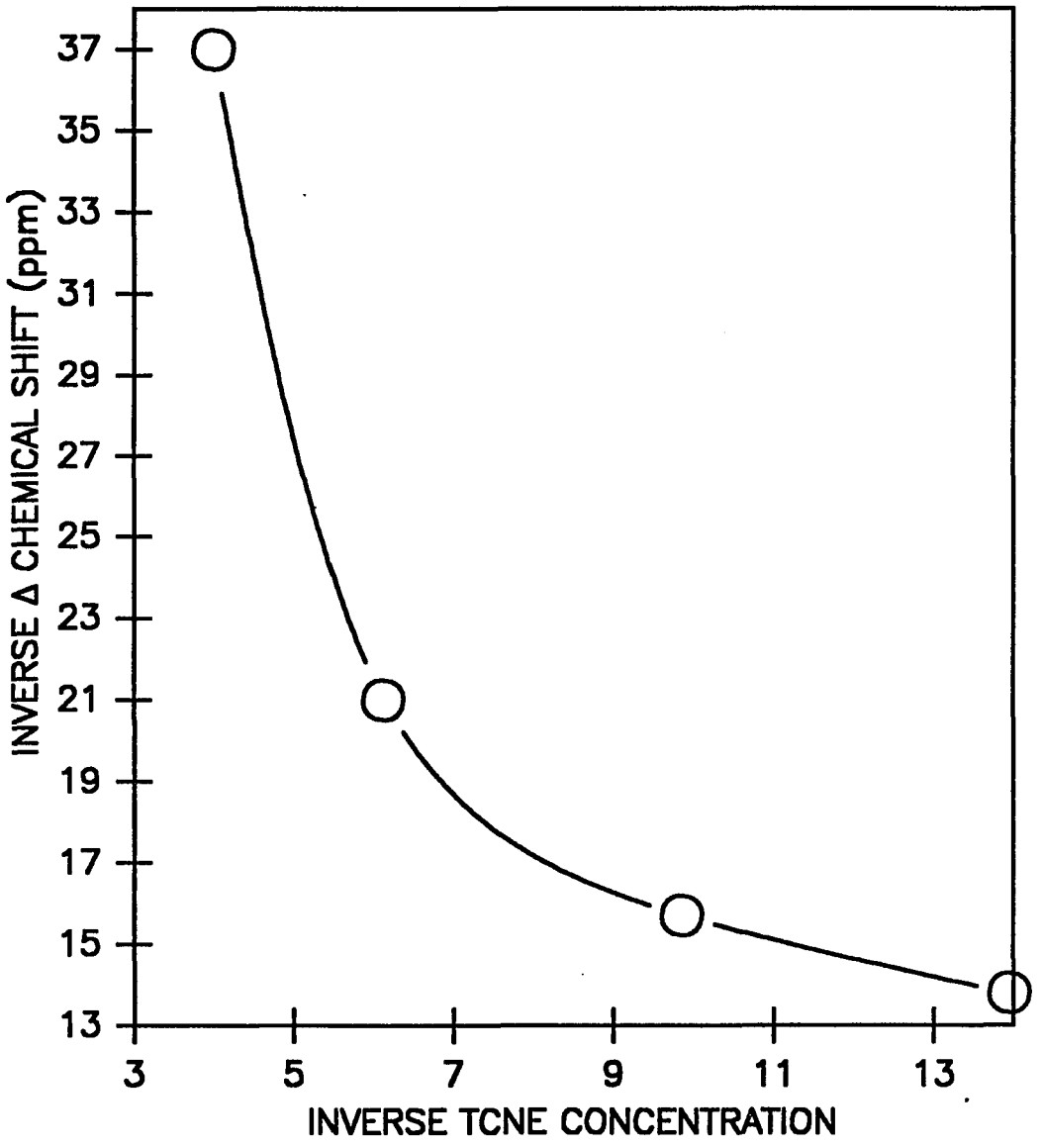

Figure IV.B.1.12: Inverse Δ chemical shift vs inverse [TCNE] for H6 of P2VP (from equation II.C.1.4)

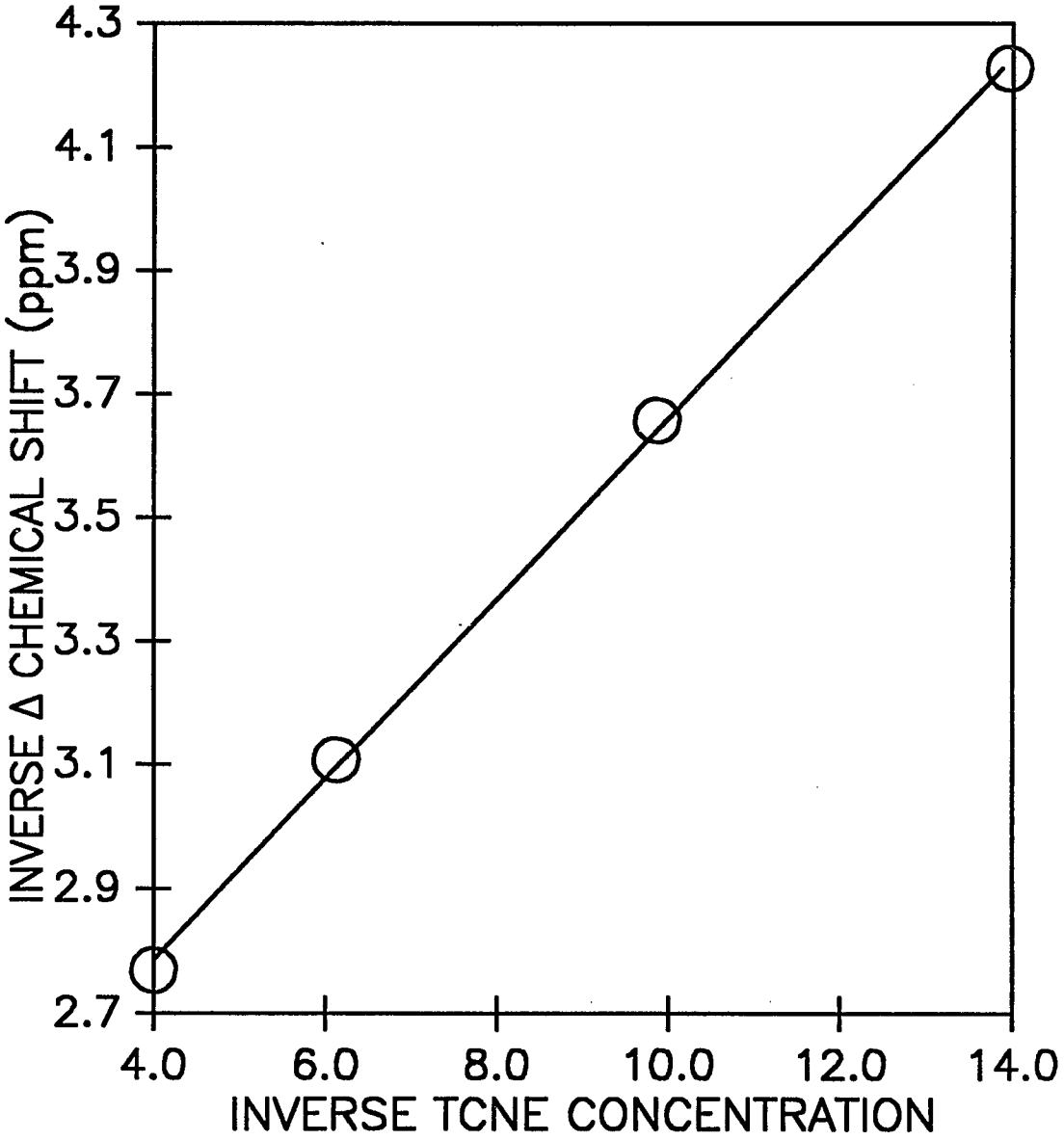

Figure IV.B.1.13: Inverse Δ chemical shift vs inverse [TCNE] for H5 of P2VP (from equation II.C.1.4)

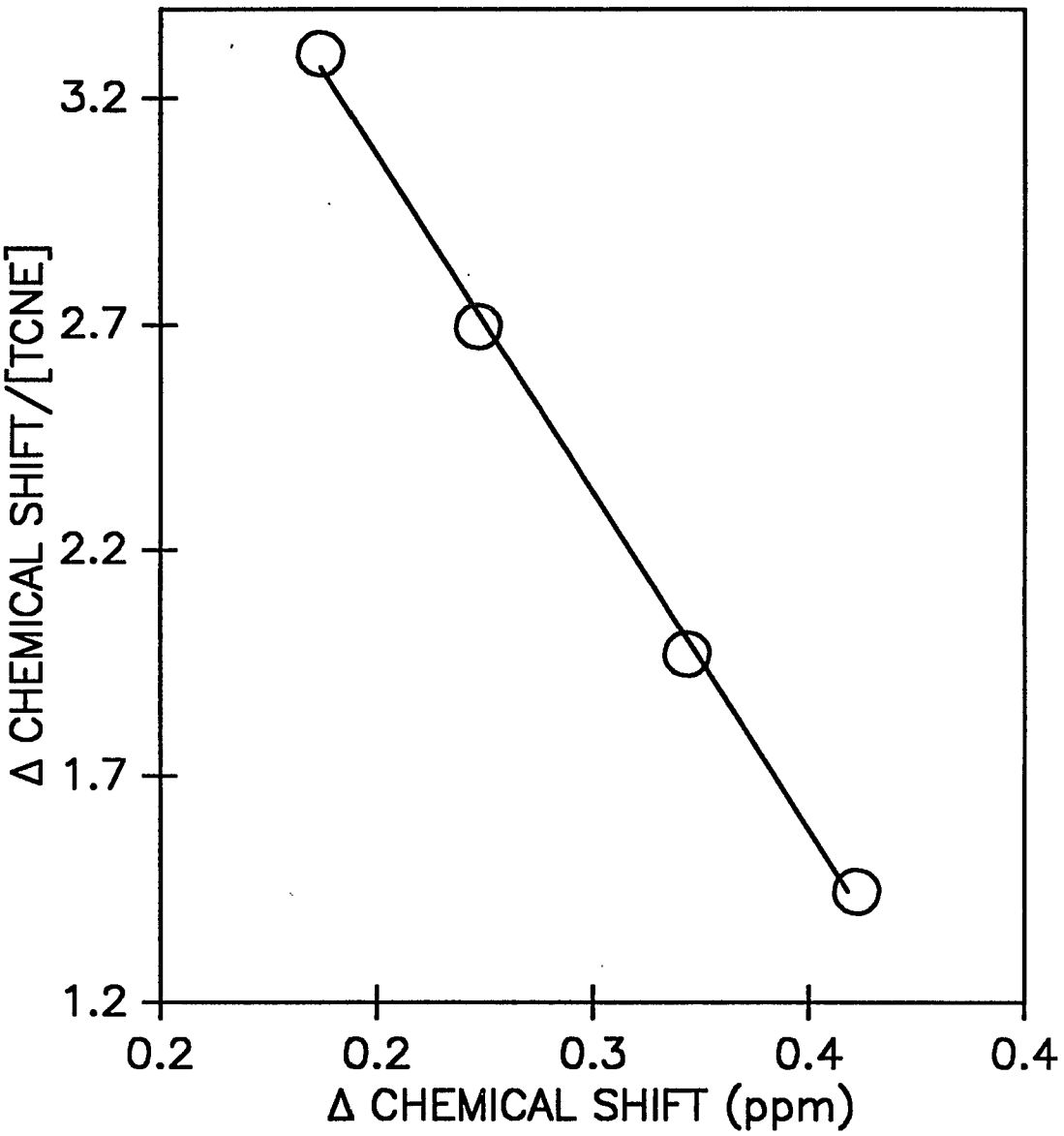

Figure IV.B.1.14: Δ Chemical shift divided by [TCNE] vs Δ chemical shift for H5 of P2VP (from equation II.C.1.5)

topographic model proposed. This model has its basis in the magnetic anisotropy of the TCNE molecule given in Figure IV.B.1.15 (50). The magnetic environment of a ring proton depends in specific ways on its placement relative to the TCNE molecule. A high field shift is induced for a proton located along the cyano bond while a low field shift is induced for a proton perpendicular to this bond. An exceptionally strong region of induced shielding from TCNE is expected below the carbon - carbon π bond. This area is expected to be placed in an exceptionally strong shielding anisotropy due to the combined effect of the two cyano groups. This region is influenced by the conical shielding field of the two cyano groups attached to the same ethylene carbon. The behavior of H_6 and the larger values of K found for H_3 may be explained by a specific topographic placement of TCNE relative to the donor ring upon complexation. This geometry would place H_6 within a region of high shielding and H_3 in a deshielding zone. To satisfy this topography TCNE must be complexed to the non - bonding electrons with the 2 ethylene carbons equal distant from the nitrogen heteroatom The planes of the pyridine ring and the TCNE molecule are mutually perpendicular with the ethylene double bond coplanar with the donor. The topographic relation described is consistent with the chemical shift behavior of H_3 and H_6 upon increasing acceptor concentration. Positions of pendent pyridine rings are more or less fixed to the 3_1 helix of the isotactic polymer. The H_3 atom of a pyridine ring is in close proximity to the nitrogen heteroatom of a neighboring ring. TCNE, if complexed as

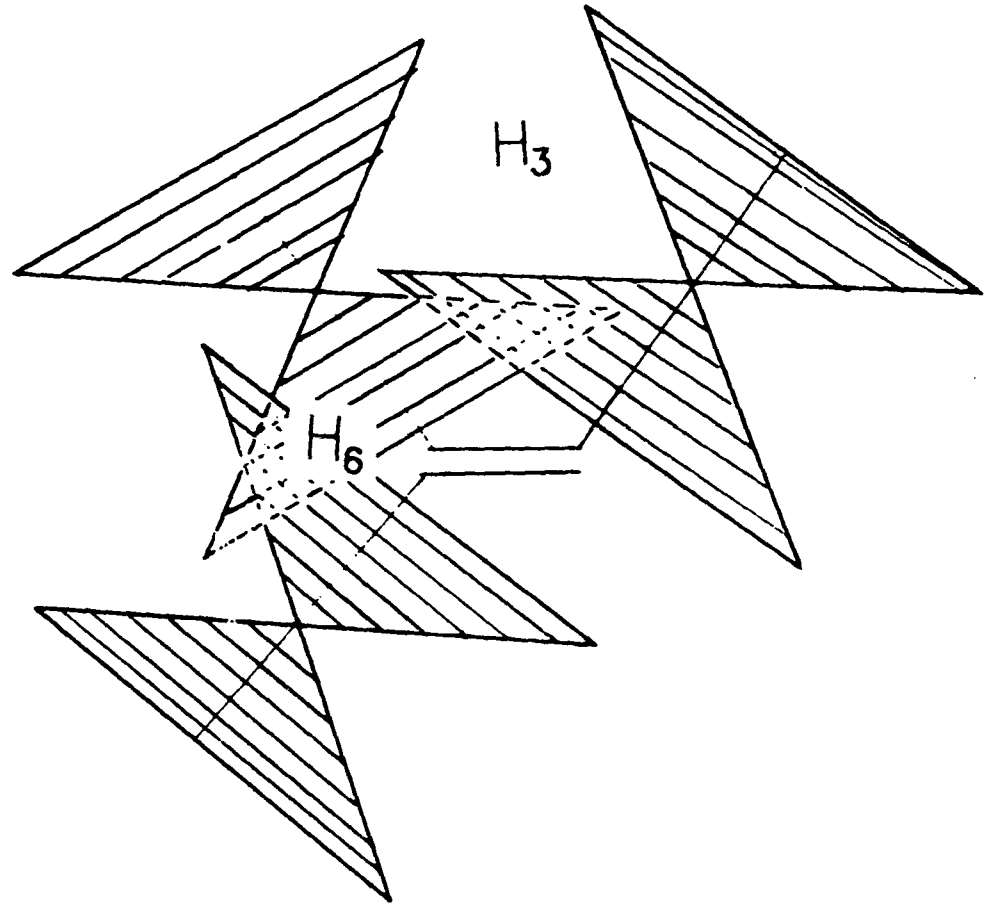

Figure IV.B.1.15: Magnetic anisotropic regions of the TCNE cyano groups
Shaded area exerts a high field shift, area perpendicular to the cyano axis exerts a low field shift. H3 is located in a low field area and H6 in a high field area.

described above, will exert on this H_3 proton a downfield shift due to its cyano groups. The complex is shown in the photograph of Figure IV.B.1.16. This downfield shift induced by magnetic anisotropy occurs concurrently with the downfield shift due to complexation. The other protons of the uncomplexed ring, being at a greater distance from the TCNE molecule, are not affected. A greater population of H_3 spins are experiencing a downfield shift than that can be attributed to complexation alone. This should result in a higher apparent equilibrium constant unique to this proton. The topographic relation described also places H_6 near the axis of the ethylene carbon - carbon π bond. This region is under the influence of the upfield shift originating from both the cyano and the ethylene groups. In contrast to the other ring protons, this effect causes both the opposite directions of chemical shifts upon complexation as well as the opposite slope in the plot of Δ vs acceptor concentration (Figure IV.B.1.11). This direction of the change of the chemical shift for H_6 is opposite to results obtained in the literature. Upon protonation of the pyridine ring all protons shift in a down field direction (46). Complexation of P2VP with the acceptor bisaacetylacetonato cobalt(II) resulted in all aromatic protons shifting in the downfield direction (51) with H_6 experiencing the greatest shift, in direct contrast to our results for H_6. For the present system the proton chemical shift must be strongly dependent upon the anisotropic magnetic environment induced by a specific topography of TCNE as described. The magnetic anisotropy exerted by TCNE must oppose the electronic effect of

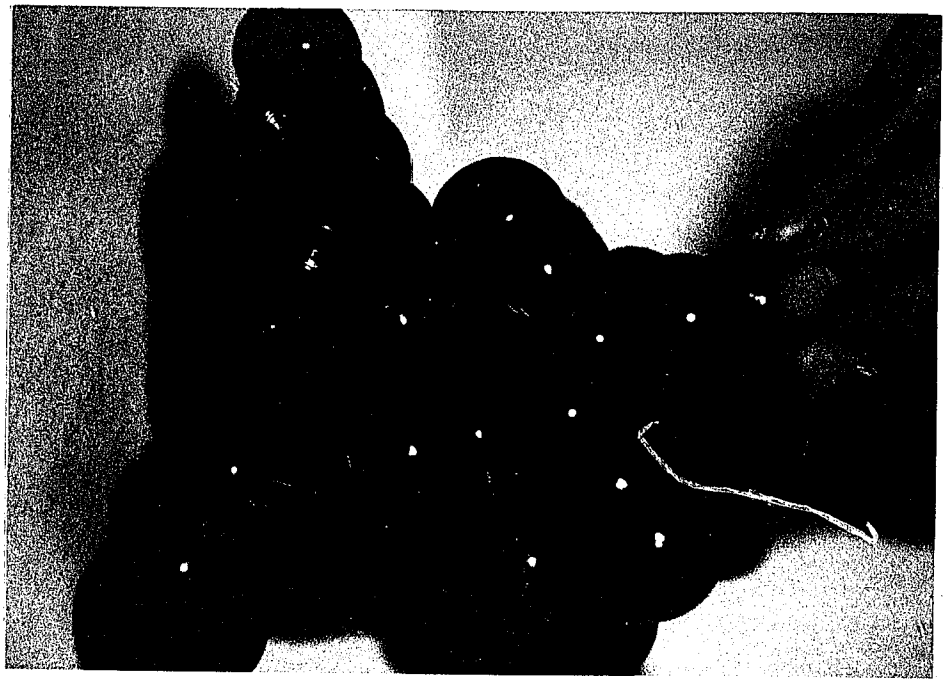

Figure IV.B.1.16: Model of the iso P2VP/TCNE charge transfer complex

complexation. Results obtained for the 2 - ethylpyridine - TCNE system reinforce the above findings.

The aromatic protons of 2EP all have downfield shifts upon complexation with TCNE (Figure IV.B.1.17). Figure IV.B.1.18 is a representative of the type of curve obtained for Δ as a function of acceptor concentration. The value of Δ_0 was well reproduced and given in table IV.B.1.8 for an order of magnitude range of initial donor concentration as calculated by the different expressions.

TABLE IV.B.1.8: Δ_0 of the varies protons derived by each equation

Equation	II.C.1.5	II.C.1.4	II.C.1.10	II.C.1.12
Proton				
H_4	.83 ±.05	.856±.008	.86 ±.03	.86 ±.03
H_3	.72 ±.04	.74 ±.01	.75 ±.03	.750±.007
H_5	.72 ±.04	.737±.007	.74 ±.02	.74 ±.02
H_6	.33 ±.01	.335±.003	.34 ±.02	.339±.004

The order obtained for Δ_0 of the different protons is given:

$$H_4 > H_3 \geq H_5 > H_6$$

This order is the same as that found for the carbon nuclei and differs from the polymeric system. The reason for the difference in order for the two systems is related to the same reason

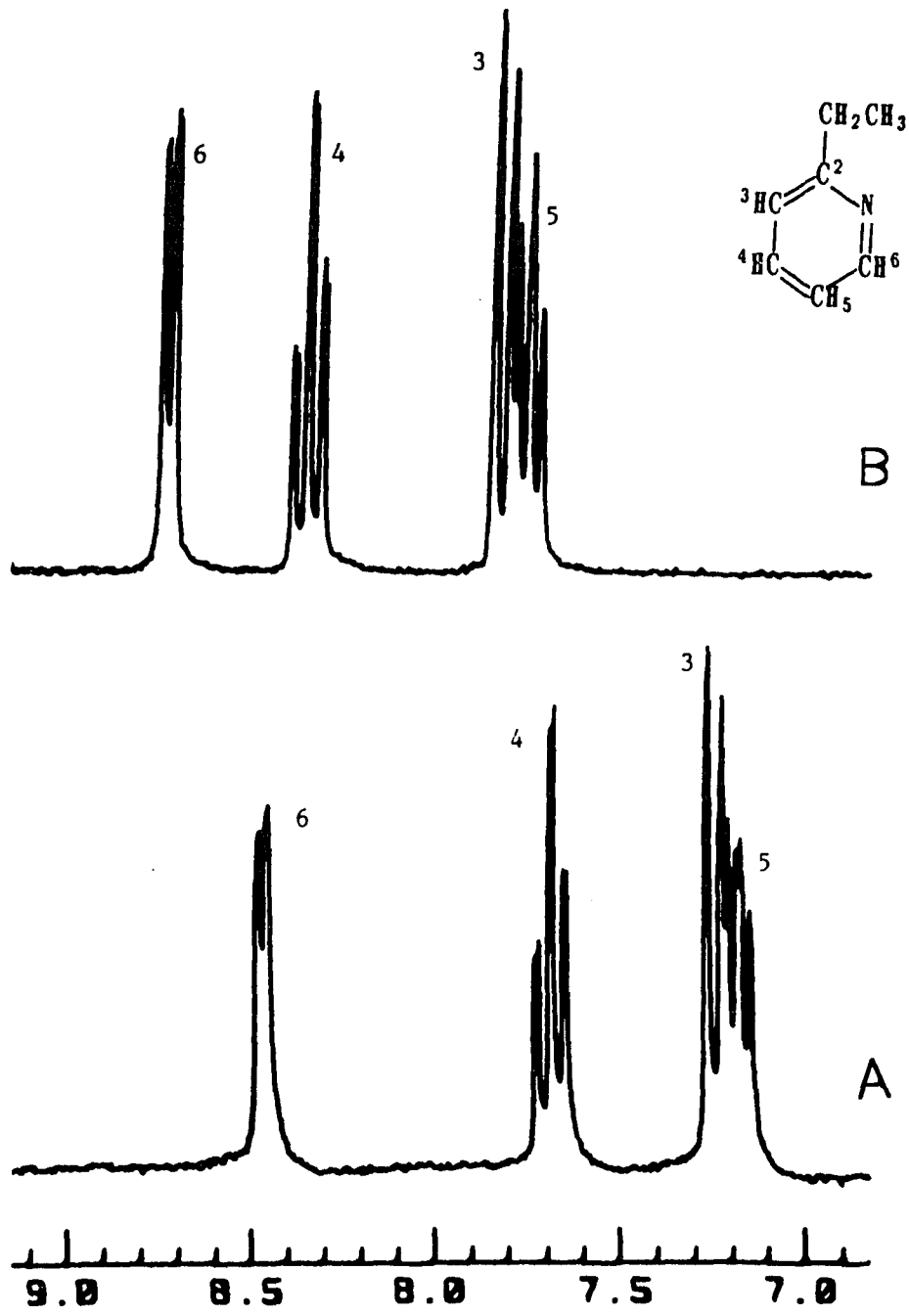

Figure IV.B.1.17: ^1H NMR spectra for 2EP in DMSO-d_6. a)free and b)in the presence of TCNE

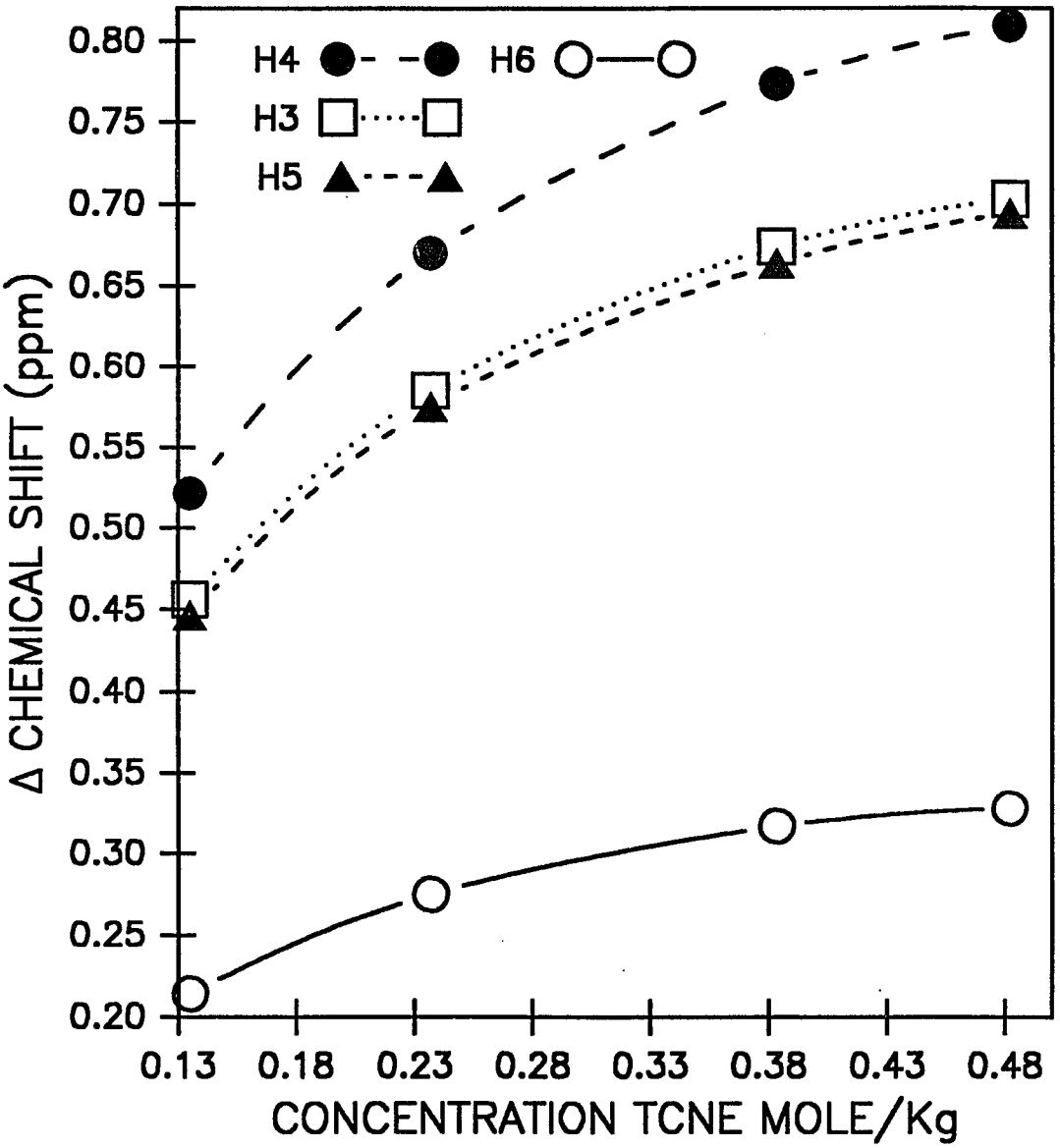

Figure IV.B.1.18: Change in chemical shift vs [TCNE] for the 2EP ring protons

yielding differences in the order for the carbon nuclei. The reason for the difference in carbon nuclei was explained by differences in overlap of the molecular orbitals of the two components. To reiterate, the alkyl group was expected to sweep an area around the site of charge transfer, leading to hindrance of complexation. This results in an increase of the distance between the TCNE ethylene π bond axis and H_6. Thus, TCNE exerts less magnetic influence on H_6 due to the rapid fall off of this effect with distance. This is further evident in that H_6 in 2EP has the smallest value of Δ_0 whereas H_6 was reported to have the greatest value of Δ_0 for the P2VP - Co(II) system (51). The influences of anisotropy and complexation are still in competition but in this case, because of the increased distance of H_6 from the source of anisotropy, complexation exerts a greater influence. H_3 was not affected because in the case of the monomeric analog there is no neighboring ring.

In evaluation of the equilibrium constant, the value was found to be concentration dependent and increased with decreasing initial donor concentration. Reproducible values were obtained only after consideration of additional unspecific shielding, AUS (section II.C.1.b). In applying this technique of extracting values for K, a correction term corresponding to a maximum correlation was considered to yield the true value for K. Figure IV.B.1.19 represents a non - linear curve obtained by use of equation II.C.1.5. Figure IV.B.1.20 is the curve obtained by AUS treatment. The value obtained by this treatment was found to be

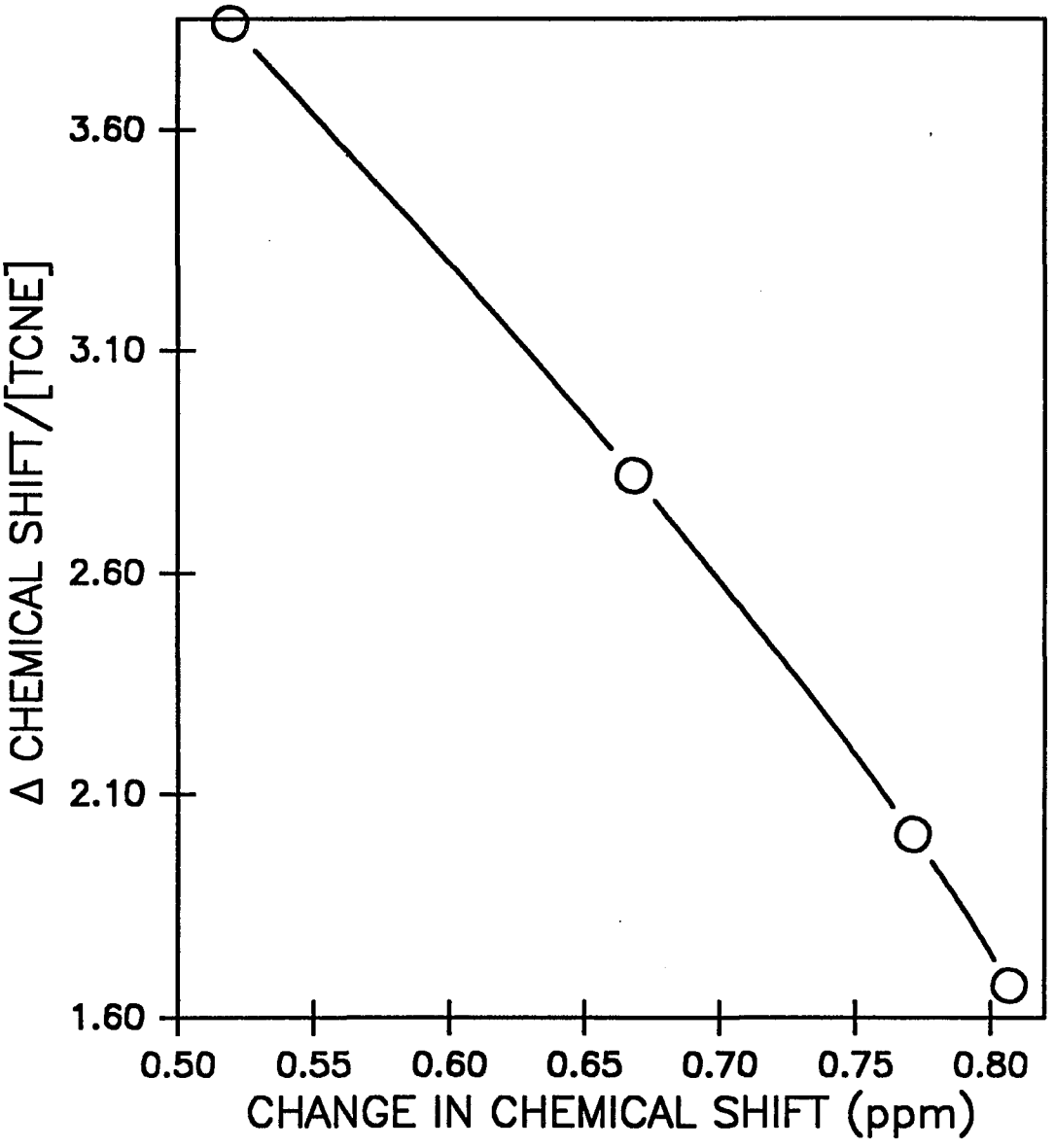

Figure IV.B.1.19: Change in chemical shift divided by [TCNE] vs change in chemical shift for H4 of 2EP

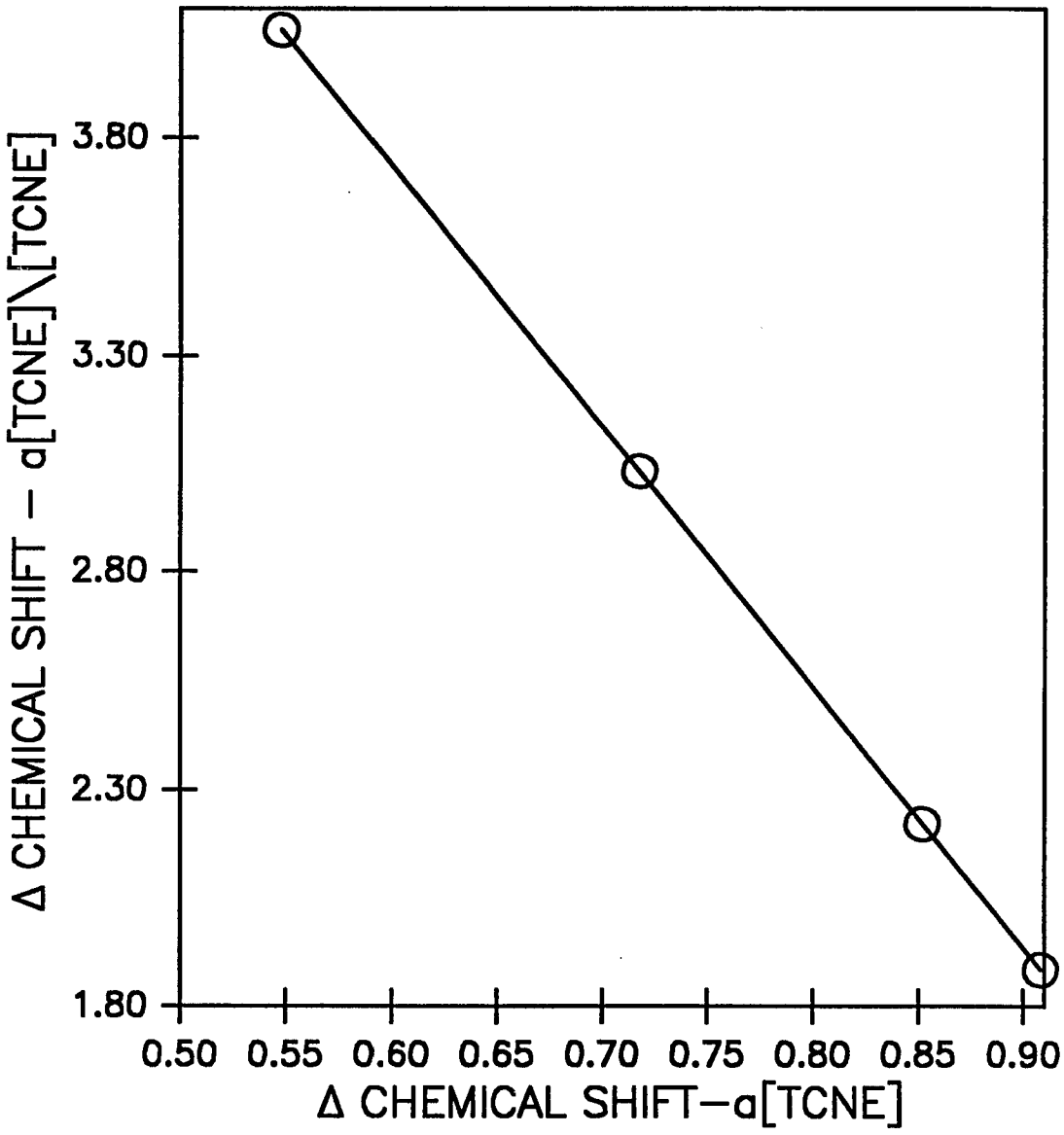

Figure IV.B.1.20: Improvement of correlation coefficient by use of AUS treatment

5.51±.37 Kg/mole for all protons of the pyridine ring. The value for the correction term, a, was consistently lower for H_6. The correction term is a measurement of AUS for the complexed nuclei and the relatively low value for H_6 indicates TCNE is less likely to approach this proton of a complex. This result reinforces the model. TCNE, when complexed as described, blocks approach of a free TCNE molecule at the site of H_6. The equilibrium constant obtained for the 2EP system also helps to verify the effect of magnetic anisotropy upon H_3 by TCNE. The topographic relation between acceptor and donor is therefore further substantiated.

Equilibrium constants were found to be significantly different between 2EP and P2VP, when P2VP was in the donor concentration range of .06 moles/Kg solution. Results obtained within the lower donor concentration for the polymer agree more closely with values obtained for 2EP, with K for P2VP being slightly higher. Clearly, a polymeric effect was demonstrated by analysis of equilibrium constants. The effect is emphasized by the need to apply AUS treatment to the monomeric analog and not the polymeric system. Higher equilibrium constants are typically explained by the acceptor becoming trapped within the polymeric domain. The acceptor coming off a pendent ring can form a complex with another ring. This occurs efficiently as the concentration of donor rings is increased within the domain. Another polymeric effect was observed by the presence of AUS in the monomeric analog but absent in the polymeric system. This difference is explained by TCNE being able to approach 2EP from

all sides while the pendent ring is blocked by the backbone. AUS is not observed because the complexed pendent ring is crowded by both the acceptor and the backbone. Free TCNE can no longer approach close enough to a complexed ring to influence the magnetic environment.

IV.C SOLID STATE NMR

Solid state NMR has been used successfully in this study to obtain important information not available by solution state NMR alone. Both position and intensity of the resonance absorption have been investigated by a variety of techniques available in the solid state experiment to yield information which complements and expands findings from the solution state. Section II.C.2 presents the basic theory of solid state NMR applied to the study of charge transfer complexes.

Figure IV.C.1 is a ^{13}C MAS absorption spectra of a)neat P2VP and b)spectrum of P2VP - TCNE complex. Chemical shifts are given in table IV.C.1.

Table IV.C.1: Chemical shifts in ppm for P2VP free and complexed

Nuclei	Free	Complexed	Difference
C_2	164.6 ± .3	160.1 ± .3	-4.6
C_6	148.7 ± .3	147.9 ± .9	-.8
C_4	135.2 ± .5	137.2 ± .5	2
$C_{3,5}$	120.8 ± .2	123.6 ± .7	2.8

The directions of change in chemical shift for the P2VP nuclei in going from the free to complexed state are the same as in solution. This suggests that the non - bonding electrons are participating in donor action and the same type of complex was formed both in solution and in the solid. The technique of solid

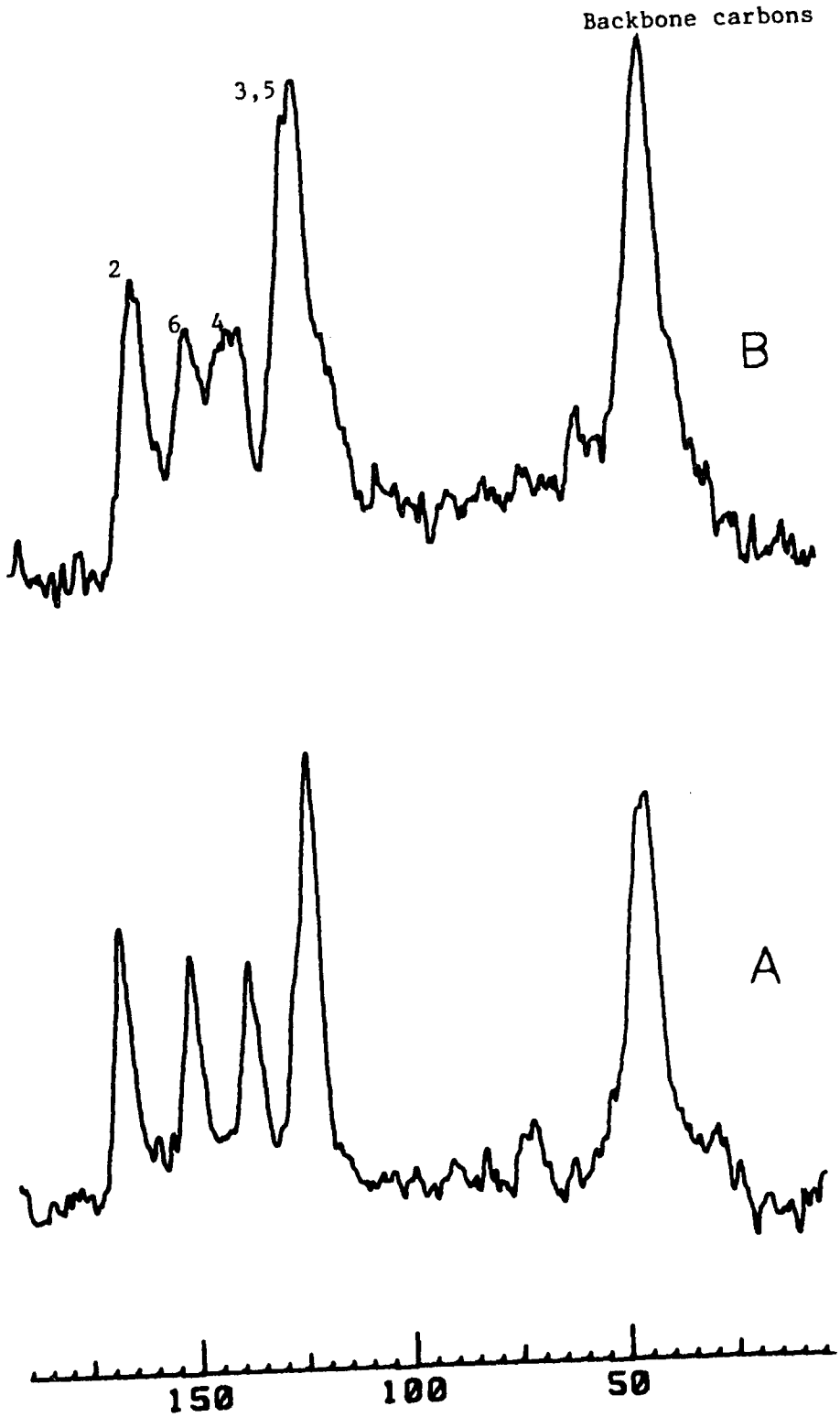

Figure IV.C.1: ^{13}C CP/MAS spectra of P2VP a)free and b)mixed with TCNE

state NMR can be used as a powerful tool in studying complexation because the pulse sequence can be manipulated in order to observe different aspects of the general Hamiltonian given in equation II.C.2.1. The absorption spectrum of Figure IV.C.1 was obtained by a typical CP/MAS experiment as described in section II.C.2. Clearly noticed is the absence of the absorption by acceptor TCNE. The acceptor, having no attached protons, was not crosspolarized under the conditions used to acquire the spectrum of Figure IV.C.1 and therefore was rendered 'invisible'. Cross - polarization and pulse sequences as discussed in section II.C.2 were applied to the systems.

Variation in contact time, T_{ct}, as described in Figure II.C.2.1 resulted in spectra in Figure IV.C.2. Graphical representations of intensity vs contact time for C_2, C_6 and the backbone carbons of P2VP are given in Figure IV.C.3. C_2 (non - protonated) has an initial build-up of magnetization which reaches a maximum at ~ 2 ms while the two backbone carbons (total of three protons attached) have passed its maximum by .4 ms and are seen to decay. C_6 (one proton attached) reaches an absorption maximum at ~ 1.8 ms. The contact time to reach these maxima reflects the number of protons most intimately associated with each individual carbon. The decay of magnetization is dependent upon the proton 'pool' and not on the proton most closely associated with a particular carbon. This is because as the contact time is increased the carbon nuclei experience polarization from proton spins not necessarily within its

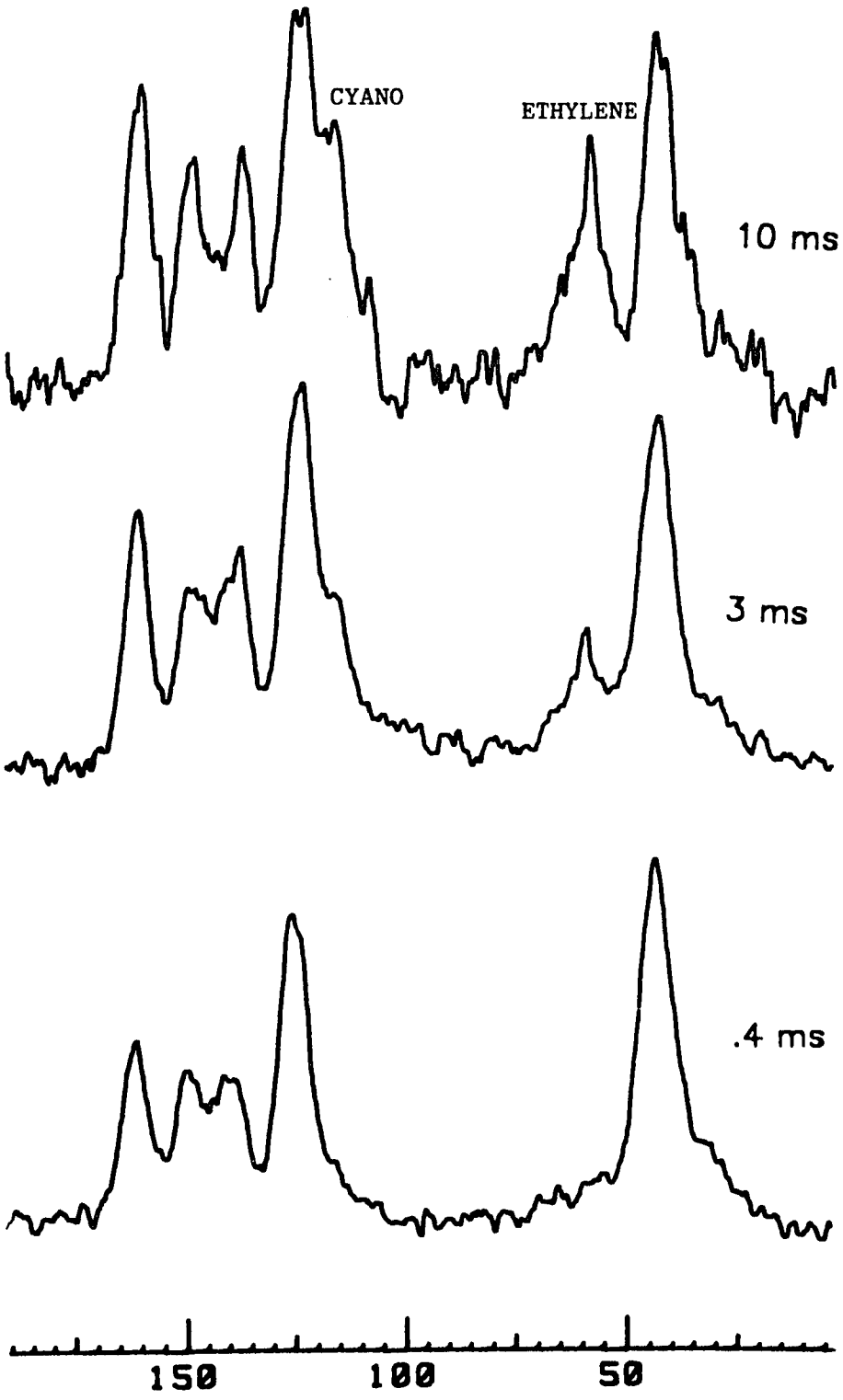

Figure IV.C.2: ^{13}C CP/MAS spectra of P2VP/TCNE complexed for different cross polarization contact times

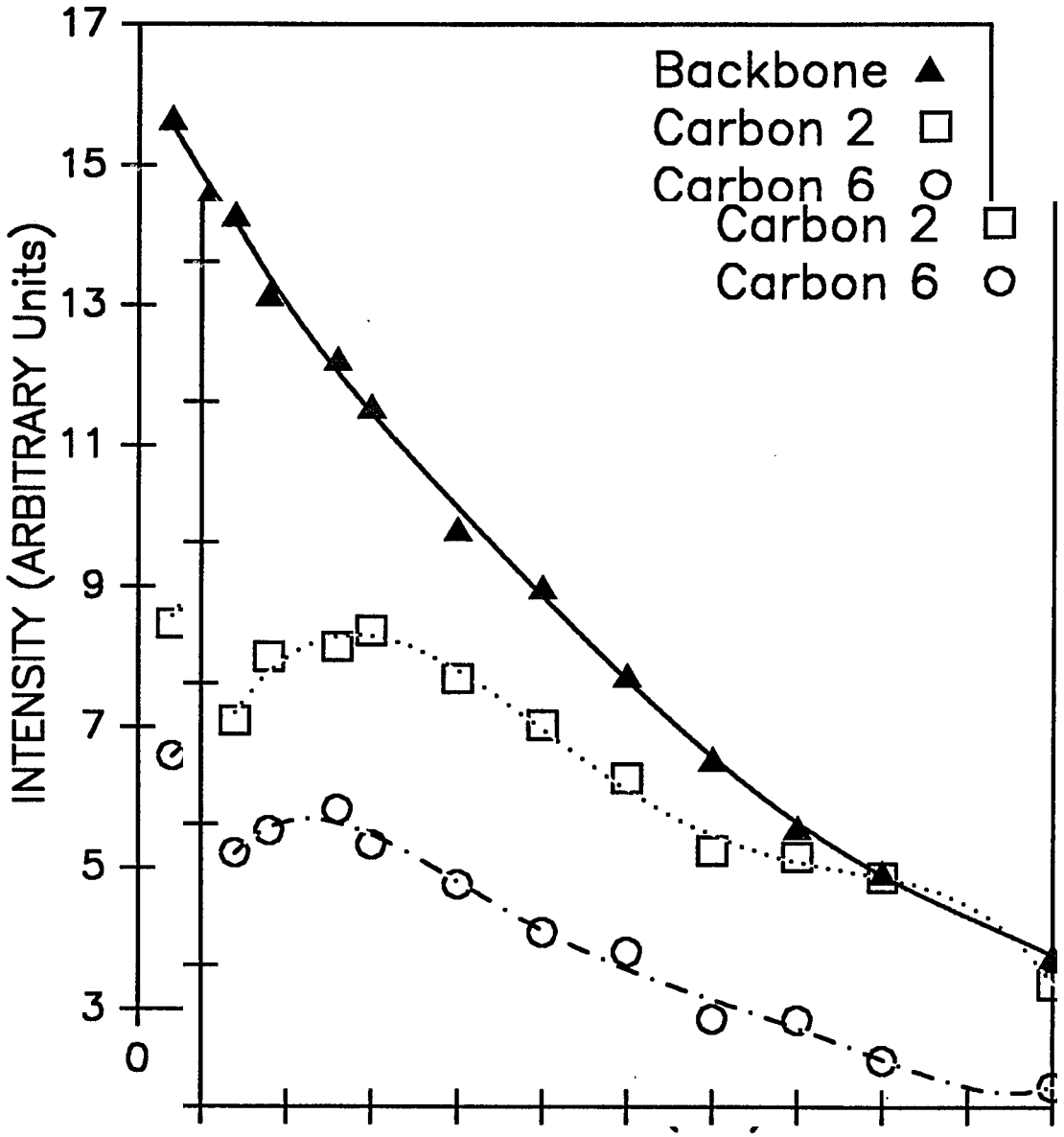

Figure IV.C.3: Intensity of C—13 absorption as a function of contact time

immediate proximity but as an average of the spin diffusion from all protons. At longer contact times, spin diffusion is lost to the lattice. Therefore cross polarization is effective within a limited proximity of ~1 nm to carbon nuclei. At longer contact times TCNE was cross polarized by the proton 'pool' on the donor. This resulted in absorptions at 58 and 116 ppm attributed to the ethylene and cyano carbon respectively. Figure IV.C.4 shows plots of ethylene and cyano carbon absorption as a function of contact time, T_{ct}. This graph clearly indicates two local maxima of contact time 1.6 and 4 ms for the ethylene carbons. The pattern for the cyano carbons indicate maxima at 2 and 5 ms. Two maxima occurring for the same absorption during the process of initial signal build-up suggests two sources of cross polarization. The rate for cross polarization is proportional to the second moment due to the proton - carbon dipolar interaction which is inversely proportional to the third power of the internuclear distance (52). This can occur if, upon complexation, the cyano groups are placed in different environments. One pair can be situated closer to the proton source and experiences more efficient cross polarization while the other pair is further removed from the proton source and is less efficiently cross polarized. This condition can be satisfied if the type of complex found in solution also exists in the solid state. It is reasonable that the maximum at 2 ms was due to the pair of cyano groups which were close to a proton source upon complexation, namely the backbone protons. The second maximum may be due to the pair of cyano groups which are

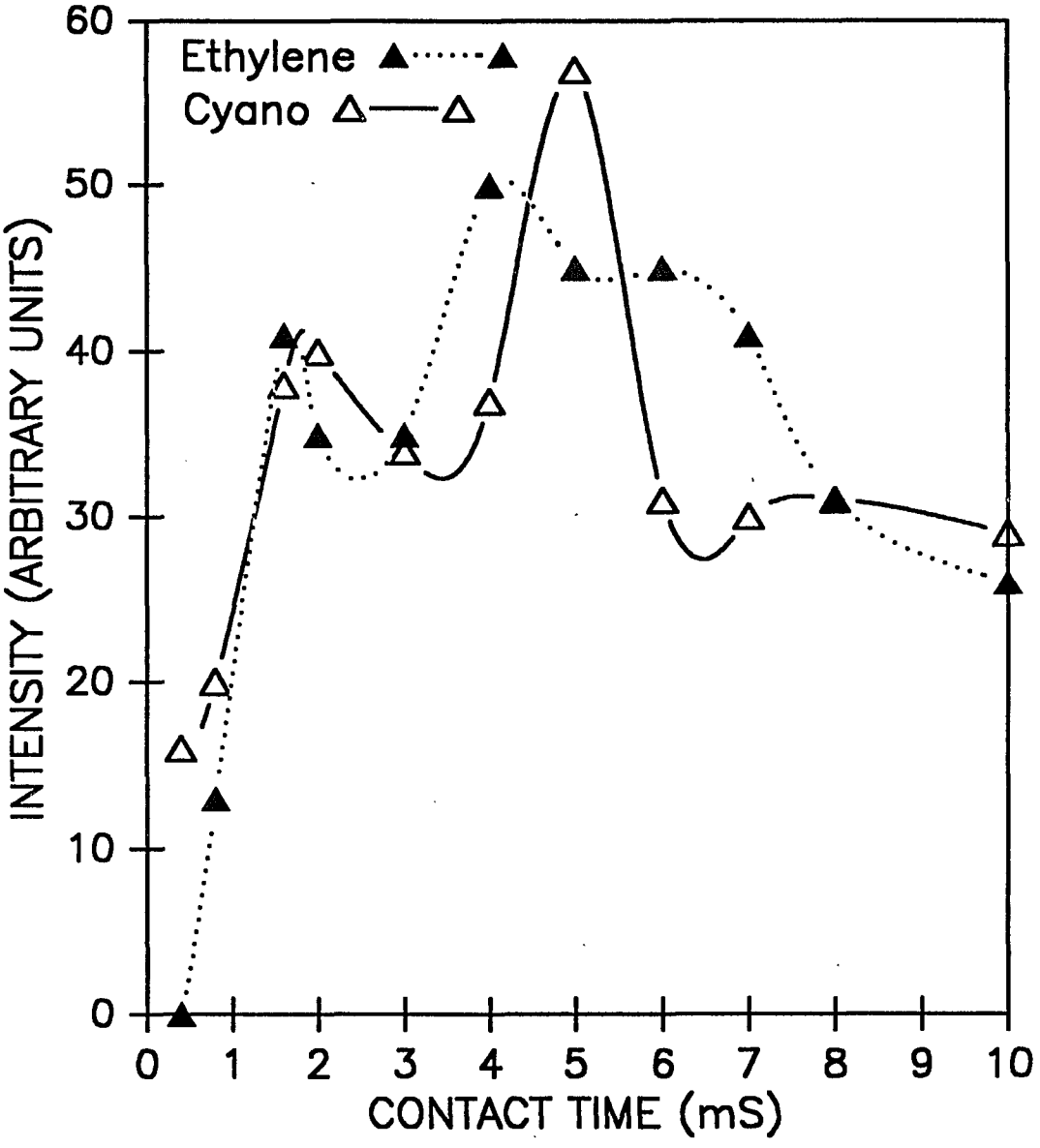

Figure IV.C.4: Intensity of C–13 absorbtion as a function of contact time for TCNE carbons

further removed from the proton pool, i.e. the pair pointing away from the backbone. The fact that they reach a maximum at only a slightly longer contact time than the ethylene carbons indicate that they are only slightly removed from the proton source. This is consistent with the suggested topography for the complex. The cyano groups are assumed to contribute to one absorption at 116 ppm. The time dependency of cross polarization for cyano carbons can be followed because they resonate at the same frequency. Certain conditions were assumed in this interpretation and follow. First, the effectiveness of cross polarization of the static dipolar environment is dependent upon the proximity of a carbon to proton spins and motion does not vary greatly for the different types of protons, e.i. aromatic and aliphatic. This assumption was justified. The aliphatic protons, being on a polymer chain, are restricted in motion and the aromatic ring has a significant barrier to rotation. $T_1\rho(H)$ processes are affected by differences in phase and not on the type of motion considered here. A second assumption was that the quantitative measurement of cyano absorption was not significantly affected by the overlap of absorption of carbons 3 and 5. This also seemed valid since the absorption at 116 ppm for carbons 3 and 5 was very small compared to its maximum at $\sim$ 124 ppm. Only the region upfield of 116ppm was integrated in obtaining the intensity for the cyano group. This assures little or no overlap by the absorption of carbons 3 and 5. An additional absorption at 136 ppm was observed when a delay was introduced in the pulse sequence as described above, *vide infra*

The decay of signal intensity as a function of contact time was observed. The contact time is given in the pulse sequence of Figure II.C.2.1 as T_{ct}. The delay for this experiment was removed so that any changes in the intensity could be related to the proton rotating - frame spin - lattice relaxation time constant, $T_1\rho(H)$, of the carbon. A relation between the intensity and the contact time was given by Stejskal et. al. (53). Under conditions of Figure II.C.2.1 with zero delay the carbon magnetization, S, was given by equation IV.C.1 (54)

$$\frac{dS}{dt} = \frac{S_0 e^{(-t/T_1\rho(H))} - S}{T_{is}} - \frac{S}{T'\rho L} \qquad \text{IV.C.1}$$

where S_0 is the maximum carbon polarization available in a matched spin - lock experiment with no dissipative processes, T_{is}, the proton - carbon matched spin - lock cross - polarization time constant and $T'\rho L$, the carbon rotating frame spin - lattice relaxation time constant in the presence of dipolar decoupling of the protons. From the condition $T'\rho L \gg T_{is}$ and $T_1\rho(H) > T_{is}$ the relation of equation IV.C.2 is given:

$$S \sim S_0 e^{(-t/T_1\rho(H))}/(1-T_{is}/T_1\rho(H)) \qquad \text{IV.C.2}$$

Thus, from a semilog plot of S vs t, $T_1\rho(H)$ can be obtained.

From the decay in carbon magnetization of the neat polymer, $T_1\rho(H)$ was found to be $\sim$ 11 ms. Upon complexation $T_1\rho(H)$ increased to $\sim$ 20 ms. Figure IV.C.5 is representative of the

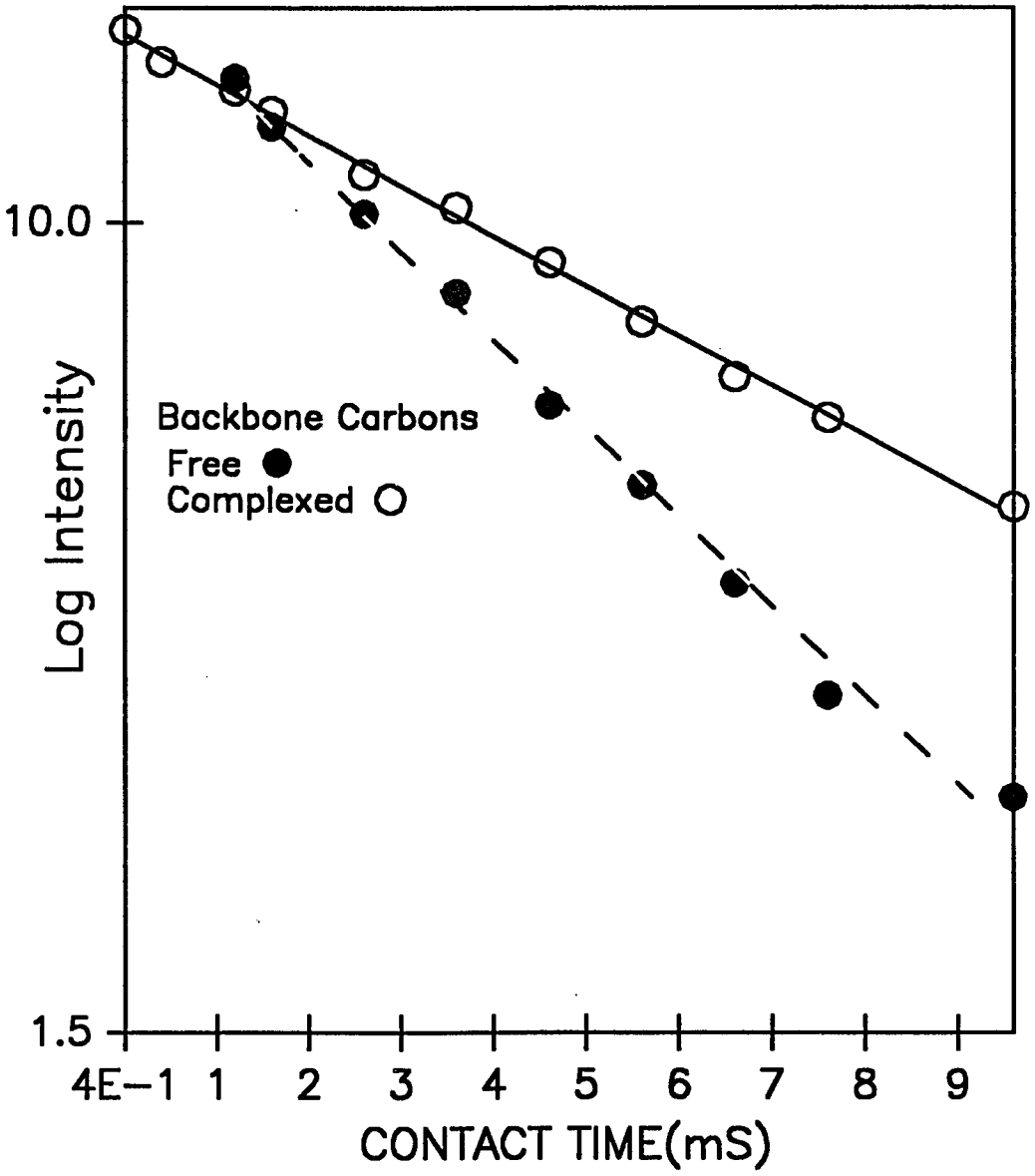

Figure IV.C.5: Semilog plot of intensity vs contact time for backbone carbons

semi - log plot. The parameter measures motion in the lower KHz range (small scale segmental motion) (55). The increased value of $T_1\rho(H)$ indicates that small scale segmental motion increased upon complexation. TCNE, upon complexation, seems to act as a plasticizer for the system. Insertion of a TCNE molecule must cause chains to move away from one another thus creating microvoids in which motion may increase.

As indicated above, observation of complexed acceptor resonance absorption was possible under proper conditions. By modifying the pulse sequence much information was obtained. In order to best interpret the results presented here a comparison was made with the work of Blann et. al. on the hexamethylbenzene (HMB) - TCNE complex. Observations were made for the isolated 1:1 HMB - TCNE charge - transfer complex with a contact time of 10 ms. The TCNE absorption was observed in the CP/MAS as low intensity peaks at 109 ppm (cyano) and 99 ppm (ethylene). The contact time was increased to as long as 20 ms without a maximum intensity being reached for the ethylene or cyano ^{13}C absorptions. The low intensity may be due to a longer distance (when compared to the present systems) of TCNE to protons on the donor, or perhaps because of ineffective transfer of polarization by methyl protons. The methyl protons disperse much of their polarization to the lattice due to rapid rotation of the group. Cross polarization is more effective for the polymeric system in transfer of polarization intermolecularly. Polarization transfer originating from methine (CH) and methene (CH_2) protons, which

experience less motion than methyl (CH_3) protons, are considered efficient (65). This condition is advantageous in the delay decoupling experiment where non - mobile protons allow the attached carbons to dephase efficiently. Protonated carbon resonance absorption can be attenuated such that only carbons interacting less efficiently by dipolar means have their intensities preserved. By this technique, non - protonated carbons can be separated from protonated carbons. Results obtained for the PVP - TCNE charge transfer complex by a delayed decoupling cross - polarization pulse sequence will be discussed and compared with the results obtained by Blann et. al (27).

Upon observation of a resonance absorption at 57.8 ppm at longer cross polarization times, a delayed decoupling experiment was deemed necessary to help varify the absorption as originating from the TCNE molecule. It was expected that resonance absorption due to TCNE would be preserved since TCNE has no directly bonded protons. Insertion of a delay of 100 μs, as described above and shown in Figure II.C.2.1, resulted in the spectrum of Figure IV.C.6a. Attenuation of the protonated carbons in the P2VP - TCNE complex reveal absorptions at approximately 161, 136, 116 and 58 ppm. The absorption at 161 is due to the non - protonated C_2 of the polymer. The remaining absorptions are attributed to TCNE. These TCNE absorptions were much different from those of TCNE complexed with HMB as observed by Blann et. al. The ethylene carbons appeared at much higher fields. The absorption of 136 ppm follows the absorption at 114

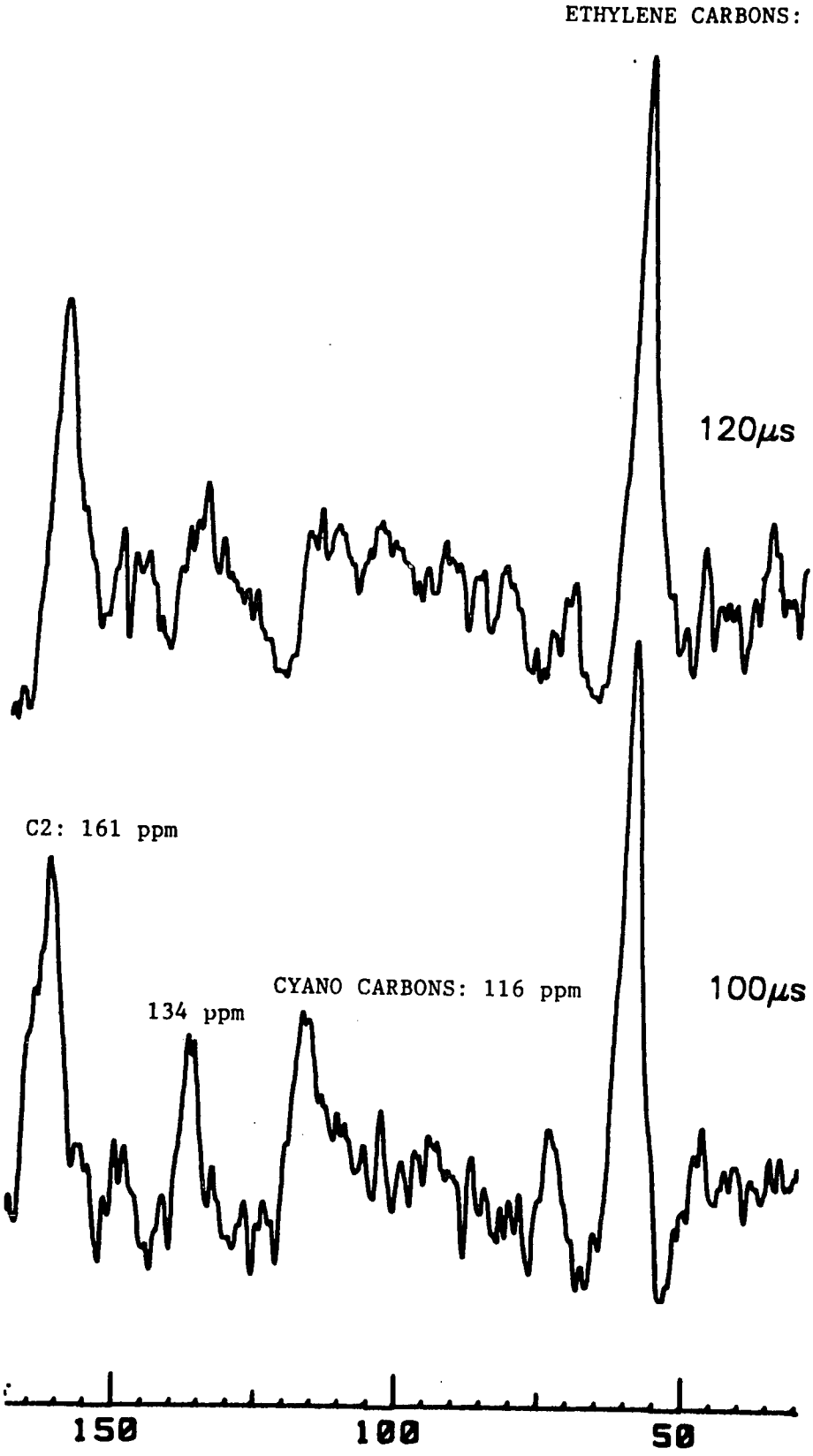

Figure IV.C.6: Delayed decoupled spectra of P2VP/TCNE

ppm in intensity when the delay was varied. Both absorptions were largely eliminated at a delay time of 120 μs as seen in Figure IV.C.6b while the absorptions at 161 and 58 ppm retain relatively large intensities.

The large upfield chemical shift observed for the ethylene carbons of TCNE for the present system compared to the chemical shift for TCNE in the HMB - TCNE complex can be attributed to electron transfer into the LUMO of the acceptor molecule, resulting in bond expansion. This leads to a high field shift, i.e. a lowering of the term $< r^{-3} >_{2pn}$ of equation IV.B.1.1. Blann et. al. had observed the cyano group carbons at 109 ppm. The 7 ppm downfield shift from 109 ppm for the present systems is surprising from the viewpoint of more efficient electron transfer as argued previously. Other factors influencing the chemical shift of the cyano group in the polymeric system relative to the hexamethylbenzene - TCNE system may be involved. It is known that the $\pi : a\pi$ systems have geometries with the plane of the TCNE molecule parallel and above the plane of the benzene ring (57,58). The intermolecular distance is 3.50 A (59) for benzene - TCNE. This would place the cyano group carbons in a region of upfield shift due to the ring current. The methyl groups, in addition, hinder the positioning of the cyano groups close to the plane of the ring. In the P4VP - TCNE system the heteroatom is in a position where the non - bonding electrons can achieve good overlap with the LUMO of the ethylene π bond. This causes the cyano group carbons to be aligned above and below the plane of

the pyridine ring and located in a region where the deshielding effect of the ring current will be strong, exerting a downfield shift influence. This difference in chemical shift, i.e. between 109 and 116 ppm, is the net result of the shielding effect in the HMB system and the deshielding effect in the present system. In the case of the P4VP system an absorption was observed at 114 ppm.

The absorption at 135 ppm observed under the conditions of the delay decoupling experiment, can not be absolutely explained at the present. It may be partly due to cyano groups of TCNE close to the polymer chain yet not complexed with a pyridine ring. These uncomplexed TCNE molecules can be associated with one another, e.g. in dimers, resulting in some of the cyano groups placed in the deshielding zones. It may also be speculated that the absorption is due to a higher symmetry of the complex with the cyano groups in magnetically different environments. This is reinforced by the lack of this additional absorption for the P4VP system. If complexation is at the nitrogen, then the cyano groups should be magnetically equivalent in the case of P4VP. Therefore an additional absorption is not expected. However, because the resonance is significantly downfield from the absorption at 116 ppm, the assignment of this absorption to the cyano carbons is highly questionable.

The extensive charge transfer from the pyridine ring to TCNE was further investigated by FT-IR. Figure IV.C.7 shows an IR

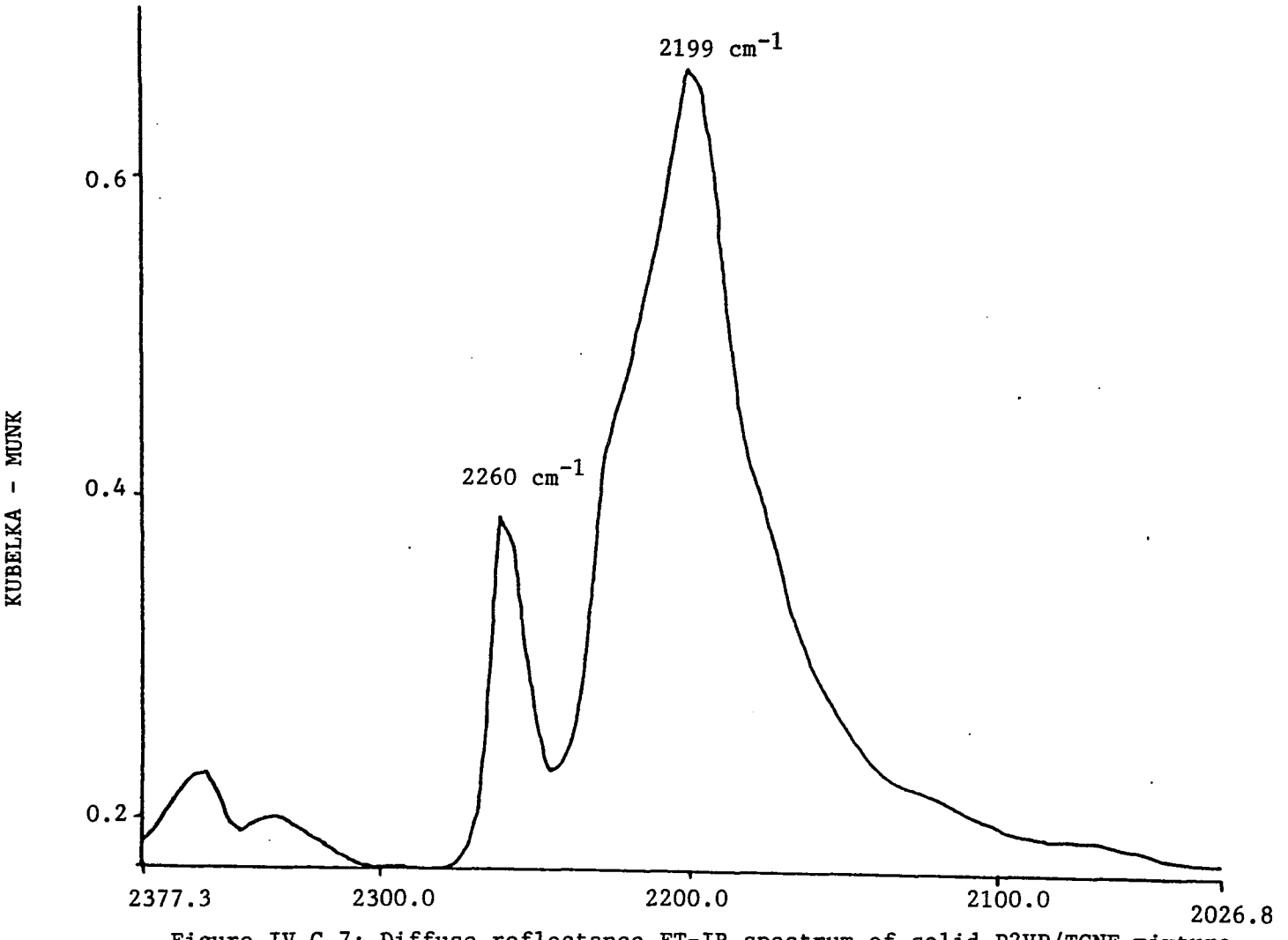

Figure IV.C.7: Diffuse reflectance FT-IR spectrum of solid P2VP/TCNE mixture

spectrum for P2VP - TCNE complex. The absorptions in the region of 2300 to 2100 cm^{-1} are due to the cyano groups. Figure IV.C.8 shows the details in this region for TCNE alone. A new strong absorption is observed at 2199 cm^{-1}. We attribute this shift toward lower wavenumber to the weakening of the C≡N bond. Charge transfer to the LUMO of the double bond leads to further increase in charge for the cyano group. The increased negative charge is expected to decrease the frequency due to a decrease in bond order (60). In the case of TCNE anion, the new absorptions are located at 2190 and 2150 cm^{-1}. Our broad absorption at 2199 cm^{-1} is in line with the expectation for partial charge transfer. This large shift compared to the case of HMB - TCNE (61) clearly supports the large upfield shift for the ethylene carbons to 58 ppm.

Based on experimental results as well as energetic considerations a complex of the type $\pi:a\pi$ must be ruled out for the P2VP - TCNE system. If it is argued that the P2VP - TCNE complex is of the same geometry as the benzoid - TCNE complexes then an absorption further downfield of 58 ppm should be observed. The possibility of two types of complexes must be ruled out since only the one absorption for the ethylene carbons was observed. It should also be noted that an absorption at ca. 116 ppm is seen in both the P2VP and P4VP systems because both systems form the same type of charge transfer complex.

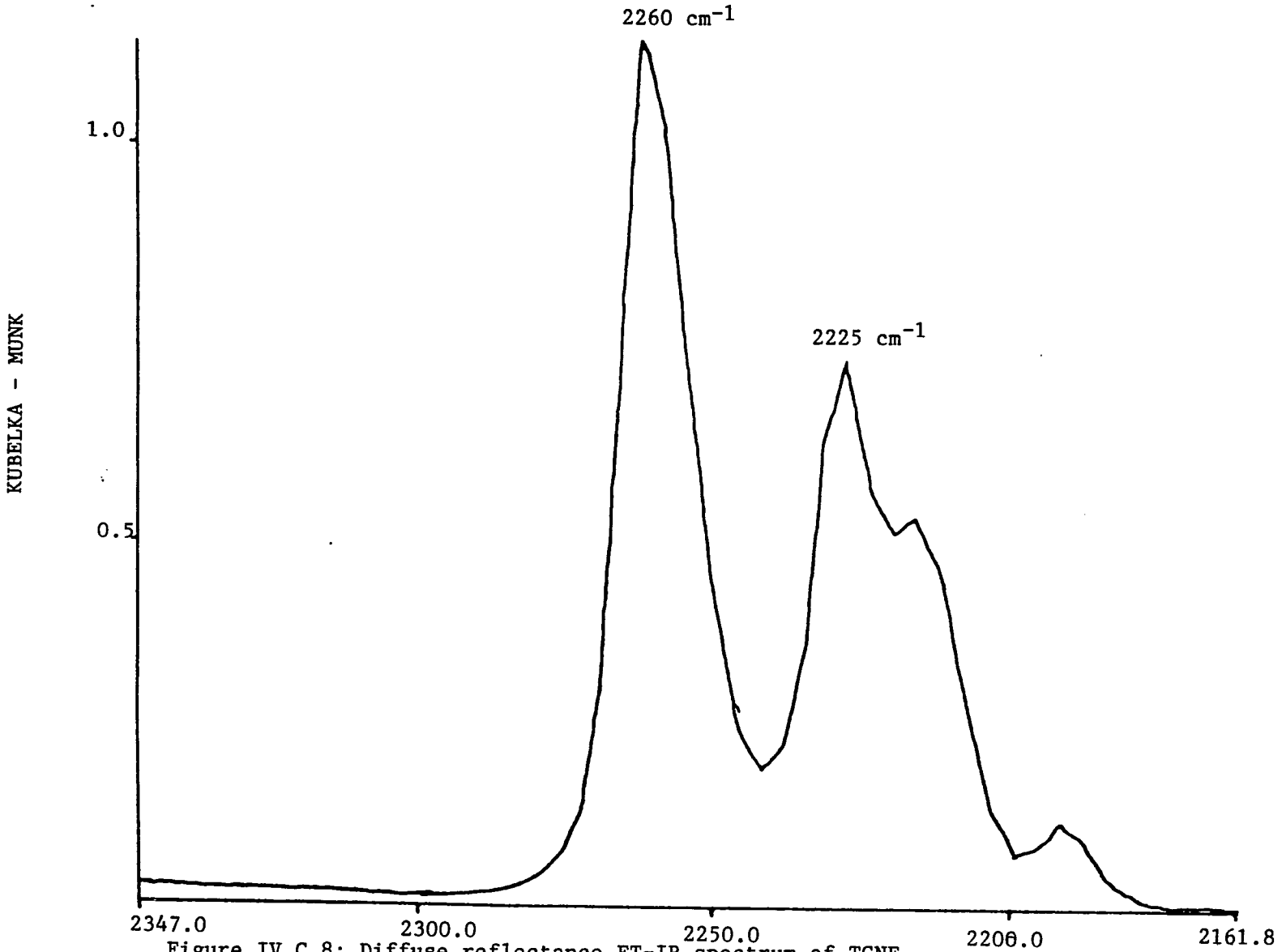

Figure IV.C.8: Diffuse reflectance FT-IR spectrum of TCNE

IV.D ELECTRON SPIN RESONANCE

Electron spin resonance absorptions were observed for the mixtures of P2VP and P4VP with TCNE. In solution the TCNE radical anion was observed (Figure IV.D.1) for both P4VP and 4EP. The nitrogen hyperfine constant, a_n, was determined to be 1.6 G, in complete agreement with the literature value for TCNE anion radical (61). Donor radicals formed for the 2EP ring and its polymer were not well resolved. Figure IV.D.2 shows a spectrum of the P2VP radical in the solid (precipitated from solution). The absorption is devoid of clear hyperfine structure. It appears to be asymmetric, most likely due to the presence of both TCNE and polymer radicals. Figure IV.D.3 represents the absorption obtained for both P4VP and poly(4-vinylpyrimidine) in the solid, i.e. a seven line spectrum with a hyperfine splitting constant of 7 G. The detailed assignment for this radical can not be established at this time. However, it can be concluded that the paramagnetic species involves delocalization into the ring. Power saturation studies indicate that one signal dominates.

The absorptions intensities were obtained over a series of ratios of TCNE to donor by double integration. For the P2VP (atactic, isotactic and low molecular weight) plots of mole spin/mole TCNE vs donor/TCNE yield maximums at a donor/TCNE ratio of 4 (Figure IV.D.4). The same treatment for P4VP yields a maximum at a ratio of 2 (Figure IV.D.5). At a one to one ratio,

the level at which solid state NMR was conducted, concentration of the paramagnetic center is ca. 1 to 2 spins per one thousand rings. This ESR data clearly shows that complete electron transfer did take place, but not to an extent to affect NMR measurement. In a separate series of experiments, at last 90% of the carbon signal was recovered for these systems.

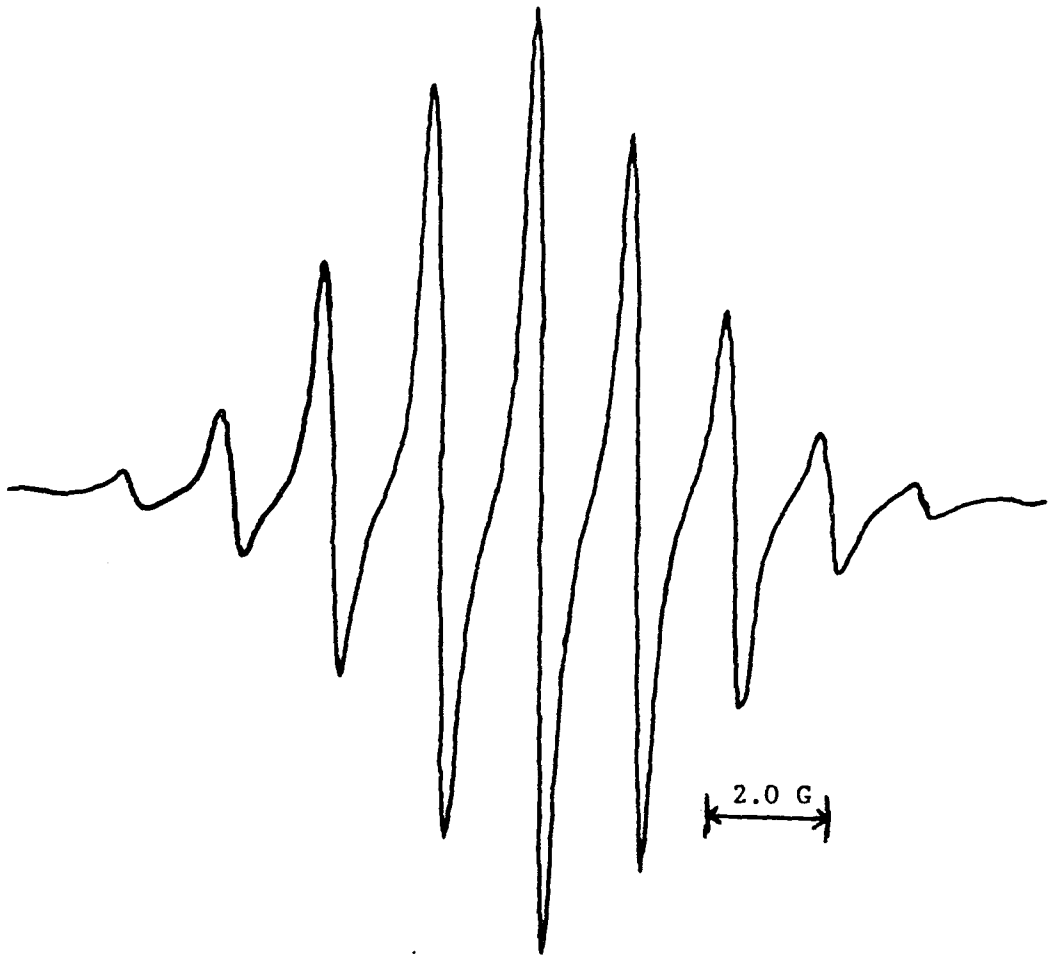

Figure IV.D.1: TCNE radical anion formed in solution of TCNE/P4VP in DMSO

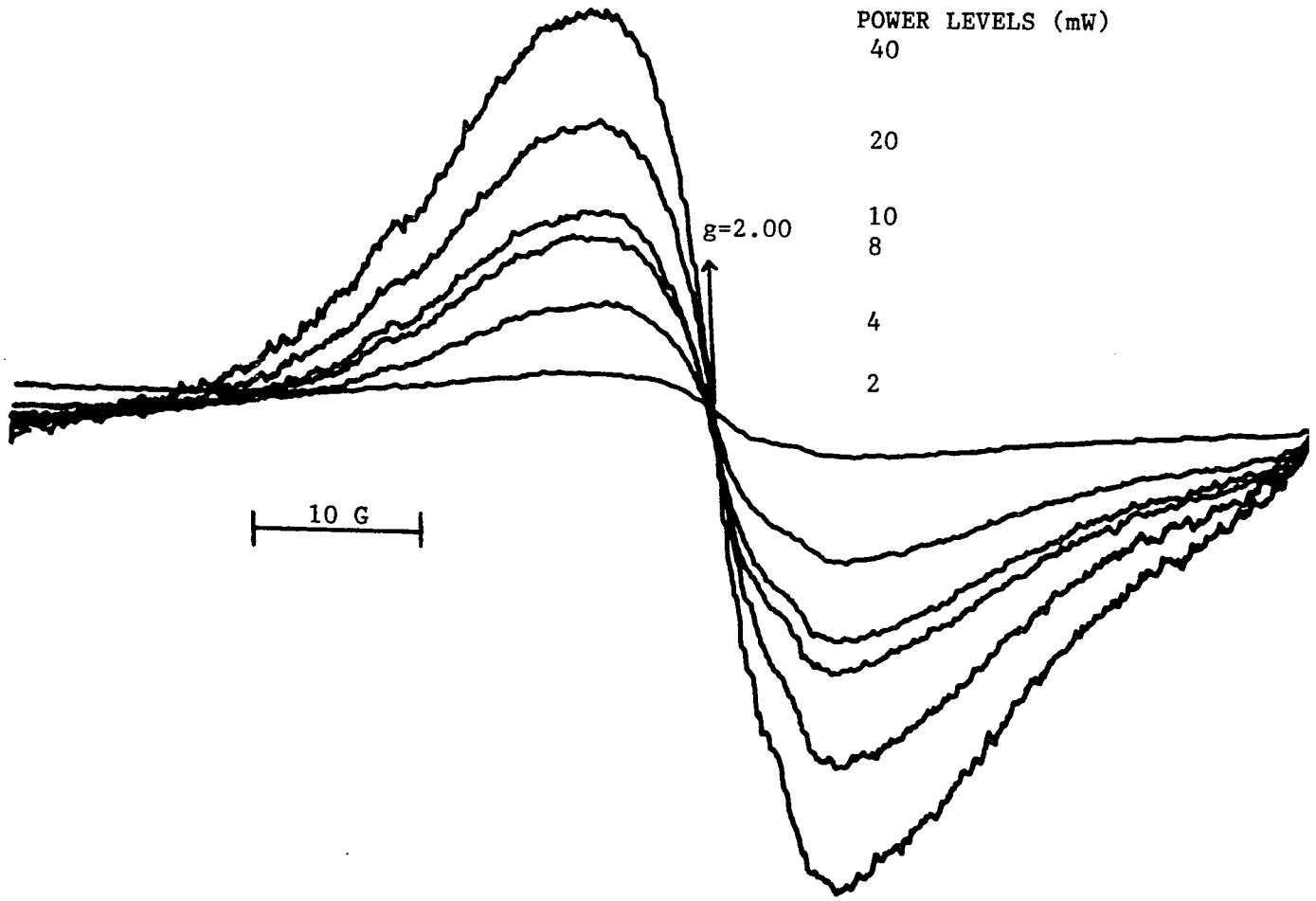

Figure IV.D.2: Spectrum of the P2VP radical formed by mixing with TCNE

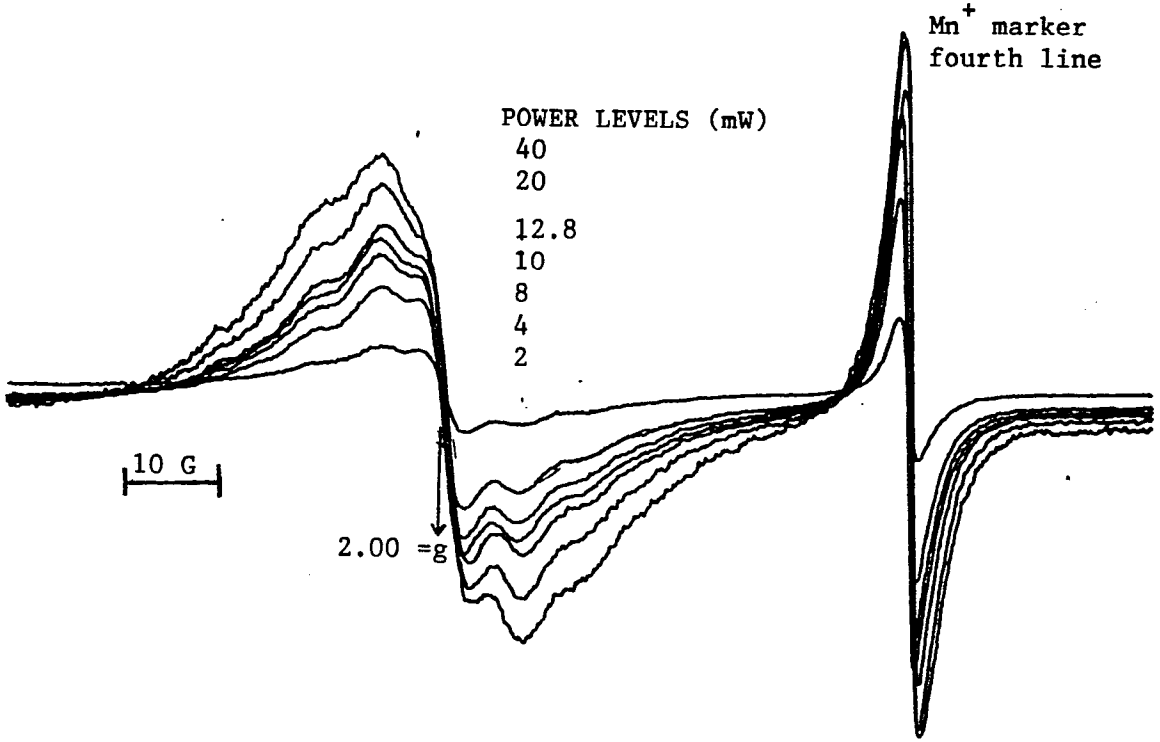

Figure IV.D.3: ESR absorption of P4VP/TCNE solid mixture

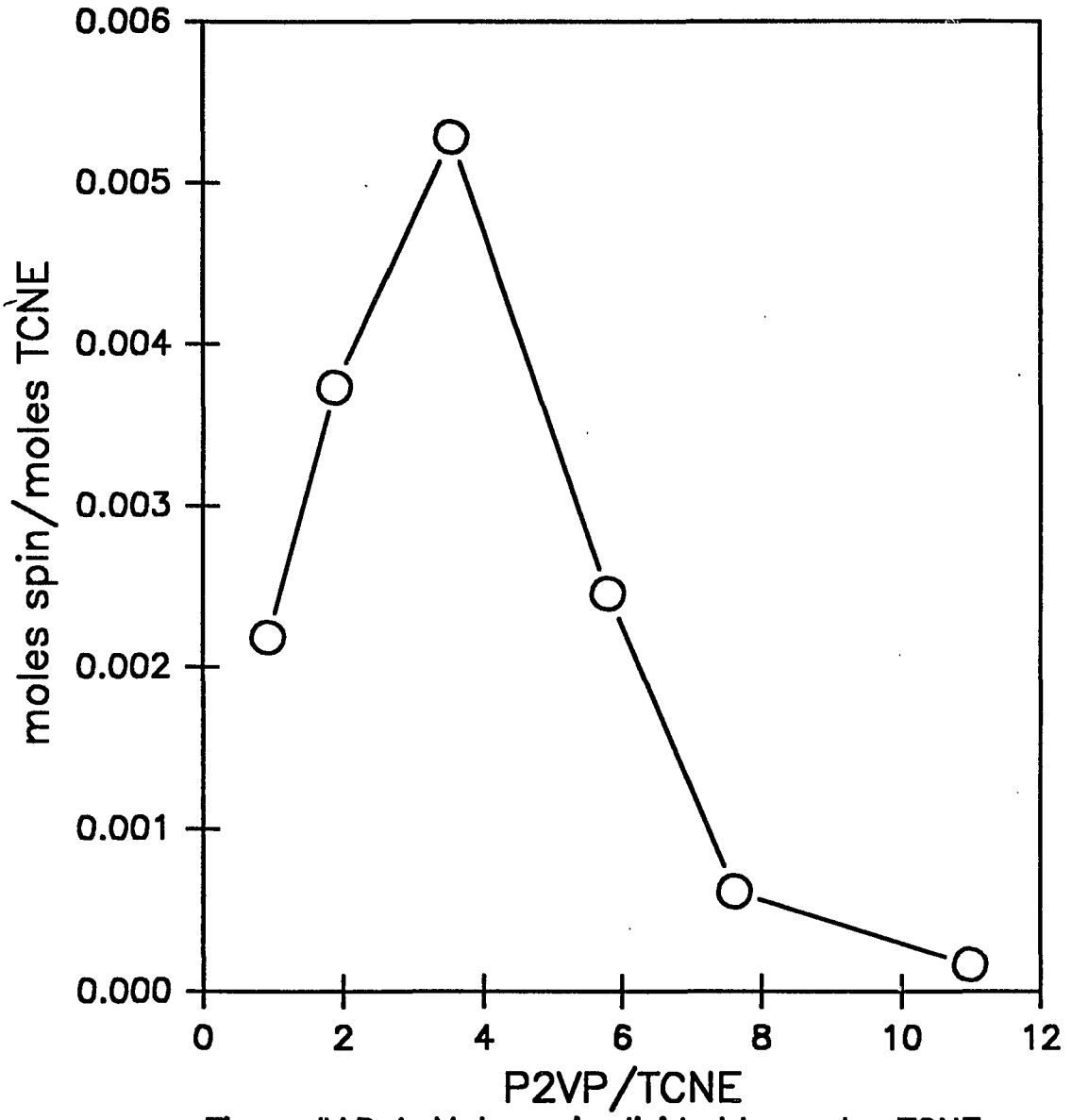

Figure IV.D.4: Moles spin divided by moles TCNE vs ratio P2VP:TCNE for P2VP

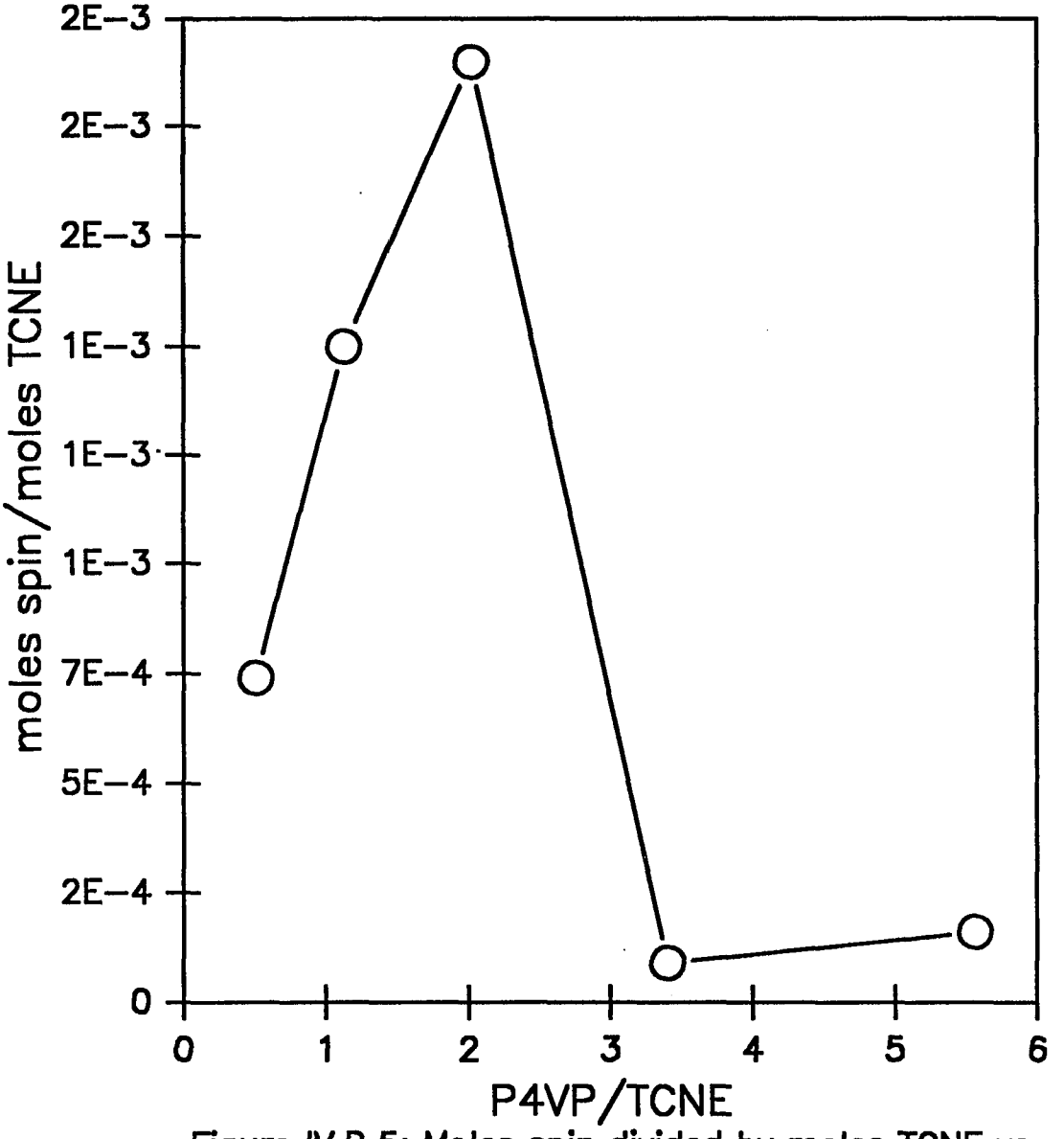

Figure IV.D.5: Moles spin divided by moles TCNE vs ratio P4VP:TCNE for P4VP

V SYNTHESIS OF POLY(4-VINYLPYRIMIDINE)

Poly(4-vinylpyrimidine) P4vPm was synthesized by a new pathway (adapted from ref. 62) as indicated in Scheme V.1.

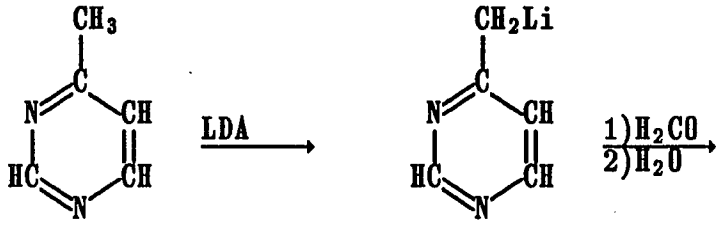

4-methylpyrimidine

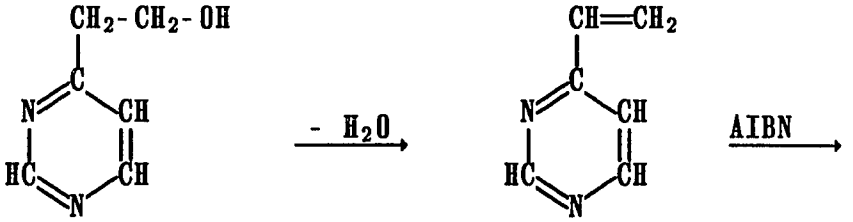

4-(β-hydroxy ethyl)-pyrimidine

4-vinylpyrimidine

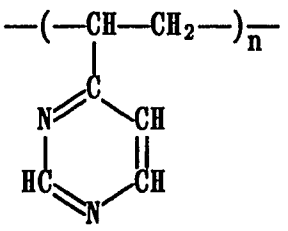

Poly(4-vinylpyrimidine)

SCHEME V.1

Product yield of the intermediate, 4-(β-Hydroxyethyl)-pyrimidine, was significantly improved over the method described by C.G. Overberger et. al. (63). This alcohol was dehydrated by three different methods, each resulting in the vinyl compound. The monomer was polymerized by AIBN thermally initiated radical

polymerization. In addition, one of the dehydration methods resulted in monomer as well as thermally polymerized P4vPm.

New synthetic methods were used to obtain the alcohol and the vinyl intermediates. Other reaction pathways attempted included: *A*) high pressure reaction of formalin solution with 4-methylpyrimidine as starting material to give the alcohol, *B*) reaction of 4-methylpyrimidine, acetic anhydride and *a*-polyformaldehyde in a sealed polymerization tube to give the vinyl compound and *C*) by reaction of 2-bromopyrimidine with vinylmagnesium bromide in THF to yield 2-vinylpyrimidine. The vinyl product was obtained from method *A* as well as that of Scheme V.1, the later gave the greater yield. The one step reaction routes, *B* and *C* were not sucessful in producing vinyl compound. A newly developed method for dehydration of the alcohol intermediate to form 4-vinylpyrimidine in high yield have also been used to establish mechanistic pathways for dehydration.

V.1 Synthesis of 4-(β-Hydroxyethyl)-pyrimidine

V.1.a Synthesis by Pyrimidinylmethyllithium intermediate

One hundred ml of a 1.5 M solution of Lithium diisopropylamide (LDA) mono(tetrahydrofuran) in cyclohexane was transferred under dry nitrogen into a 1000 ml 3-neck-flask equipped with a magnetic stirrer. To this solution 500 ml of THF was added. Freshly distilled 4-methylpyrimidine (106 mmoles) was

then added. The reaction mixture became dark red in color. To this solution of newly formed 4-pyrimidinyllithium dry formaldehyde gas was added. The gas was generated by heating dry α-formaldehyde at high temperature (200 - 210^{0}C). The generated formaldehyde gas was passed through a drying tube filled with phosphorus pentoxide and collected in a trap at -78^{0}C. This purified formaldehyde was allowed to condense slowly into the reaction solution by warming the trap to room temperature. The reaction flask was partially submerged in an ice bath. The solution was allowed to react for an hour and then placed in a separatory funnel. Water was added to the solution until no more lithium hydroxide precipitate formed. The water and the organic layer were subjected to distillation to remove the solvents.

The water layer contained alcohol and was free from 4-methylpyrimidine. The alcohol of the water layer was then purified further. After the removal of most of the water, a precipitate together with a high boiling red liquid remained. THF was used to collect the product from the liquid and the solid. The solid was then refluxed in THF to further remove any trapped alcohol. The solid was redisolved in water and the process repeated. The solvent, THF, was removed from the isolated product. Addition of methanol to the remaining liquid led to the formation of a precipitate. Final removal of the precipitate, THF and methanol resulted in 5.6 grams of highly pure product.

The organic layer also contains product but to a lesser extent. After removal of solvent, methanol was added and the removal of the formed precipitate resulted in ≈ 2 grams of pure product.

A total of 7.8 grams of alcohol containing small amounts of methanol was isolated. Quantitative proton NMR measurement with cyclohexane as an internal standard indicated an amount of 0.062 moles of product, a percent yield of 58%. About 0.12 grams of methanol could not be removed from the product. Figure V.1.1 shows a proton NMR spectrum with its assignment for the isolated product.

V.1.b Synthesis of 4-(β-Hydroxyethyl)-pyrimidine by high pressure reaction

An alternative method used to obtain the alcohol was by reacting 4-methylpyrimidine with a formalin solution under nitrogen pressure as described (64). A typical reaction mixture contained twenty grams of 4-methylpyrimidine (0.19 moles) in 40 ml of H_2O, thirty grams of 37% formalin (0.33 mole) and a catalytic amount of piperidine (0.7 g). The reaction was carried out under nitrogen pressure (ca. 170 - 180 psi) at 160 - 165°C for at least 6 hours. Although alcohol had formed, the mixture contained a large amount of starting material.

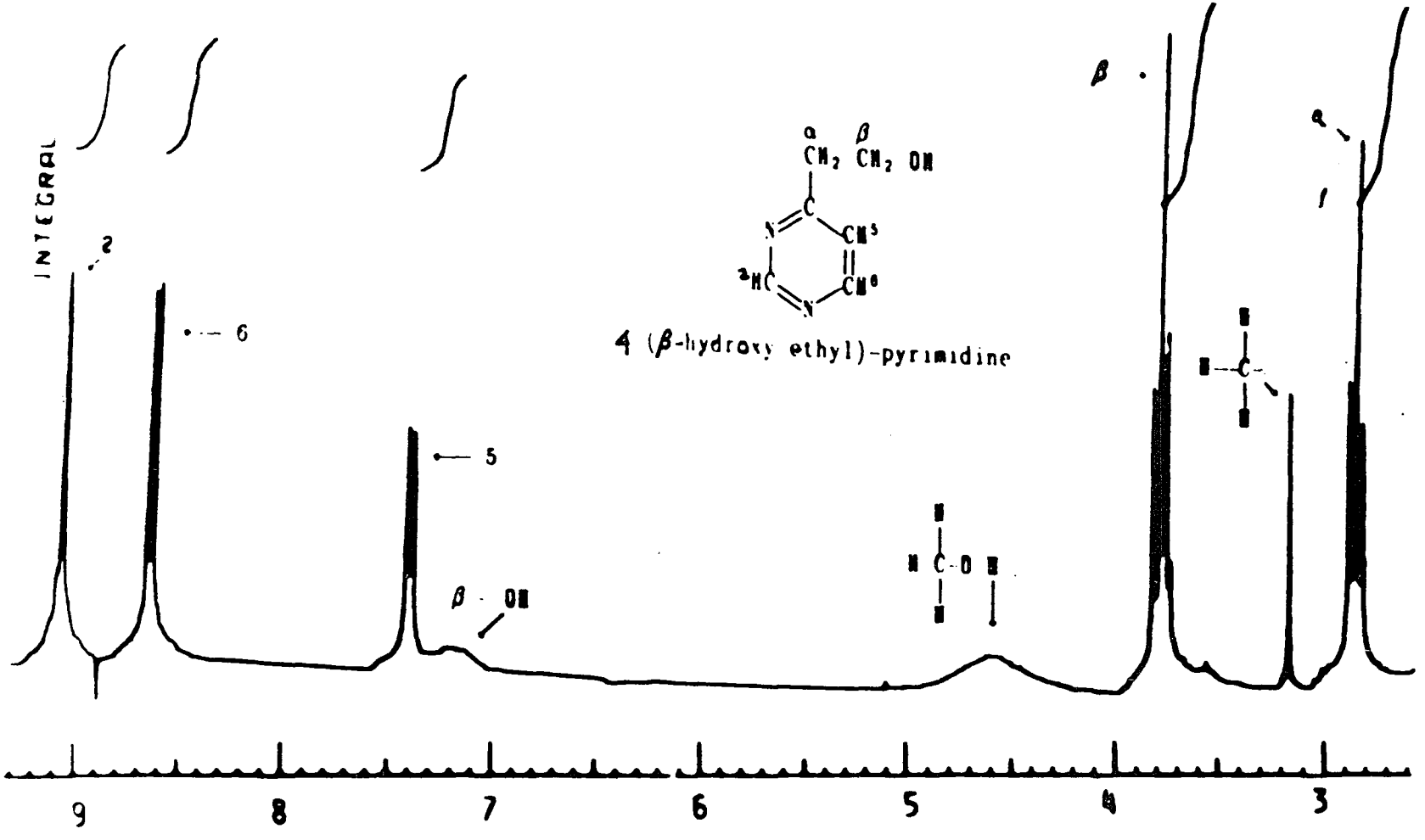

Figure V.1.1: Proton NMR spectrum of isolated alcohol

V.2 SYNTHESIS OF 4-VINYLPYRIMIDINE

To the resulting alcohol either anhydrous sodium sulfate or sodium hydroxide and 4,4'-methylenebis(2,6-di-*t*-butyl)phenol as inhibitor were added. The temperature was slowly raised to a maximum of ≈150°C inside a Kuegelrohr distillation apparatus under vacuum (64). This resulted in monomer and regeneration of starting material.

A second method used to dehydrate the alcohol was to add the alcohol dropwise to hot sodium hydroxide. The base was heated to 160°C under reduced pressure. A receiving flask was submerged in a dry ice/acetone bath. Alcohol was added dropwise to the hot *NaOH* and a mixture of water and 4-vinylpyrimidine was collected. Also present was a large amount of starting material. Other attempts to form the vinyl compound were made and are discussed below.

The excellent leaving group, bromine, of 2 bromopyrimidine is doubly-activated toward nucleophilic substitution. Pyridines are known to be easily alkylated by organolithium reagents. Therefore alkylation by vinylmagnesium bromide was also considered a viable synthetic pathway. A solution of 2-Bromopyrimidine (0.009 moles in dried THF) was placed in a 3-neck flask. All transfers took place in a dry box. 9 ml of 1 M vinylmagnesium bromide was placed in a delivery funnel under

nitrogen gas. The vinyl group was delivered to the reaction vessel dropwise over 2.5 minutes in a dry nitrogen atmosphere. The solution, kept in as ice bath, was stirred by a magnetic stirrer. No sign of a reaction was observed so the mixture was kept at room temperature. The solution became darker and cloudy. The vinyl product was not detected in this mixture.

The combined monomer obtained from different dehydration experiments is given in Figure V.2.1. Starting material, not entirely separated from the monomer, was regenerated upon dehydrating and can be seen as low intensity absorptions upfield to each of the vinyl aromatic absorptions.

The conventional method of dehydrating the alcohol is to add the alcohol to hot base while maintaining a vacuum. This method results in low yields partially due to the regeneration of starting material. It would be of interest to demonstrate the mechanism of dehydration as well as to improve the per cent yield of the vinyl group. Dehydration may follow two pathways as indicated in Schemes V.2.1 and V.2.2.

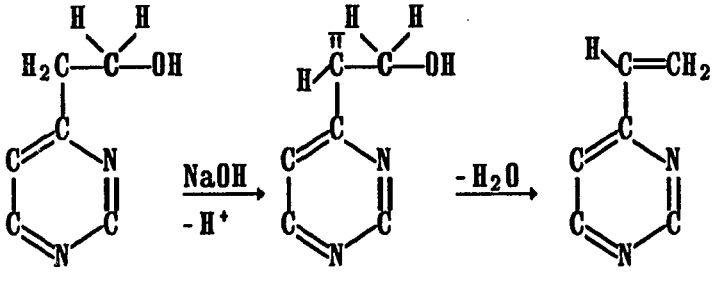

SCHEME V.2.1

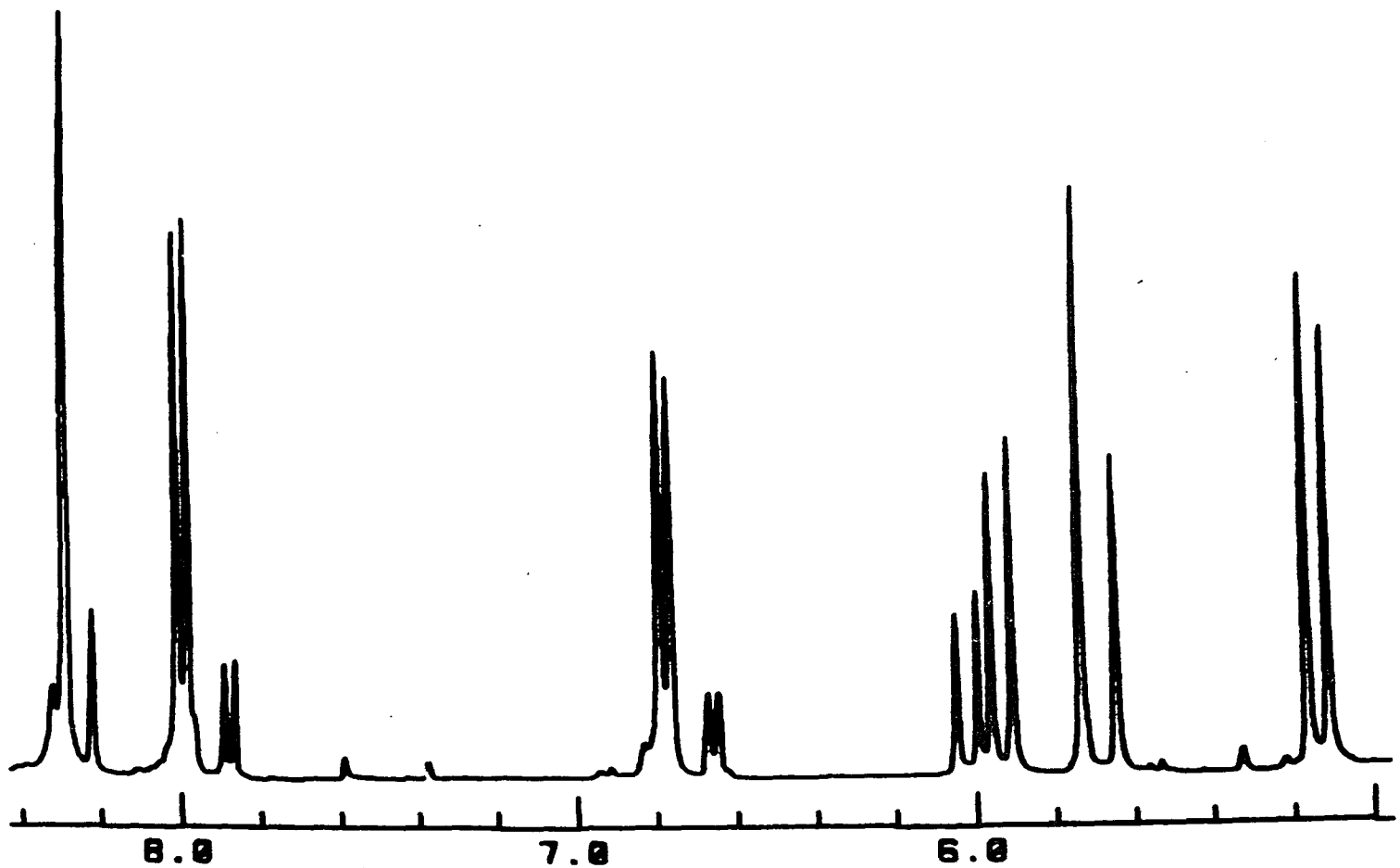

Figure V.2.1: Proton NMR spectrum of monomer obtained by dehydration of alcohol with base

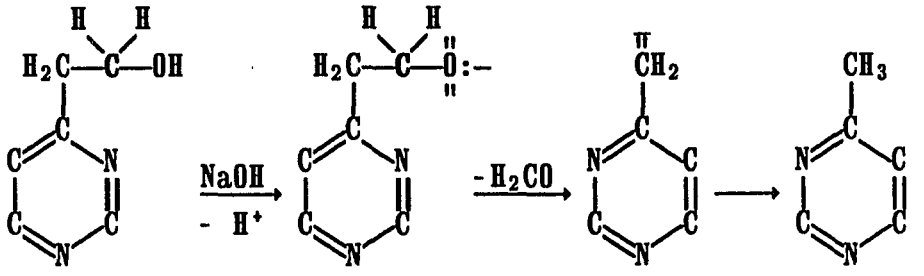

SCHEME V.2.2

It is evident that the vinyl group will form only if the α-hydrogen is more acidic then the β-hydroxy hydrogen. The α-carbanion is highly resonance stabalized by the nitrogen heteroatoms in the ortho and para positions. Regeneration of the starting material (Scheme V.2.2) also has as an intermediate the carbanion but it is generated by first abstraction of the β-hydroxy hydrogen. Formation of the vinyl compound will be preferred if the α-hydrogen is more acidic then the β-hydroxy hydrogen. Contributing to the stability of the β-hydroxy hydrogen may be the formation of the six member hydrogen bonded structure as shown in Figure V.2.2

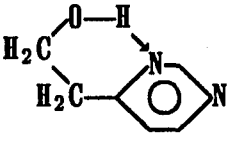

FIGURE V.2.2: Hydrogen bonding in 4-(β-hydroxy ethyl)-pyrimidine

Evidence for the above is obtained by refluxing 4-(β-hydroxy ethyl)-pyrimidine in acidic anhydride. If the β-hydroxy hydrogen were to attack the anhydride linkage acetic acid and 4-pyrimidine

acetate would result without formation of the vinylic compound. 4-vinylpyrimidine can form if the α-methylene hydrogen attacks the anhydride linkage first resulting in acetic acid and the secondary carbanion. Formation of the carbanion will result in removal of the hydroxy group as in scheme V.2.1, with the formation of an additional mole of acetic acid. The alcohol was refluxed in acetic anhydride for 2.5 hours. The mixture was separated into two parts by distilling at the boiling point of acetic anhydride. The proton NMR of the distillate is given in figure V.2.3 which clearly indicates formation of the vinyl compound. A high intensity absorption at 2.1 ppm is attributed to acetic anhydride. An absorption at 1.98 ppm corresponded to an absorption at 10.8 having three times the area as expected for acetic acid. The ^{13}C NMR spectrum corresponds the the proton spectrum. The ^{1}H nmr spectrum of the solution remaining in the distillation flask is given in Figure V.2.4. This also shows formation of the vinyl compound as well as a small amount of alcohol occuring as broad low intensity absorptions slightly upfield of the vinyl aromatic protons. No starting material was detected by proton or carbon NMR in either of the two portions. These results show the reaction proceeding by a resonance stabilized α-carbanion intermediate formed preferably to Abstraction of the β-hydroxy hydrogen. The structure of Figure V.2.2 is concluded to be responsible for stability of the hydroxy hydrogen.

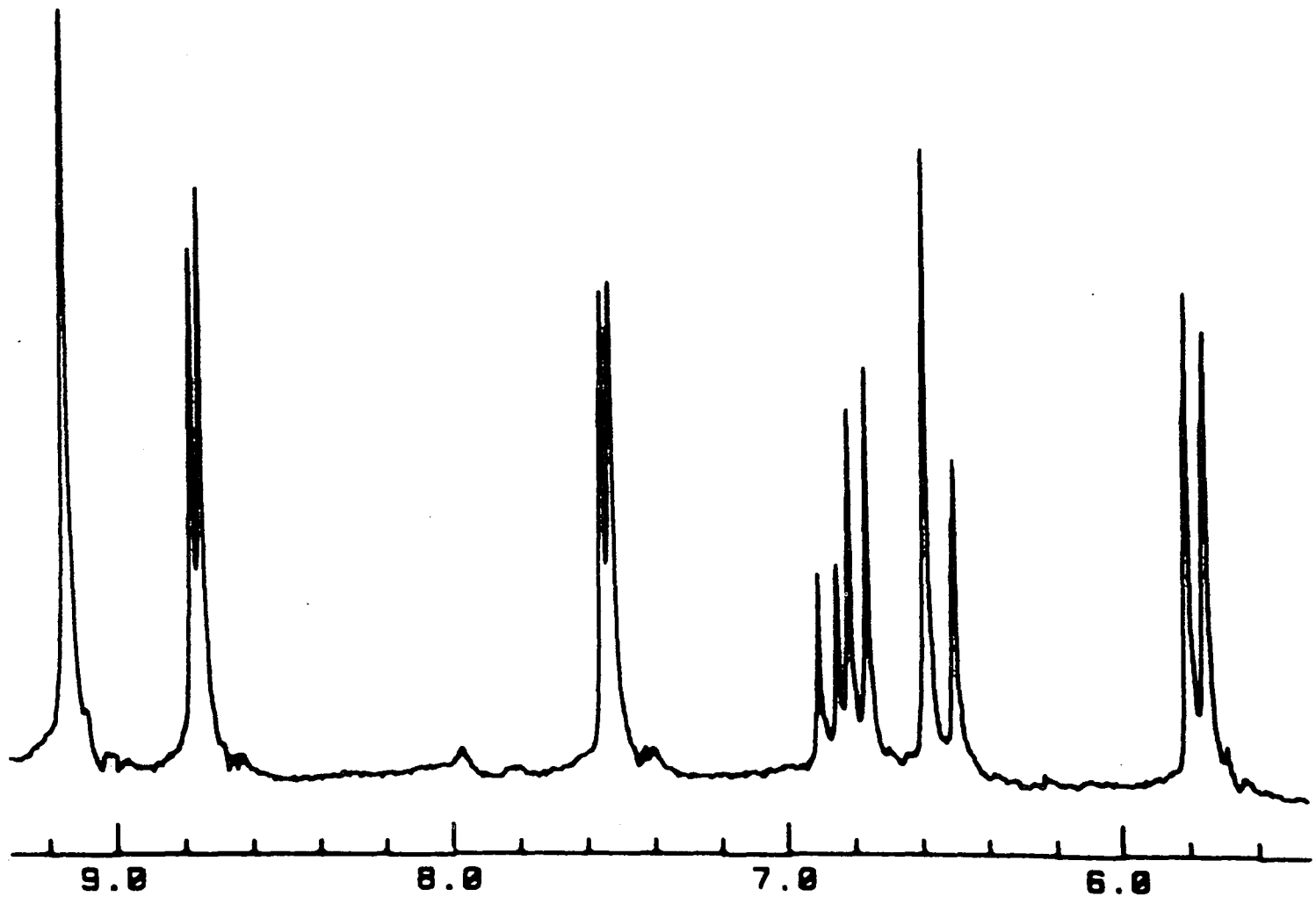

Figure V.2.3: Proton NMR spectrum of distillate from acetic anhydride reaction showing monomer

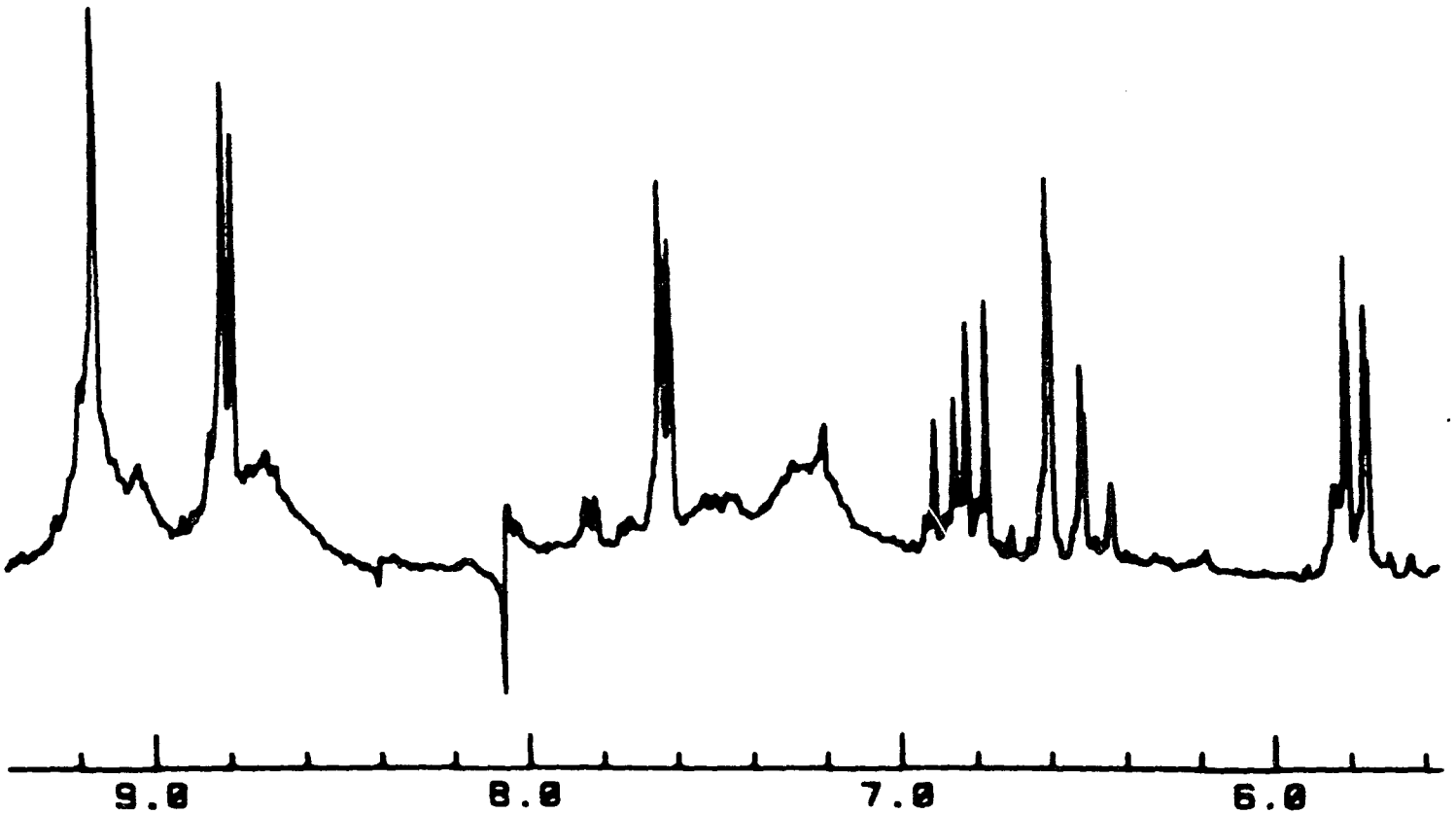

Figure V.2.4: Proton NMR spectrum of distillant of acetic anhydride reaction showing monomer

V.3 FORMATION OF POLY(4-VINYLPYRIMIDINE)

The monomer was polymerized by thermally (65°C) initiated AIBN radical polymerization in toluene under nitrogen for 10 hours. The insoluble polymer gel was dissolved in methanol and precipitated from ether at least twice. Figure V.3.1.a shows a ^{13}C NMR spectra of a purified sample of poly(4-vinyl)pyrimidine. An important side reaction in the dehydration method by use of the Kuegelrohr distillation apparatus is the possible formation of poly(4-vinylpyrimidine). The solid which remained was washed in methanol whereby the insoluble solid was removed by centrifugation. The solid was washed with acetone until no color appeared in the wash. After removing the acetone a light brown powder was isolated. The supernatant of the methanol wash was treated with acetone to give a precipitate. Further washings with acetone yielded the same powder as above. Figure V.3.1.b is a ^{13}C CP/MAS NMR spectrum of the isolated powder.

The reaction sequence outlined in Scheme V.I was a modification of the method of A. Ohsawa *et.al.* (62) whereby formation of tertiary alcohols were reported . The reaction involved generation of methyllithium from methylpyridazines. The alcohol was generated *in situ* by addition of the appropriate ketone. The current yield of 56% for 4-(β-hydroxy ethyl)-pyrimidine is a substantial improvement over the previously reported value of 26%. Products of dehydration of

4-(β-hydroxyethyl)-pyrimidine in acetic anhydride has lead to a mechanistic pathway involving a stable α-carbanion intermediate. The method also introduces a new and efficient method in the

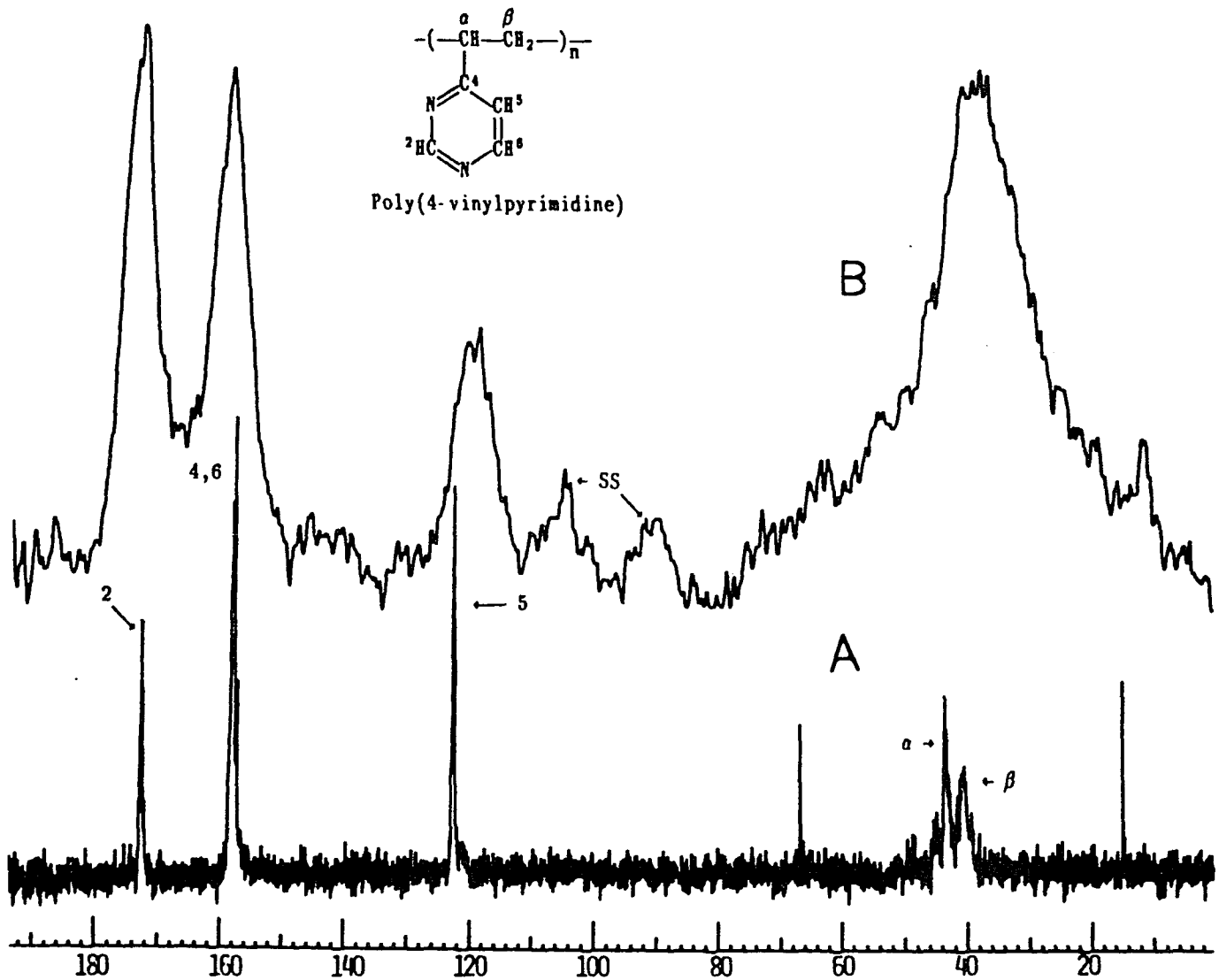

Figure V.3.1: a) C-13 NMR spectrum of poly(4-vinylpyrimidine) in THF and
b) CP/MAS of isolated powder. SS denotes spinning side bands

dehydration of such alcohols which have the potential to stabilize the hydroxy hydrogen towards attack by such reagents.

VI CONCLUSIONS

For iodine as the acceptor in polymeric charge transfer systems, polymer size and tacticity as well as the characteristics of the solvent were shown to be significant factors in determining the nature and extent of electron transfer. The ability of solvent to form hydrogen bonds was important in the formation of triiodide in the presence of certain donors. Donors of low molecular weight, i.e. pyridine and low molecular weight P2VP, did not form triiodide as readily as high molecular weight P2VP. Tacticity also determined the extent of triiodide formation. In poor solvents, isotactic P2VP behaved in a manner similar to low molecular weight P2VP in its ability to form triiodide. This is attributed to spatial distribution of the donor moieties. Isotactic and low molecular weight polymers are restricted in their ability to form domains of high donor concentration. High molecular weight polymer was shown to lead to domains of donor rings favorable for triiodide formation due to coiling of its chain. Unlike its behavior in methylene chloride, in chloroform isotactic polymer formed triiodide. This can be attributed to increased helical to coil transitions in chloroform. Complete electron transfer to form triiodide is promoted by solvents with high dielectric constant and strong tendency to form hydrogen bonds. Compared to methylene chloride, chloroform with a lower dielectric constant but stronger tendency to act as a donor in hydrogen bonding is more conducive to the formation of triiodide. In chloroform, the

polymer tends to assume a random coil conformation and charge separation to form inner complex and monoiodide is facilitated by hydrogen bonding with the outer complex.

Nuclear magnetic resonance gave important information in the study of charge transfer complexes of isotactic P2VP and 2-ethylpyridine with tetracyanoethylene. The difference in the order of the change in chemical shift of the pure complex, Δ_0, for the polymer and 2EP was attributed to the extent of electron transfer in the two complexes. The polymer demonstrated a larger degree of electron transfer due to better overlap of the non-bonding electrons with the π orbital of TCNE. Better overlap is due to a fixed position of the pyridine ring relative to the backbone. In 2EP, the alkyl group freely rotates and prevents TCNE from approaching the non-bonding electrons efficiently. The direction of change of carbons 2 and 6 was upfield while carbons 3, 4 and 5 moved downfield in both the polymer and 2EP upon complexation. This was explained by a redistribution of electron density within the aromatic framework as well as a change in bond order. Bond order for carbons 2 and 6 decrease while polarization effect on carbons 3, 4 and 5 dominate the chemical shift upon charge transfer complexation.

Equilibrium constants for the polymer as determined by proton NMR were found to be ca. 8.4 Kg/mole in a donor concentration of 0.04 mole/Kg and 21 Kg/mole in a donor concentration of 0.06 mole/Kg. Equilibrium constants as

determined by carbon NMR in a concentration of 0.06 mole/Kg agreed with that from proton NMR. The higher value at high concentration was attributed to an increase of polymer domains which contribute to a higher probability of TCNE being trapped in a domain of high donor concentration. The monomer did not demonstrate this concentration effect. In order to calculate the equilibrium constant for the small molecule, additional unspecific shielding had to be considered. Upon correcting for additional shielding the equilibrium constant was found to be ca. 5.5 Kg/mole. The H_6 proton demonstrated the least need for correction which was attributed to complexed TCNE restricting approach of a free TCNE molecule to the H_6 proton. The polymer did not demonstrate a need for such treatment because the ring of the complex is blocked from all sides. An apparent equilibrium constant for H_3 was found to be twice that of H_4 and H_5. H_6 showed change in chemical shift opposite to the remaining protons. Such behavior for H_3 and H_6 was not observed for the 2EP - TCNE complex. These results were explained by the magnetic anisotropy of TCNE. A topographic model of the complex was proposed based on these findings.

FT-IR data indicate significant extent of electron transfer to the strong acceptor TCNE. ESR spectroscopy clearly shows that complete electron transfer takes place but not at a significant level, i.e. less than 0.5 mole per cent of TCNE being converted to its anion radical.

REFERENCES

1 R.S. MULLIKEN, J. PHYS. CHEM., *56*, 801(1952)

2 R.S. Mulliken, Recl. trav. Chim. Pays-Bar Belg., *75*, 845(1956)

3 a)R.S. Mulliken, J. Chim. Phys., 611(1964) b)R.S. Mulliken J. Chim. Phys. ,Phys.-Chim. Biol. *61*, 20(1964)

4 Wynter, Hill, Bledose, Shenoy and Ruby; J. Chem. Phys. *30*, 3872(1962)

5 M. Kryszewski, Polymer Letter, *4*, 595(1966)

6 Molecular Complexes: A Lecture and Reprint Volume, Wiley, 1969; R.S. Mulliken and W.B. Person, ch 2

7 H.A. Benesi and J.H. Hildebrand; J. Am. Chem. Soc., *71*, 2703(1949)

8 R. Bhattacharga and S. Basu; Trans. Faraday Soc. *54*, 1286(1958)

9 R.L. Scott, Recl. traz. Chim. Pays-Bas Belg., *75*, 787(1956)

10 M.W. Hanna and A.C. Ashbough; J. Phys. Chem., *67*, 811(1964)

11 P.J. Berkely, Jr., and M.W. Hanna; J. Phys. Chem., *67*, 846 (1964)

12 E.D. Becker, U. Liddel and J.N. Shoolery; J. Mol. Spectroscopy, *2*, 1(1958)

13 T.C. Nehman and A.I. Popov; J. Phys. Chem., *70*, 3688(1966)

14 R. Foster and C.A. Fyfe; Prog. in NMR Spec., Vol.4, 1(1969)

15 R. Foster and C.A. Fyfe; Trans. Faraday Soc., *61*, 1626(1965)

16 Foster, Hammick and Wardley; J. Chem. Soc., 3817(1953)

17 K.A. Connors and J.A. Mollica, J. Pharm. Sci., *55*, 772(1966)

18 M. Nakano, N.I. Nakano and T. Higuchi. J. Phys. Chem., *71*, 3954(1967)

19 R. Sahai, G.L. Loper, S.H. Lin and H. Eyring; Proc. Nat. Acad. Sci. USA, *71*, 1499(1974)

20 K.A. Connors, Binding Constants, Wiely, 1987, p198

21 T. Gramstad and O. Mundheim, Spectrochimica acta,

28A, 1405(1972)

22 T. Gramstad and E.D. Becker, J. Mol. Struct., *5*, 253(1970)

23 H. Stamm, W. Lamberty and J. Stafe; J. Am. Chem. Soc., *102*, 1529(1980)

24 H. Stamm and W. Lamberty; Tetrahedron, *37*, 565(1981)

25 D.A. Deranleau, J. Am. Chem. Soc., *91*, 4044(1969)

26 N.J. Rose and R.S. Drago, J. Am. Chem. Soc., *81*, 6138,6141(1959)

27 W.G. Blann, C.A. Fyfe, J.R. Lyerla and C.S. Yannoni J. Am. Chem. Soc., *103*, 4030(1981)

28 S.J. Opella, M.H. Frey; J. Am. Chem. Soc., *101*, 5854(1979)

29 S.J. Opella, M.H. Frey and T.A. Cross; J. Am. Chem. Soc., *101*, 5856(1979)

30 S.J. Wyard, J. Sci. Inst., *42*, 769(1965)

31 G. Natta, J. Polym. Sci., *51*, 487(1961)

32 L.I. Katzin, J. Chem. Phys., *21*, 490(1953)

33 L.M. Julien, W.E. Bennett and W.B. Person; J. Am. Chem. Soc., *91*, 6915(1969)

34 A.D. Awtrey and R.E. Connick; J. Am. Chem. Soc., *73*, 1842(1951)

35 R.E. Buckles, J.P. Yuk and A.I. Popv; J. Am. Chem. Soc., *74*, 4379(1952)

36 C. Reid and R.S. Mulliken; J. Am. Chem. Soc., *76*, 3869(1954)

37 J. Kleinberg, E. Colton, J. Sattizahn and C.A. VanderWerf J. AM. Chem. Soc., *75*, 447(1953)

38 B.I. Sazhin and Yu. I. Vasilenok; Vysokomol. Soyed. *A10*, 1408(1968)

39 T. Tomono, E. Hasegawa and E. Tsuchida; J. Polym. Sci., Polym. Chem. Ed. *12*, 167(1974)

40 Ref. 6, ch. 10 and ref. 2

41 V.G. Krishna and B.B. Bhowmik; J. Am. Chem. Soc., *90*, 1700 (1968)

42 M. Karplus and J.A. Pople; J. Chem. Phys., *38*, 2803(1963)

43 Interpretation of C13 NMR Spectroscopy, F.W. Wehrli and T. Wirthlin, Heyden and Son Ltd. 1976 ch. 2

44 T. Tokuhiro and G. Frainkel; J. Am. Chem. Soc., *91*, 5005(1969)

45 W. Adam, A Grimison, R. Hoffmann and C.Z. de Ortiz; J. Am. Chem. Soc., *90*, 1509(1968)

46 R.J. Pugmire and D.M. Grant; J. Am. Chem. Soc., *90*, 697(1986)

47 J.P. Larkindale and D.J. Sinkin; J. Chem. Phys., *55*, 5048(1971)

48 Y. Abe, A.E. Tonelli and P.J. Flory; Macromol. *3*, 29(1970)

49 A.E. Tonelli, Macromol. *6*, 682(1970)

50 Nuclear Magnetic Resonance Spectroscopy: a physicochemical view, Robin K. Harris

51 N. Higuchi, T. Hiraoki and K. Hikichi; Polymer Journal, *11*, 139(1979)

52 A. Pines, M.G. Gibby and J.S. Waugh; J. Chem. Phys., *59*, 569(1973)

53 E.O. Stejskal, J. Schaefer, M.D. Sefcik and R.A. McKay; Macromolecules, *14*, 275(1981)

54 E.O. Stejskal, J. Schaefer and T.R. Steger; Symp. Faraday Soc., *18*, 56(1979)

55 L.C. Dickinson, P. Morganelli, C.W. Chu, Z. Petrovie, W.J. MaCknight and J.C.W. Chien; Macromolecules, *21*, 338 (1988)

56 L.B. Alemany, D.M. Grant, R.J. Pugmire, T.D. Alger and K.W. Zilm, J. Am. Chem. Soc., *105*, 3133(1983)

57 W.C. Herndon and J. Feuer; J. Am. Chem. Soc., *90*, 5914(1968)

58 M.J. Mobley, K.E. Rleckhoff and E.M. Volght; J. Phys. Chem., *81*, 800(1977)

59 J.L. Lippert, M.W. Hanna and P.J. Trotter; J. Am. Chem. Soc., *91*, 4035(1969)

60 J.C. Moore, D. Smith, Y. Youhne and J.P. Devlin; J. Phys. Chem., *75*, 325(1971)

61 W.D. Phillips, J.C. Rowell and S.I. Weissman; J. Chem Phys. *33*, 626(1960)

62 A. Ohwawa, T. Uezu and H. Igeta; Chem. Pharm. Bull., *27*, (4) 916(1979)

63 C.G. Overberger and I.C. Kogon; J. Am. Chem. Soc., *76*, 1879 (1954)

64 M. Furue, K. Sumi and S. Nozakura; J. Pol. Sci: Polymer Letters Ed. *20*, 291(1982)